Fed-batch cultivations for high-yield production of tissue engineering related bio-molecules

Von der Naturwissenschaftlichen Fakultät

der Gottfried Wilhelm Leibniz Universität Hannover

zur Erlangung des Grades

Doktor der Naturwissenschaften

Dr. rer. nat.

genehmigte Dissertation

von

M. Sc. Ran Chen

geboren am 05.09.1981, in Hubei, China

2011

Referent: **Prof. Dr. Thomas Scheper**

Korreferent: **Prof. Dr. Bernd Hitzmann**

Datum der Promotion: **10. 05. 2011**

Erklärung

Hierdurch erkläre ich, dass die vorliegende Dissertation selbstständig verfasst und alle benutzten Hilfsmittel sowie evtl. zur Hilfeleistung herangezogene Institutionen vollständig angegeben wurden.

Die Dissertation wurde nicht schon als Diplom- oder ähnliche Prüfungsarbeit verwendet.

Hannover, Mai 2011

Ran Chen

Acknowledgments

First of all, I would like to give my heartily thanks to Prof. Dr. Robert Faurie and Prof. Dr. Thomas Scheper, who kindly provided me the opportunity to continue my research work in the Institute for Technical Chemistry (TCI) and made this dissertation possible.

My great appreciation goes to my advisor, Prof. Dr. Thomas Scheper, for constant guidance, tolerance, encouragement and patience as well as financial support over my Ph.D. study. I consider him not only as a professor but a caring father. I am sure what I learnt from him will benefit through my life.

I am grateful to Prof. Dr. Bernd Hitzmann, whom I considered to be my co-advisor, for valuable suggestion, discussion and help on fed-batch cultivation experiments as well as being my co-referee.

I would like to acknowledge PD Dr. Ursula Rinas, for continuous support and fruitful advice on FGF-2 production and purification.

I would like to thank Prof. Dr. Jürgen Alves for being my third examiner.

Special thanks to Jinu John, who worked with me on *E. coli* cultivation for 3 years. Without her help and assistance I could not accomplish the work presented here.

I would also like to thank many past and present members of our institute. Special thanks to Bastian Rode and Christian Endres, who help me a lot on working with bioreactor and PSA determination. I would also like to thank Magda Tomala, who worked with me on the expression and purification of FGF-2 at small scale. Many thanks to Yangxi Zhao, for the collaboration on the downstreaming processes of FGF-2 production. I appreciate Dr. Ingrida Majore and Antonina Lavrentieva, who did a nice work on testing the bioactivity of FGF-2. I would like to thank all the colleagues at the TCI, for providing a comfortable working atmosphere, especially Ismet Bice who is always ready to help me.

Thanks go to Silvana Taubeler-Gerling, Dipl.-Biol. Maike Wesemann, PD Dr. Kirsten Haastert, Susann Müller, Olmer Ruth, Dr. Robert Zweigerdt and Prof. Dr. Ulrich Martin

from Hannover Medical School (MHH), for their beautiful work on the activity test of FGF-2.

I would also like to give my appreciation to Dr. Sascha Beutel, Dr. Frank Stahl and PD Dr. Cornelia Kasper for the inspiration and support of my work.

I would like to thank Martin Pähler and Martina Weiß for purchasing chemicals and technique assistance.

Many thanks to all the people at mechanical and electronic workshop, for helping me to solve so many problems with the fermentation system.

I appreciate all the help I received from TCI and Leibniz University of Hannover during my 4 years stay which are too numerous to mention here.

Finally, my heartfelt thank to my parents, my wife and my brother for their endless love, encouragement and support. This work could not be done without them.

Abstract

In this thesis, fed-batch cultivations for effective production of two tissue engineering related bio-molecules: polysialic acid (PSA) and human basic fibroblast growth factor (FGF-2) are described.

The PSA production in *Escherichia coli* (*E. coli*) K1 in batch and fed-batch cultivations is investigated. Three different cultivation strategies were used, namely batch cultivation, fed-batch cultivation with a constant specific growth rate of 0.25 h^{-1} and fed-batch cultivations with a constant glucose concentration of 0.1 g l^{-1} and 0.05 g l^{-1}. A flow injection analysis (FIA) system supported by an extended Kalman filter (EKF) was used for on-line measuring and controlling of the glucose concentration in the culture broth. The results demonstrated that compared to the batch cultivation, both fed-batch strategies have greatly improved the PSA productivity and acetate formation was prevented. The highest level of PSA yield on glucose (0.043 g g^{-1}) was obtained in fed-batch cultivation at a constant glucose concentration of 0.05 g l^{-1} with a final PSA concentration of 1.35 g l^{-1} in the reactor. The results from the four cultivation experiments further revealed that PSA production was correlated to the specific growth rate of the cells and the optimal specific growth rate for PSA production in *E. coli* K1 was 0.32 h^{-1}.

A biotechnological process for the effective production of FGF-2 in high quantity and quality is presented. Fed-batch cultivations of *E. coli* BL21 at two constant specific growth rates (0.35 h^{-1} and 0.15 h^{-1}) were performed. The higher expression level (42 mg g^{-1} dry cell) of FGF-2 with higher time-space yield of soluble protein (0.056 g l^{-1} h^{-1}) was achieved by fed-batch cultivation at a constant specific growth rate of 0.35 h^{-1}. For the purification, a new combination of cation exchange membrane chromatography and heparin-sepharose affinity chromatography was applied. A novel anion exchange membrane chromatography was used in the polishing step to remove endotoxins and DNAs, yielding $\geqslant$ 98 % pure FGF-2 as determined by RP-HPLC. This new process yielded about 200 mg of pure FGF-2 from 1.9 l culture broth. A carrier-free formulation was developed for the lyophilization and long-term storage of FGF-2 using sucrose as a stabilizer. The purified FGF-2 was endotoxin-free and demonstrated a high mitogenic activity on mesenchymal stem cell-like cells (EC_{50} = 0.13 ng ml^{-1}) and NIH-3T3 cells (EC_{50} = 0.10 ng ml^{-1}). It has also been successfully tested on neuronal differentiation of PC 12 cells and keeping primate ESC (embryonic stem cell) and human iPSC (induced pluripotent stem cell) pluripotent at cooperation institutes, which proved purified FGF-2 was suitable for using in cell culture. A preliminary stability test demonstrated that lyophilized FGF-2 powder has an average residual water content of 1.90 %. And the freeze-dried protein was stable after 17 days storage at 37 °C, 1 month at room temperature or 2 month at 4 °C.

Keywords: polysialic acid; fed-batch cultivation; human basic fibroblast growth factor

Zusammenfassung

In dieser Arbeit werde Fed-Batch Kultivierungen für die effektive Produktion von zwei Tissue Engineering relevanten Biomoleküle: Polysialinsäure (PSA) und menschliche basischer Fibroblasten Wachstumsfaktor (FGF-2), beschrieben.

Die Produktion von PSA in *Escherichia coli* (*E. coli*) K1 durch Batch und Fed-Batch Kultivierungen wurde untersucht. Drei verschiedenen Fermentationstrategien wurden verwendet, nämlich Batch, Fed-Batch mit einer konstanten spezifischen Wachstumsrate von 0,25 h^{-1} und Fed-Batch mit konstanten Glucose-Konzentrationen von 0,1 g l^{-1} oder 0,05 g l^{-1}. Ein Fließ-Injektions-Analyse (FIA) System mit einem erweiterten Kalman-Filter (EKF) wurde eingesetzt für das on-line Monitoring und die Regelung der Glucose Konzentration in der Kulturbrühe. Meine Ergebnisse wiesen auf, dass die beiden Fed-Batch Strategien im Vergleich zum Batch die Produktivität von PSA erheblich verbessert haben und die Bildung von Acetat eliminiert wurde. Die höchste Ausbeute von PSA zu Glucose war 0,043 g g^{-1}, die bei der Fed-Batch Kultivierung mit einer konstanten Glucosekonzentration von 0,05 g l^{-1} erhalten wurde. Dabei betrug die End-Konzentration von PSA im Reaktor 1,35 g l^{-1}, d.h. die Produktion von PSA ist mit der spezifischen Wachstumsrate der Zellen korreliert und die optimale spezifische Wachstumsrate für die Herstellung in *E. coli* K1 beträgt 0,32 h^{-1}.

Ein komplett neues biotechnologisches Verfahren zur Produktion von FGF-2 mit hoher Quantität und Qualität wurde auch in dieser Arbeit erarbeitet. Dazu wurde die Fed-Batch Kultivierung von *E. coli* BL21 mit zwei unterschiedlichen spezifischen konstanten Wachstumsraten (0,35 h^{-1} und 0,15 h^{-1}) durchgeführt. Die höhere Expression von FGF-2 (42 mg g^{-1} Trockenbiomasse) erfolgte bei eine Wachstumsrate von 0,35 h^{-1}. Dabei errichte man eine höhere Raum-Zeit-Ausbeute an löslichem Protein (0,056 g l^{-1} h^{-1}). Eine neue Kombination von Kationenaustauschermembran Chromatographie und Heparin-Sepharose Affinitätschromatographie begünstigte die Aufreinigung von FGF-2. Außerdem wurde eine neuartige Anionenaustauschermembran Chromatographie als Polierschritt zum Entfernen der Endotoxine und DNAs verwendet. Die durch RP-HPLC bestimmte Ausbeute des reinen FGF-2 lag über 98 %. Dieses Kosten günstige Verfahren liefert etwa 200 mg von reinem FGF-2 aus 1,9 l Kulturbrühe. Eine Träger-freie Formulierung war bereits für die Gefriertrocknung und Lagerung von FGF-2 entwickelt worden, dabei war Saccharose als Stabilisator eingesetzt. Das aufgereinigte FGF-2 zeigte eine hohe mitogenetische Aktivität in mesenchymalen Stammzell-ähnlichen Zellen (EC_{50} = 0,13 ng ml^{-1}) und NIH-3T3 Zellen (EC_{50} = 0,10 ng ml^{-1}). Weitere in unseren Koorperationsinstituten durchgeführte Aktivität-Tests, z.B Testen für die neuronale Differenzierung der PC 12 Zellen und der Erhalt der Pluripotenz von Primaten ESC (embryonalen Stammzellen) sowie menschliche iPSC (induzierte pluripotente Stammzellen), erzielten auch ausgezeichnete Ergebnisse. Darüber hinaus wurde nachgewiesen, dass das lyophilisierte FGF-2 Pulver einen durchschnittlichen Restwassergehalt von 1,90 % hat. Deswegen kann das gefriergetrocknete Protein stabil bleiben nach der Lagerung von 17 Tagen bei 37 °C, 1 Monat bei Raumtemperatur oder 2 Monate bei 4 °C.

Stichworte: Polysialinsäure; Fed-Batch Kultivierung; menschliche basischer Fibroblasten Wachstumsfaktor

Table of Contents

1. Introduction

Tissue engineering is a rapidly evolving field which combines the knowledge of biology, biochemistry, medicine, material scicence and engineering to develope new biological replacements in order to repair, maintain or improve tissue/organ functions (Skalak and Fox, 1988).

In the past 20 years, remarkable progresses were achieved in this relatively "young" area (Atala, 2006; Koh and Atala, 2004; Shieh and Vacanti, 2005; Stock and Vacanti, 2001). Nowadays, stem cell researches have become an important aspect of tissue engineering (Bianco and Robey, 2001; Lanza et al., 2007; Leo and Grande, 2006; Polak and Bishop, 2006). And finding biodegradable polymers as scaffold materials become another significant area (Hutmacher, 2001; Ifkovits and Burdick, 2007; Ma and Elisseeff, 2006; Yang et al., 2001, 2002).

Cytokines play an important role in various cellular processes such as cell proliferation, differentiation, migration, adhesion (Babensee et al., 2000; Lee, 2000). Therefore they are widely used as supplements in stem cell cultivations. In this thesis a biotechnological process for the production of an extensively used cytokine-human basic fibroblast growth factor (FGF-2) is described. Additionally, an optimum fed-batch strategy for the production of a promising biodegradable scaffold material-polysialic acid (PSA) is also presented.

For PSA production, batch cultivation, fed-batch cultivations with two different control strategies were performed. PSA yields on glucose were compared and the best cultivation condition for PSA production was identified. For FGF-2 production, efficient production of FGF-2 was achieved by fed-batch cultivation of *Escherichia coli* BL21 and a new purification process was developed using membrane adsorber technology. The purified protein was identified to be endotoxin-free and bioactive. It has been successfully tested in cultivating PC12 cells, embryonic stem cells and induced pluripotent stem cells, etc.

The production processes decribed in this thesis support large-scale preparation of PSA and FGF-2 at low-cost, thus will be benefical to the furture tissue engineering researches.

2. Theoretical background

2.1 Cultivation of *Escherichia coli*

Fermentation processes are utilized for the production of various biological products such as amino acids, antibiotics, proteins and enzymes. Among all the organisms used in fermentation, *Escherichia coli* (*E. coli*) is the most commonly used. Since recombinant DNA technology emerged in 1970s, *E. coli* has become the most widely used prokaryotic expression system for the production of heterologous proteins.

The cultivation of *E. coli* is usually carried out in a stirred tank bioreactor. Air is sparged into the medium and well distributed by a mechanical stirrer. In order to maintain suitable growth conditions for the cells, temperature, pH value and dissolved oxygen concentration in the reactor are controlled.

2.1.1 Cultivation medium

Cultivation mediums can be divided into two major types, complex medium and defined medium. A complex medium contains some components whose chemical composition is unknown, such as yeast extract, beef extract or peptone. The most commonly used complex medium for *E. coli* cultivation is LB medium (Luria-Bertani medium). However, the composition of complex media may be different from batch to batch which makes cultivation results not reproducible. While in defined medium all the chemical components are known. A defined medium usually contains carbon sources, nitrogen sources, trace elements and vitamins. The most commonly used carbon source is glucose and ammonium salts are often used as nitrogen sources. Trace elements and vitamins are used at very low concentrations for the better growth of the cells. Defined medium is often used in high cell density cultivation of *E. coli*.

2.1.2 Measurement and control

Common on-line measurements of cultivations including pH value, temperature and dissolved oxygen concentration as well as the CO_2 and O_2 content in the exhaust gas. Robust and precise sensors have been developed to monitor these parameters. However, many important process variables are still difficult to measure on-line such as biomass

concentration, acetate concentration and glucose concentration in the reactor. Therefore, in the past two decades, many new approaches were developed for on-line process monitoring.

For example, the use of non-invasive methods such as 2D-fluorescence spectroscopy (Lindemann et al., 1998; Marose et al., 1998) and in-situ microscopy (Bittner et al., 1998; Joeris et al., 2002) to monitor bioprocesses has been applied. A detailed review see (Marose et al., 1999). On-line analytical instruments based on flow injection analysis (FIA) system have been developed and tested (Schügerl et al., 1993; Schügerl et al., 1996; Steube and Spohn, 1994). Software sensors based on extended Kalman filter (EKF), fuzzy logic, adaptive controller and artificial neural network (ANN) have been exploited for on-line state estimation of bioprocesses (Chéruy, 1997; Chen et al., 2004; de Assis and Filho, 2000; do Carmo Nicoletti et al., 2009). A thorough review is given in (Schügerl, 2001).

2.1.3 Operation modes

There are three main cultivation techniques, known as batch, continuous and fed-batch operations.

In batch cultivations, all nutrients are put into the reactor at the beginning of the cultivation and cells are harvested at the end of the cultivation. While in continuous cultivations, fresh medium is fed into the reactor at a constant rate (i.e. dilution rate) and meanwhile the culture broth is taken out at the same rate. Therefore, the growth rate of the cells can be controlled by manipulating the dilution rate.

Fed-batch cultivations usually starts with an initial batch phase and afterwards growth limiting substrates are fed into the bioreactor at a controlled rate. By changing the feed rate, cell growth rate can be easily controlled at the desired set point. Using this method, the oxygen transfer limitation and acetate formation in batch cultivations could be avoided and high cell density in the bioreactor could be achieved. Therefore, fed-batch cultivation has been widely used in industrial fermentations. A typical fed-batch cultivation is shown in Fig. 2.1.

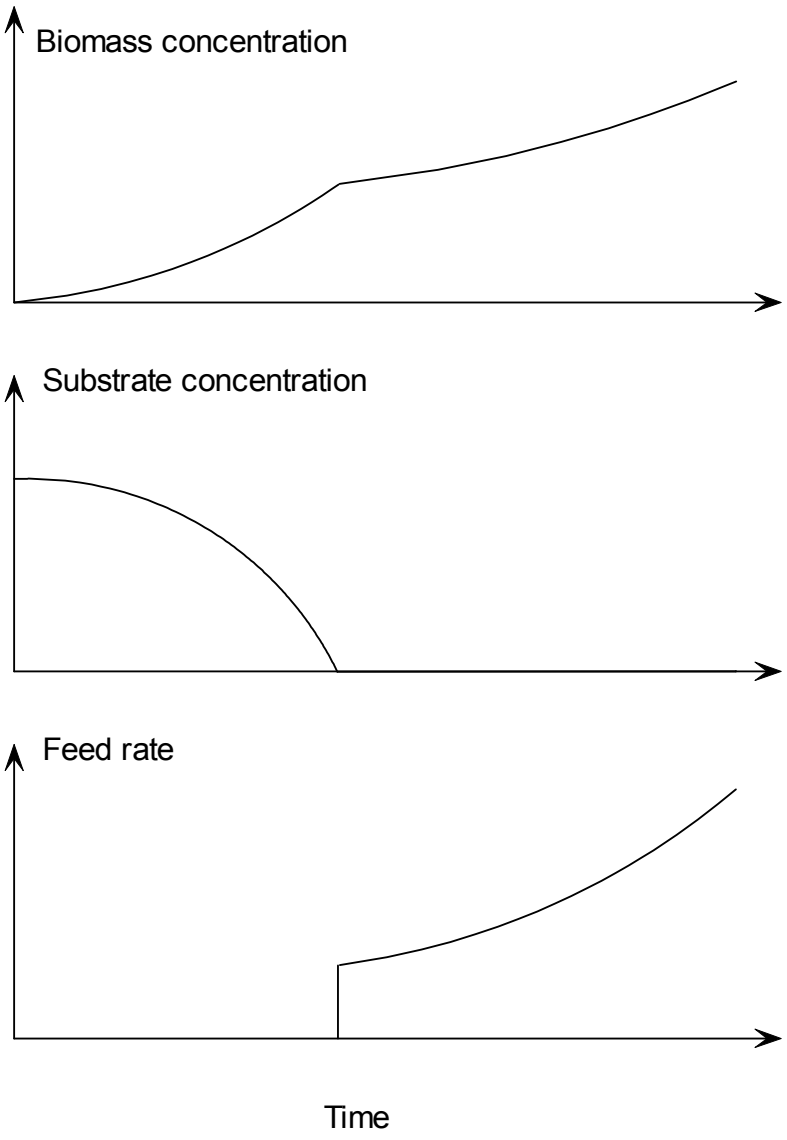

Fig. 2.1Diagram of a typical fed-batch cultivation.

2.1.4 Limiting factors in *E. coli* cultivation

2.1.4.1 Medium

E. coli needs various nutrients to support its proper growth, such as carbon, nitrogen, phosphorus, sulfur, magnesium, potassium, iron, manganese, zinc and copper (Gunsalus et al., 1960). However, most of the medium components become growth inhibitors when their concentrations in the medium reach a critical value. For example, glucose at a concentration above 50 g l^{-1}, ammonium above 3 g l^{-1}, phosphorus above 10 g l^{-1}, iron

above 1.15 g l^{-1}, magnesium above 8.7 g l^{-1}, copper above 0.0042 g l^{-1} are known to inhibit the growth of *E. coli* (Riesenberg, 1991). Therefore, cultivations should always start with initial nutrients concentrations below the critical values.

2.1.4.2 Oxygen supply

Due to the low solubility of oxygen in water, oxygen supply is a common limiting factor in *E. coli* cultivations. Several methods have been developed to increase oxygen supply in a bioreactor. For example, increasing air flow rate or stirrer speed, mixing air with oxygen or using pure oxygen and pressurizing the reactor (Riesenberg, 1991). Moreover, new air separation system using membrane gas separation technology has been developed (Wang et al., 1988). This system can convert ambient air into oxygen enriched air with oxygen content up to 50 % (Fass et al., 1989).

2.1.4.3 Acetate formation

In aerobic conditions, when *E. coli* is cultivated on excess glucose will cause the excretion of acetate into the medium. This glucose induced acetate formation phenomenon is also called as bacterial Crabtree effect (Rinas et al., 1989), which could result in up to 15 % of glucose being converted into acetate (Holms, 1986). However, acetate concentration above 2 g l^{-1} was known to affect cell growth as well as reduce recombinant protein productivity (Bauer et al., 1990; Koh et al., 1992; Sakamoto et al., 1994; Turner et al., 1994b).

As the main by-product of *E. coli* cultivation, acetate formation during cultivation processes has been intensively studied. In 1982, Doelle et al. (1982) observed acetate production from excess glucose. Meyer et al. (1984) proposed thresholds for acetate formation in chemo-stat cultures with both defined and complex medium. Majewski and Domach (1990) predicted that restrictions might exist in the capacity of the oxidation chain. Han et al. (1992a) further suggested that limited oxidation capacity of the TCA (tricarboxylic acid) cycle might be the reason for acetate formation.

Many approaches have been developed to avoid acetate accumulation in *E. coli* cultivations. Such as using fed-batch technique to limit glucose supply (Lee, 1996); replacing glucose with glycerol (Korz et al., 1995) or fructose (Aristidou et al., 1999); using metabolic engineering to change metabolic pathway (Bauer et al., 1990); using dialysis to remove

acetate (Märkl et al., 1993; Nakano et al., 1997) and using a probing feeding technology (Åkesson et al., 1999).

2.2 Fed-batch cultivation of *E. coli*

Because of the high volumetric yield of the desired product, fed-batch has become the most popular technique for high cell density cultivation of *E. coli*. Simple carbon source feeding strategies can be developed based on mathematical models of *E. coli* growth with limited substrate. Thus, demand of substrate by the cells can be easily calculated.

Other more advanced feeding methods involve the application of direct or indirect feedback control systems. Indirect feedback control system utilize feedback signal from the on-line measuring of actual cultivation parameters such as pH value and dissolved oxygen concentration. The system feed carbon substrate according to the sudden change of these paprameters. While in direct feedback control system, the feedback signal is directly come from the on-line monitoring of substrate concentrations. By comparing the feedback signal with the set point, the system adds feed medium to the reactor in order to keep the substrate concentration at the set point.

Comprehensive reviews of various control strategies for *E. coli* cultivations are in (Konstantinov and Yoshida, 1992; Lee, 1996; Riesenberg and Guthke, 1999; Wlaschin and Hu, 2006; Yee and Blanch, 1992).

2.2.1 Bioprocess models

Bioprocess models can be divided into four different types. If the model treats all the cells independently (i.e. every cell is different), it is a segregated model (Tsuchiya et al., 1966). If the model considers all the cells as the same, it is a non-segregated model (Fredrickson et al., 1970). Moreover, if the model includes the reactions inside the cells, it is a structured model. However, if the model considers the cell as an entirety without internal reactions, it is an unstructured model.

Among all the bioprocess models, unstructured non-segregated models are the simplest. They treat the cells as the same and internal reactions inside the cells are not considered. The most widely used unstructured non-segregated model is the Monod growth model

(Monod, 1949). In this model the cell growth kinetics can be described using specific growth rate-μ and Monod substrate saturation constant-K_m (Eq. 1.1).

$$\mu = \mu_{max} \frac{S}{K_m + S} \tag{1.1}$$

Here S is the substrate concentration, μ_{max} is the maximum specific growth rate and K_m is the limiting substrate concentration when half maximum specific growth rate is reached ($\mu = \frac{\mu_{max}}{2}$). The cell growth can be described as (Eq. 1.2):

$$\frac{dX(t)}{dt} = \mu X(t) \tag{1.2}$$

And the substrate consumption can be written as (Eq. 1.3):

$$\frac{dS(t)}{dt} = -\frac{\mu X(t)}{Y_{X/S}} \tag{1.3}$$

Therefore, a fed-batch cultivation carried out in an ideal stirred tank bioreactor could be described by the following equations (Eq. 1.4-1.6):

$$\frac{dX(t)}{dt} = \frac{\mu_{max} S(t)}{K_m + S(t)} X(t) - \frac{\dot{V}_F(t)}{V_R(t)} X(t) \tag{1.4}$$

$$\frac{dS(t)}{dt} = -\frac{\mu_{max} S(t)}{K_m + S(t)} \frac{X(t)}{Y_{X/S}} + \frac{\dot{V}_F(t)}{V_R(t)} (S_0 - S(t)) \tag{1.5}$$

$$\frac{dV_R(t)}{dt} = \dot{V}_F(t) \tag{1.6}$$

Where, $X(t)$ – concentration of biomass at time t (g l^{-1});

$S(t)$ – concentration of substrate at time t (g l^{-1});

μ_{max} – maximum specific growth rate (h^{-1});

K_m – Monod substrate saturation constant (g l^{-1});

$\dot{V}_F(t)$ – feed rate at time t (l h^{-1});

$V_R(t)$ – culture volume at time t (l);

S_0 – substrate concentration of feed solution (g l^{-1});

μ – specific growth rate (h^{-1});

$Y_{X/S}$ – yield coefficient (g g^{-1}).

Although the real bioreactor is far away from ideal, this model is still useful in fed-batch cultivation design and control.

2.2.2 Control strategies

A control strategy is used to determine the amount of feed medium to be added into the reactor at a specific time. Many control strategies have been developed in order to meet this requirement (Johnson, 1987). They can be roughly divided into two types: open-loop and closed-loop control strategies.

2.2.2.1 Open-loop control

An open-loop control system control the feeding pump directly based on given parameters and a process model. However, since there is no feedback the open-loop control system does not know whether its control is successful or not. In most fed-batch cultivations with open-loop control, the substrate feed rate $\dot{V}_F(t)$ is calculated by the process model in order to keep a constant specific growth rate of the cells. For Monod model, the substrate feed rate could be calculated from Eq. 1.5, by assuming a constant substrate concentration in the bioreactor ($\frac{dS}{dt} = 0$) (Eq. 1.7):

$$\dot{V}_F(t) = \mu_{max} \frac{S(t)}{K_m + S(t)} \frac{X(t)}{Y_{X/S}} \frac{1}{S_0 - S(t)} V_R(t) \qquad (1.7)$$

The numerically calculated substrate feed rate could be used for feeding control directly.

This strategy has been successfully used in various fed-batch cultivations (Jenzsch et al., 2006; Korz et al., 1995; Paalme et al., 1990). However, in order to get high quality control, initial values given to the Monod model especially initial biomass concentration must be precisely determined. Since small deviations of initial biomass concentration at the

beginning of the fed-batch phase will lead to significant errors at the end of the cultivation. Moreover, the control system can not detect or correct these errors due to the lack of feedback. Therefore, closed-loop control system is exploited in order to obtain a more accurate and robust control.

2.2.2.2 Closed-loop control

A closed-loop control system uses feedback signal from the on-line measurements of cultivation parameters for accurate control. The system compares the feedback signal with the set point and then adjusts the feeding pump accordingly.

Many important process variables can be used for indirect feedback control, such as pH value (Honda et al., 1998; Lee and Chang, 1993; Sugimoto et al., 1999) and dissolved oxygen concentration (Cutayar and Poillon, 1989; Konstantinov et al., 1990; Mori et al., 1979; Yang and Maa, 1998; Yano et al., 1991). In these strategies, the feed media is added when glucose is exhausted as shown by a sudden increase in dissolved oxygen concentration or pH value, which is also called DO-stat and pH-stat. However, the disadvantage of these strategies is the cultivation conditions are not stable. The cell states are kept changing between starvation and glucose availability since the feeding is non-continuous. Therefore, direct feedback control system was developed.

Direct feedback control system is more advanced than indirect feedback system. According to the feedback of current substrate concentrations in the reactor, the control system can calculate the amount of feed media to be delivered to the reactor in order to reach the substare set point. This type of control system has already been used in various fed-batch cultivations (Horn et al., 1996; Kleman et al., 1991; Sakamoto et al., 1994). However, the glucose concentrations in the culture broth are usually very low during the fed-batch phase. In most cases they are even lower than the detection limit of exsiting commercial on-line measurement devices. Therefore, robust and accurate on-line glucose measurement systems are required for high quality control. Direct feedback from on-line monitoring of acetate concentrations has also been applied in fed-batch cultivations by Shimizu et al.(1988) and Turner et al.(1994a). However, accurate on-line acetate measurement devices are also needed.

2.2.3 Flow injection analysis (FIA)

Flow injection analysis (FIA) technique was first introduced by Růžička and Hansen in 1975. It is based on "the injection of a liquid sample into a moving, nonsegmented continuous liquid carrier stream. The injected sample forms a zone, which is then transported toward a detector that continuously records the changes in absorbance, electrode potential, or other physical parameter resulting from the passage of the sample material through the flow cell" (Růžička and Hansen, 1975). Since that time, this automated system has been widely used in various aspects (Stewart, 1981; Trojanowicz, 2000). The principles and components of FIA are described in (Růžička and Hansen, 1988).

Different FIA systems have been developed for the on-line monitoring of glucose concentrations. Most of them are based on an enzymatic method using glucose oxidase (GOD) to catalyze the oxidation of *D*-glucose to H_2O_2 and *D*-glucono-*δ*-lactone. The latter one is then hydrolyzes to gluconic acid (Eq. 1.8). Thus, either the oxygen consumed in this reaction could be measured by an amperometric detector (Kumar et al., 2001; Male et al., 1997; Schügerl et al., 1991; Van Putten et al., 1996) or GOD is combined with peroxidase (POD) which can react with the formed H_2O_2, afterwards the glucose concentration can be measured colorimetrically (Benthin et al., 1992; Garn et al., 1989; Valero et al., 1990).

$$\text{Glucose} + O_2 + H_2O \xrightarrow{\text{GOD}} \text{Gluconic acid} + H_2O_2 \qquad (1.8)$$

In our institute, an automated FIA system has been developed for the on-line monitoring of bioprocess (Brandt and Hitzmann, 1994; Hitzmann et al., 1996; Hitzmann et al., 1997; Hitzmann et al., 1995). This system has been successfully applied in on-line monitoring of various cultivations (Umoh et al., 1996; Van Putten et al., 1995; Weigel et al., 1996).

2.2.4 Extended Kalman filter (EKF)

In 1960, R.E. Kalman described a recursive method for solving the process state estimation problem and afterwards it was named the Kalman filter. Since then, this powerful filter has been widely used in various aspects, such as linear state estimation, computer image recognition, satellite navigation and radar tracking (Sorenson, 1985). The mathematical

algorithm of Kalman filter was well elucidated by (Brown and Hwang, 1992; Jacobs, 1993; Kalman, 1960; Maybeck, 1979; Meinhold and Singpurwalla, 1983).

The extended Kalman filter (EKF) expands the application of Kalman filter into nonlinear area. EKF "can compensate for the missing process data by a prior knowledge about the process. At each individual time step when new measurement data become available, the EKF determines a new estimate from the data obtained one step before, the model prediction and the value determined from the measurements. The new estimate is a weighted average of these three data, where the EKF determines the weights from the reliabilities that are attributed to the measurement values, the measurement uncertainties, the model equations and the last estimate" (Gnoth et al., 2008). Therefore, the estimated values by EKF are closer to the actual values than the original measurement values. A detailed formulation of EKF can be found in (Analytic Sciences Corporation. Technical Staff and Gelb, 1974; Kopp and Orford, 1963; Lee and Ricker, 1994; Reif and Unbehauen, 1999).

EKF has been widely used in fermentation processes (Stephanopoulos and Park, 1991; Stephanopoulos and San, 1983), such as yeast cultivation (Bellgardt et al., 1986), *E. coli* cultivation (Dubach and Märkl, 1992; Hilaly et al., 1994) and cultivations of other organisms (Ghoul et al., 1991; Náhlík and Burianec, 1988; Weuster-Botz et al., 1997; Zhang and Su, 2002) even industrial production process (Wilson et al., 1998). In recent years, EKF is combined with fuzzy logic (Simutis et al., 1992), neural network (Liu, 1999), etc. for more sophisticated process control.

In our institute, an EKF control system has been established based on on-line measuring of glucose concentration using the FIA system (Hitzmann et al., 2000). It has been successfully used in fed-batch cultivation of yeast (Arndt and Hitzmann, 2004; Klockow et al., 2008) and *E. coli* (Arndt et al., 2005; Kleist et al., 2003) at different glucose concentration set points.

3. Optimization of polysialic acid production using different cultivation strategies

3.1 Introduction

3.1.1 Sialic acid

Sialic acid was first isolated from bovine submaxillary mucin as a saccharide-like component by Gunnar Blix in 1936. Till now, the sialic acid family has more than 50 members which are widely distributed in nature (Angata and Varki, 2002). Sialic acids play an important role in the chemical and biological diversity of glycoconjugates (Kelm and Schauer, 1997; Schauer, 1985; Schauer et al., 1982) and can also regulate many cellular and molecular interactions (Schauer, 2009). Moreover, different cell sialoglycosylation patterns could be found during cell development, aging and oncogenesis processes (Rosenberg, 1995).

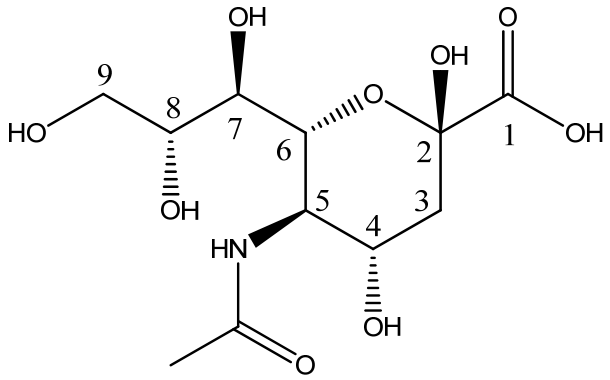

Fig. 3.1 Structure of *N*-acetyl-neuraminic acid (Neu5Ac).

N-acetyl-neuraminic acid (Neu5Ac, see Fig. 3.1) is the most extensively studied member in the sialic acid family. It is also considered to be the origin of other family members (Schauer, 1982). Therefore, "sialic acid" is also refers to Neu5Ac in the literature.

3.1.2 Polysialic acid

In 1957, Barry and Goebel (1957) first isolated colominic acid from the culture broth of *E. coli* K235. Later, Barry (1958) found that colominic acid was a polymer of Neu5Ac.

Further study revealed that colominic acid was a low-molecular-weight homopolymer of Neu5Ac (McGuire and Binkley, 1964). Polysialic acid (PSA) is a high-molecular-weight homopolymer which consists of sialic acids with up to 200 residues (Pelkonen et al., 1988; Rohr and Troy, 1980).

3.1.2.1 Structure

The most common structure of PSA is the Neu5Ac polymer with α2,8-linkage (Fig. 3.2).

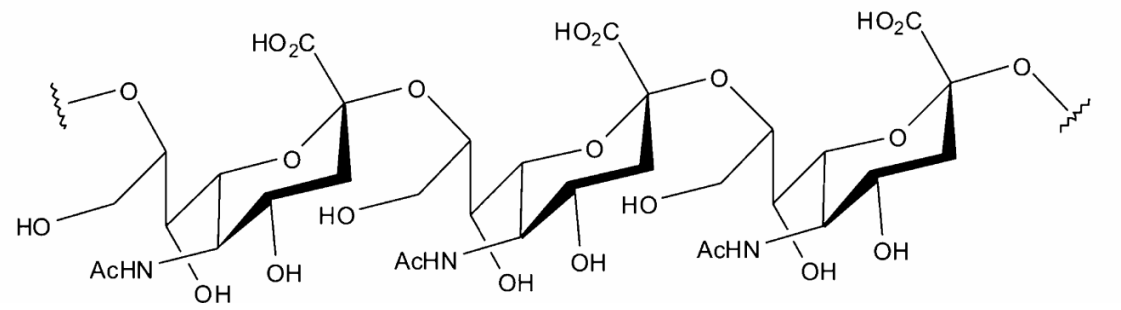

Fig. 3.2 Structure of α2,8-linked poly-5-*N*-acetyl-neuraminic acid. This figure has been adapted from Rode et al.(2008).

3.1.2.2 Biological functions and applications

PSA is the major macromolecular ingredient found in vertebrate brains (Finne, 1982) and plays an important role in the regulation of various cell contact interactions (Acheson et al., 1991). In the nervous system, PSA participates in various cell processes such as cell migration, axonal guidance and synaptogenesis (Bruses and Rutishauser, 2001). Moreover, neuronal regeneration could be induced in adult brain when PSA synthesis was reactived (El Maarouf et al., 2006).

PSA is a biodegradable polymer and its degradation products are non-toxic (Gregoriadis et al., 1993). Moreover, it is a biocompatible material and does not evoke immune response (Moreno et al., 1985). These properties make it very suitable to be used in drug delivery system (Gregoriadis et al., 2000).

Most recent studies demonstrate that PSA is a promising biomaterial for cell culture, tissue engineering and biomedical applications. Stark et al. (2008) used PSA as coating material to cultivate Hep-G2 and PC 12 cells. Same results were obtained comparing to

conventional coating materials (e.g. collagen I, hyaluronic acid and poly-*L*-lysine). Haile et al. (2007) cultivated glial and neuronal cells on PSA, good results were also obtained. Due to high solubility in water, PSA could not be used as biomaterial directly. Berski et al. (2008) have synthesized a hydrogel based on PSA and tested it as a scaffold material. They found this hydrogel can be controllably degraded by endosialidase and it was suitable as growth supporting material for PC 12 cells. Steinhaus et al. (2010) immobilized PSA on glass surfaces and found that it could aid nerve regeneration.

3.1.2.3 PSA of *E. coli*

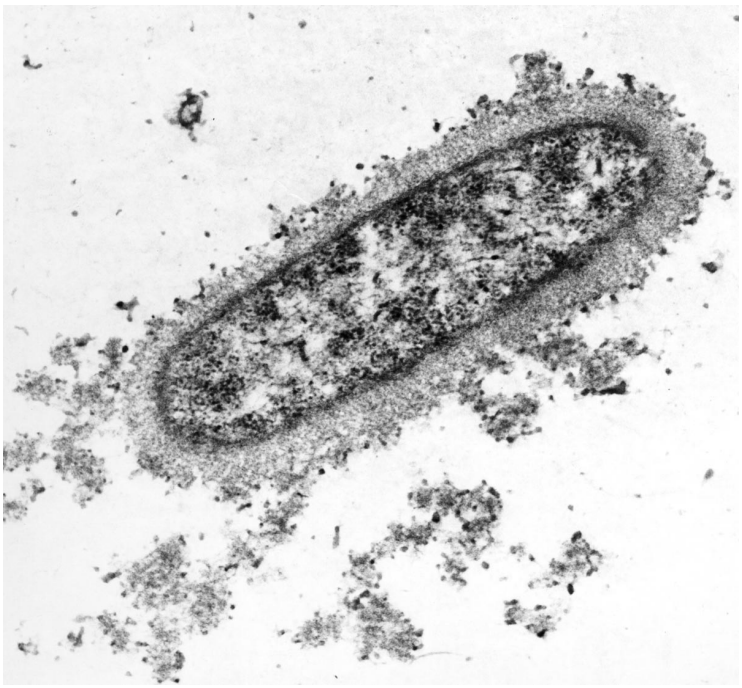

Fig.3.3 Transmission electron microscopy of *E. coli* K1. This figure has been adapted from Vimr et al.(2004).

PSA is produced by some bacteria as their capsules, such as *Neisseria meningitidis*, *E. coli*, group B *streptococci*, *Haemophilus ducreyi* and *Pasteurella hemolytica* (Mizanur and Pohl, 2008). In *E. coli* K1, the capsule PSA belongs to the group 2 bacterial capsules, which consists of linear homo α2,8-linked Neu5Ac residues (Whitfield, 2006). This capsule also covers the bacterial specific antigens and protects the bacteria from being recognized by the host immune system (Moxon and Kroll, 1990). The biosynthesis process of PSA in *E. coli*

K1 was well elucidated by Bliss and Silver (1996), Whitfield (2006) and Steenbergen and Vimr (2008). The pattern of *E. coli* K1 capsule is shown in Fig. 3.3.

3.1.2.4 Production

In nature, PSA only presents in several materials at a very low level, such as swallow's nests, whey from cheese production, chalaza and egg membranes (Kapre and Shaligram, 2010). Therefore it was mainly produced by microbial fermentation.

Several groups have studied the production of PSA with different bacterial strains. The early studies were mainly focused on optimizing medium and cultivation conditions. Orskov et al. (1984) and González-Clemente et al. (1990) found that PSA production was temperature regulated. Rodríguez-Aparicio et al. (1988) reported that PSA production in bacteria was depended on temperature as well as pH value and aeration of the medium. Zhan et al. (2002) cultivated *E. coli* K235 in batch and fed-batch cultivations with controlled pH value of 6.4, a PSA yield of 2,600 mg l^{-1} was obtained. However, they were using expensive sorbitol as carbon source. Liu et al. (2010) cultivated *E. coli* K235 by maintaining a sorbitol concentration around 20 - 40 g l^{-1} in the medium during the fed-batch phase, the final PSA concentration reached 5,399 mg l^{-1}. Kapre and Shaligram (2010) have also developed a process for the production and purification of PSA as described in a patent.

In our group, Rode et al. (2008) have established a biotechnological process for the production and purification of long chain PSA in *E. coli* K1. In this study, we are focusing on maximizing the efficiency of PSA production. For this purpose, different cultivation strategies were applied for the cultivation of *E. coli* K1and a comparison of PSA yield on glucose was performed.

This work was cooperated with Jinu John from the group of Bernd Hitzmann at the TCI.

3.2 Bacterial strain

A clinical isolated wild type strain *E. coli* B2032/82 serotype K1was used throughout this study. The strain was stored as a 50 % (v v^{-1}) glycerol stock at - 80 °C.

3.3 Experiments

3.3.1 Preculture and medium

A complex medium (Appendix 6.2.1.1) was used as preculture medium. The preculture was prepared by inoculating a glycerol stock into 100 ml medium in a 500 ml shaking flask and was subsequently incubated on a rotary shaker at 37 °C, 120 rpm for 10-12 h. Then it was directly used to inoculate the bioreactor. A synthetic medium was prepared according to Rode et al. (2008) and used for the batch and fed-batch cultivation of *E. coli* K1, as described in Appendix 6.2.1.2. The media were sterilized by autoclaving at 121 °C for 20 min.

3.3.2 Bioreactor cultivations

Cultivations were carried out at 37 °C in a stirred tank bioreactor with 2 l working volume (Bio-Stat® B, B. Braun Biotech, Melsungen, Germany) throughout this study. The initial culture conditions were the following: initial culture volume = 1.5 l (1.7 l for fed-batch cultivation at a constant glucose concentration of 0.1 g l^{-1}), air flow rate = 1.5 l min^{-1} (1.7 l min^{-1} for fed-batch cultivation at a constant glucose concentration of 0.1 g l^{-1}), pH value = 7.5, stirrer speed = 800 rpm. The pH value was maintained at 7.5 by addition of 10 % (w v^{-1}) NaOH. Automatic control of pH value, temperature and dissolved oxygen were done by the digital control unit of the bioreactor. The concentrations of oxygen and carbon dioxide in the exhaust gas were determined by Modularsystem S710 (SICK MAIHAK GmbH, Reute, Germany) gas analyzer. All the on-line measurement data were recorded by the RISP software (real-time integrating software platform, Institute for Technical Chemistry, Leibniz University of Hannover). Antifoam reagent (Desmophen VP PU 21lK01, Bayer MaterialScience AG, Leverkusen, Germany) was added when needed. Culture broth volume changes by off-line sampling were manually corrected by subtracting the sampling volume from the culture broth volume. The construction of bioreactor system is shown in Appendix 6.4. The concentrations of biomass, glucose and acetate in the reactor were determined as described in Appendix 6.3.1.

For fed-batch cultivations, during the fed-batch phase, the concentration of dissolved oxygen was kept constant at 30 % air saturation by adjusting the stirrer speed (0-

1,200 rpm). And the feeding solution was placed on a balance to record the consumption of glucose over time (density of glucose feeding solution was 1.0487 g cm^{-3}).

3.3.3 PSA determination

The PSA concentrations in all samples were determined using a modified thiobarbituric acid method described by Rode et al. (2008). The analytical procedure was described in Appendix 6.3.2.

3.3.4 Process modeling

3.3.4.1 Modeling of batch cultivation

A simple Monod model was used (Eq. 3.1-3.4) to modeling the batch cultivation. The oxygen limitation during the exponential growth phase was not considered.

$$\mu = \mu_{max} \frac{S(t)}{K_m + S(t)} \tag{3.1}$$

$$\frac{dX(t)}{dt} = \frac{\mu_{max} S(t)}{K_m + S(t)} X(t) \tag{3.2}$$

$$\frac{dS(t)}{dt} = -\frac{\mu_{max} S(t)}{K_m + S(t)} \frac{X(t)}{Y_{X/S}} \tag{3.3}$$

$$Y_{X/S} = \frac{\Delta X}{\Delta S} \tag{3.4}$$

Here, $X(t)$ – concentration of biomass at time t (g l^{-1});

$S(t)$ – concentration of substrate (glucose) at time t (g l^{-1});

μ_{max} – maximum specific growth rate (h^{-1});

K_m – Monod substrate saturation constant (g l^{-1});

μ – specific growth rate (h^{-1});

$Y_{X/S}$ – yield coefficient (g g^{-1}).

3.3.4.2 Modeling of fed-batch cultivation at a constant specific growth rate

To control the fed-batch cultivation, a process model based on the Monod model with limited substrate and for an ideal stirred tank bioreactor was developed using the following equations (Eq. 3.5-3.9):

$$\frac{dX(t)}{dt} = \frac{\mu_{max} S(t)}{K_m + S(t)} X(t) - \frac{\dot{V}_F(t)}{V_R(t)} X(t) \tag{3.5}$$

$$\frac{dS(t)}{dt} = -\frac{\mu_{max} S(t)}{K_m + S(t)} \frac{X(t)}{Y_{X/S}} + \frac{\dot{V}_F(t)}{V_R(t)} (S_0 - S(t)) \tag{3.6}$$

$$\mu = \mu_{max} \frac{S(t)}{K_m + S(t)} \tag{3.7}$$

$$\frac{dV_R(t)}{dt} = \dot{V}_F(t) \tag{3.8}$$

$$\dot{V}_F(t) = \mu_{max} \frac{S(t)}{K_m + S(t)} \frac{X(t)}{Y_{X/S}} \frac{1}{S_0 - S(t)} V_R(t) \tag{3.9}$$

Where, $\dot{V}_F(t)$ – feed rate at time t (l h^{-1});

$V_R(t)$ – culture volume at time t (l);

S_0 – substrate concentration of feed solution (g l^{-1});

The ordinary differential equations were solved numerically on-line by a MS-DOS program Neu-ork (Institute for Technical Chemistry, Leibniz University of Hannover) using the Runge-Kutta method of 4th order. To calculate the feed rate, a constant substrate concentration in the reactor was assumed ($\frac{dS}{dt} = 0$). Thus, Eq. 3.9 was obtained from Eq. 3.6. The estimated feed rate was directly used to control the feeding pump.

3.3.4.3 Modeling of fed-batch cultivation at a constant glucose concentration

For modeling the bioprocess, a process model was developed based on the Monod growth model and an ideal stirred tank bioreactor (Arndt et al., 2005). The process model consists of five ordinary differential equations (Eq. 3.10-3.14).

$$\frac{dX(t)}{dt} = \frac{\mu_{max} S(t)}{K_m + S(t)} X(t) - \frac{\dot{V}_F(t)}{V_R(t)} X(t) \quad (3.10)$$

$$\frac{dS(t)}{dt} = -\frac{\mu_{max} S(t)}{K_m + S(t)} \frac{X(t)}{Y_{X/S}} + (S_0 - S(t)) \frac{\dot{V}_F(t)}{V_R(t)} \quad (3.11)$$

$$\frac{d\mu_{max}(t)}{dt} = 0 \quad (3.12)$$

$$\mu = \mu_{max} \frac{S(t)}{K_m + S(t)} \quad (3.13)$$

$$\frac{dV_R(t)}{dt} = \dot{V}_F(t) - \dot{V}_S \quad (3.14)$$

Here, $\dot{V}_S$ – sample flow rate of the FIA system (l h^{-1}).

3.3.5 FIA system and EKF

A flow injection analysis (FIA) system was applied (Appendix 6.4.2) for the on-line measurement of glucose concentration in the culture broth. As a fast and accurate measurement system, FIA can measure a glucose concentration down to 0.02 g l^{-1} with a standard deviation of 0.0025 g l^{-1}. The response time was 3 minutes which made it suitable for on-line measurement. A sample module (Flownamics E19, IUL Instruments GmbH, Königswinter, Germany) with a ceramic membrane (pore size of 0.22 µm) was used to continuously take cell-free medium from the reactor (sample flow rate 36 ml h^{-1}). The samples (24 µl) were injected into the carrier stream and mixed with a glucose oxidase solution (36 µl, 500 U ml^{-1}), which was injected by a second injector. The amount of oxygen used to oxidize glucose was determined by an oxygen electrode (Anasyscon, Hannover, Germany), from which the glucose concentration was calculated. The control of the FIA system and the evaluation of the measurements were carried out by a computer program CAFCA (computer assisted flow control and analysis) (Hitzmann et al., 1995).

In order to minimize the glucose measurement noise and to estimate the biomass concentration, the maximum specific growth rate and the volume of the reaction broth, an extended Kalman filter (EKF) was applied (Arndt and Hitzmann, 2004) (Appendix 6.4.2). This program was running on a separate PC and received the glucose measurement data through a serial connection.

The Kalman filter not only provided estimated data of glucose concentration but also estimated data of biomass concentration, maximum specific growth rate and volume of the culture broth. The feeding pump rate was controlled based on these parameters and a PI (Proportional Integral) controller which was calculated using the following equations (3.15-3.17):

$$\dot{V}_F(t_i) = \dot{V}_{FF}(t_i) + \dot{V}_{FB}(t_i) \tag{3.15}$$

$$\dot{V}_{FF}(t_i) = \mu_{max}(t_i) \frac{S(t_i)}{K_m + S(t_i)} \frac{X(t_i)}{Y_{X/S}} \frac{1}{S_0 - S(t_i)} V_R(t_i) \tag{3.16}$$

$$\dot{V}_{FB}(t_i) = \dot{V}_{FB}(t_{i-1}) + q_0\big(S_{set} - S(t_i)\big) + q_1(S_{set} - S(t_{i-1})) \tag{3.17}$$

Here, $\dot{V}_F(t_i)$ – feed rate at time t_i (l h^{-1});

$\dot{V}_{FF}(t_i)$ – feed rate of feedforward part of the controller at time t_i (l h^{-1});

$\dot{V}_{FB}(t_i)$ – feed rate of feedback part of the controller at time t_i (l h^{-1});

S_{set} – substrate set point (g l^{-1}).

Eq. 3.16 was the feedforward part of the controller, which derived from Eq. 11 by assuming a constant glucose concentration in the reactor ($\frac{dS}{dt} = 0$). Eq. 3.17 is a digital PI controller; the parameters were obtained by simulation to be q_0= 1.4 l^2 g^{-1} h^{-1} q_1= -1.1 l^2 g^{-1} h^{-1}. If a negative pump rate was calculated by the controller, the pump rate would be set to zero and the digital PI part would be started again.

The parameters of extended Kalman filter were obtained by simulation (data not shown) and presented in Table 3.1. The system construction is shown in Fig. 3.4.

Table 3.1 Parameters of extended Kalman filter

Parameter	Name	Value
Q[1, 1]	Spectral density matrix element of process noise (respect to X)	0.001 g^2 $l^{-2}h^{-1}$
Q[2, 2]	Spectral density matrix element of process noise (respect to S)	0.001 g^2 $l^{-2}h^{-1}$
Q[3, 3]	Spectral density matrix element of process noise (respect to μ_{max})	0.05 l h^{-3}

Q[4, 4]	Spectral density matrix element of process noise (respect to V_R)	0	$l^2\ h^{-1}$
Q[i, j]	Spectral density matrix element of process noise ($i \neq j$)	0	
P[1, 1]	Initial condition of estimation error covariance (respect to X)	0.1	$g^2\ l^{-2}$
P[2, 2]	Initial condition of estimation error covariance (respect to S)	0.02	$g^2\ l^{-2}$
P[3, 3]	Initial condition of estimation error covariance (respect to μ_{max})	0.2	h^{-2}
P[4, 4]	Initial condition of estimation error covariance (respect to V_R)	0	l^2
P[i, j]	Initial condition of estimation error covariance ($i \neq j$)	0	
R	Measurement error covariance	0.01	$g^2\ l^{-2}$

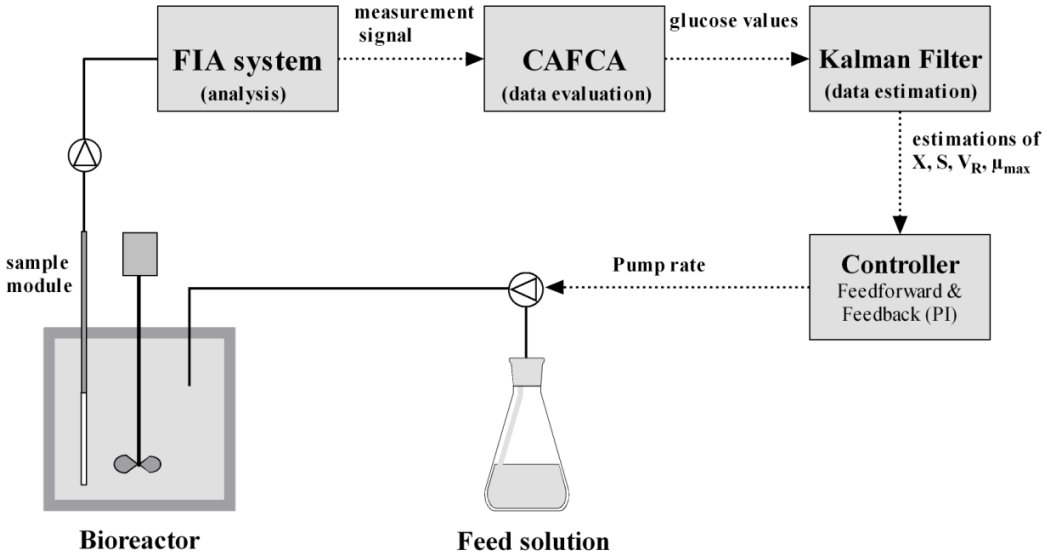

Fig.3.4 Flow chart of the control loop for keeping a constant glucose concentration in the culture broth.

3.4 Results

3.4.1 Batch cultivation of *E. coli* K1

A batch cultivation with an initial glucose concentration of 18 g l^{-1} was performed as the first step for studying the PSA production in *E. coli* K1. An overview of the cultivation process is illustrated in Fig. 3.5 and Fig. 3.6.

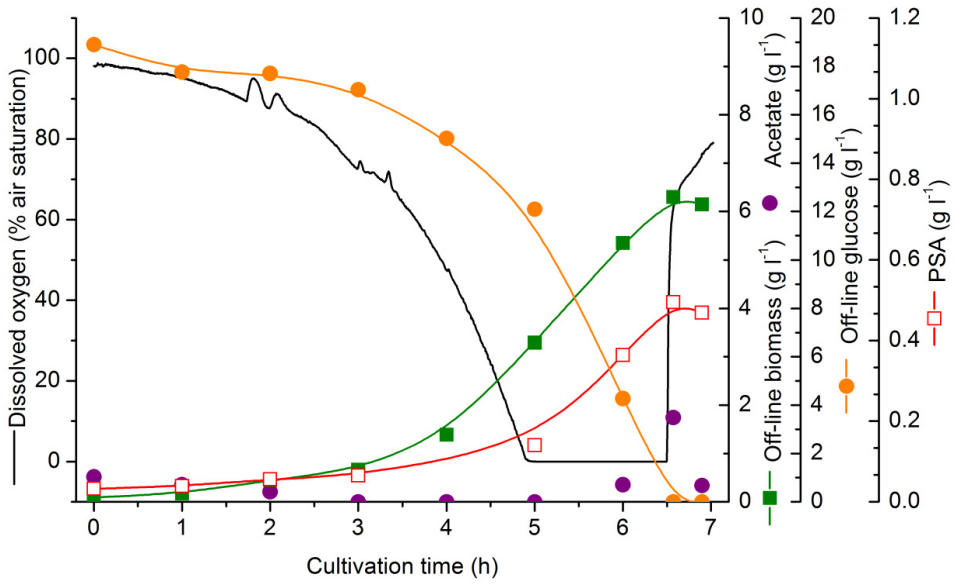

Fig. 3.5 Time profile of batch cultivation with an initial glucose concentration of 18 g l^{-1}.

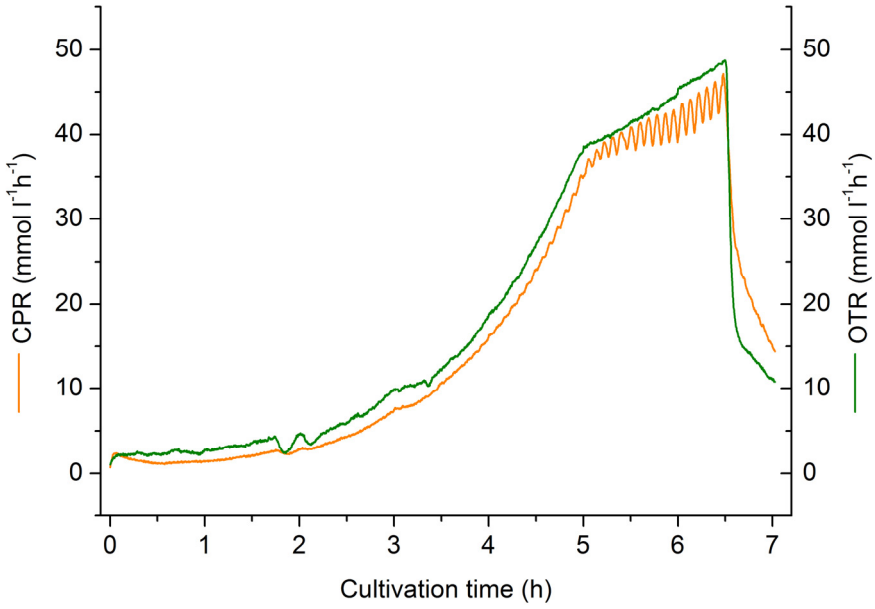

Fig. 3.6 OTR and CPR of the batch cultivation.

As shown in Fig. 3.5, during batch cultivation cells were grown at a high specific growth rate of approximately 0.7 h^{-1}. At 6.5 h, when glucose was exhausted, the highest acetate

level was reached (1.74 g l^{-1}) and afterward the acetate was consumed by the cells. The PSA production was consistent with the biomass formation pattern and the final PSA concentration was 0.47 g l^{-1}. After 4.9 h the reactor could not provide sufficient oxygen to the cells, which led to the decrease of dissolved oxygen concentration to zero. From this time onwards, OTR (oxygen transfer rate) and CPR (carbon production rate) (Fig. 3.6) (calculated according to the equations in Appendix 6.4.3) were also exhibiting another growth pattern, indicating that anaerobic respiration as well as aerobic oxidation occurred.

The oxygen transfer limitation, the high amount of acetate production and the low PSA productivity indicated that the batch cultivation was suboptimal. Therefore, fed-batch cultivations were exploited. Considering that the specific growth rate of 0.7 h^{-1} used in the batch cultivation was higher than the critical specific growth rate for acetate formation, a lower specific growth rate (0.25 h^{-1}) was tested in the following fed-batch cultivation.

3.4.2 Fed-batch cultivation at a controlled constant specific growth rate

In this fed-batch cultivation experiment, an open-loop control system was utilized. The feed rate was calculated on-line only based on the kinetic model. The system construction is described in Appendix 6.4.1.

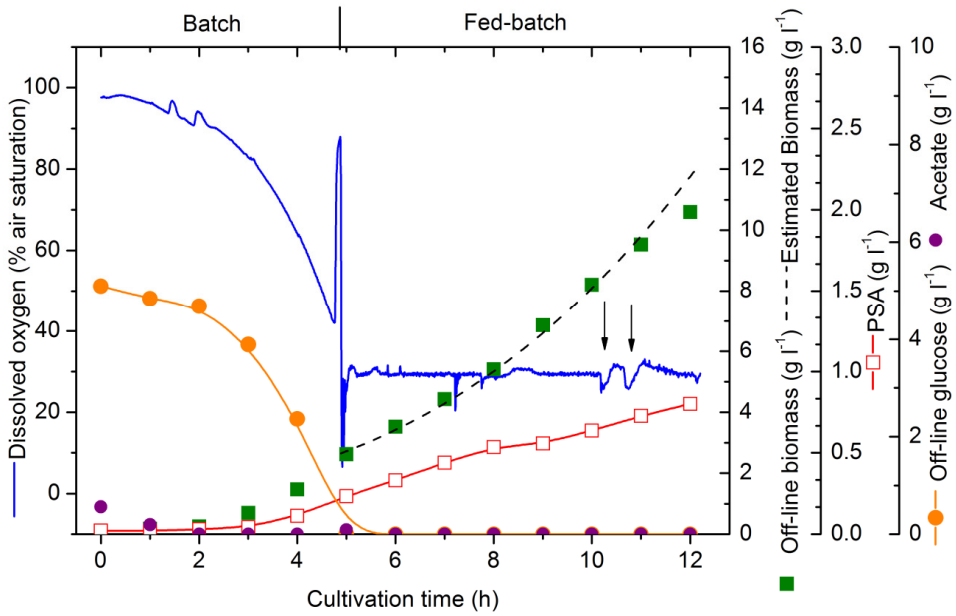

Fig.3.7 Time course of fed-batch cultivation at a constant specific growth rate of 0.25 h^{-1}. The arrows indicate the time when antifoam reagent was added.

This fed-batch cultivation was carried out at a specific growth rate set point of 0.25 h^{-1} in order to reduce acetate formation. The process profile is demonstrated in Fig. 3.7. The initial values of model parameters given to Neu-ork program are summarized in Table 3.2.

Table 3.2 Initial values given to the Neu-ork program for fed-batch cultivation of *E. coli* K1 at constant growth rate of 0.25 h^{-1}.

Parameters	$X(t_0)$ (g l^{-1})	$V_R(t_0)$ (l)	S (g l^{-1})	S_0 (g l^{-1})	$Y_{X/S}$ (g g^{-1})	K_m (g l^{-1})	μ_{set} (h^{-1})
Values	2.625	1.45	0.04	100	0.39	0.05	0.25

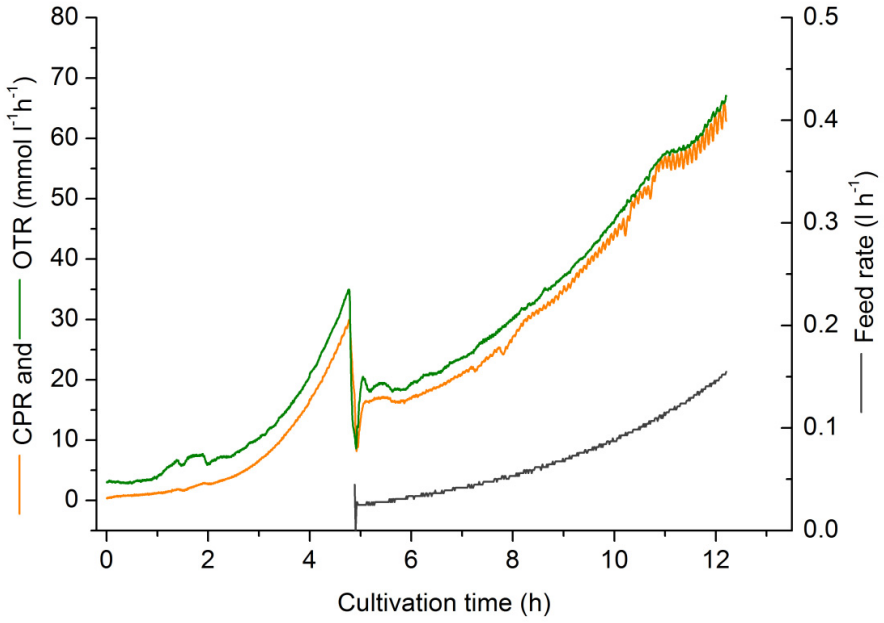

Fig. 3.8 OTR, CPR and feed rate of fed-batch cultivation at a constant specific growth rate.

As demonstrated in Fig. 3.7, after the unlimited growth in the batch phase (μ= 0.72 h^{-1}) until 4.9 h, the fed-batch phase was started at a specific growth rate of μ_{calc}= 0.24 h^{-1} (calculated from off-line measurements), which was very close to the set point (μ_{set}= 0.25 h^{-1}). During the fed-batch phase the dissolved oxygen was maintained at 30 % air saturation and no acetate formation was observed (Fig. 3.7); the glucose concentration in the culture broth was almost 0 g l^{-1} all the times. The estimated biomass values were consistent with the off-line biomass values until 11 h (Fig. 3.7). Beyond that point, a small

negative deviation of the determined biomass concentrations in comparison to the estimated values was observed. Perhaps the cells were not able to keep their growth on the growth rate set point at the end of the cultivation. The final biomass concentration was 10.6 g l^{-1} and the final PSA concentration reached 0.8 g l^{-1}. The OTR, CPR and feeding profile are shown in Fig. 3.8. The cultivation had to be stopped at 12 h since the culture volume (1.9 l) reached the maximum capacity of the reactor.

3.4.3 Fed-batch cultivations at controlled constant glucose concentrations

Although in the fed-batch cultivation described above no acetate was formed and a higher PSA concentration (0.8 g l^{-1}) was obtained, the cells were grown under glucose limitation during the whole feeding phase as it is a substrate limited feeding. Therefore, fed-batch cultivations with a constant glucose concentration in the culture broth were performed.

In this cultivation strategy, a feedforward/feedback closed loop control system was used. The feed rate was calculated based on the estimated values of the process variables. The construction of the cultivation system is described in Appendix 6.4.2.

3.4.3.1 Glucose concentration set point of 0.1 g l^{-1}

In this fed-batch cultivation, glucose limitation was avoided by keeping a constant glucose concentration of 0.1 g l^{-1} in the culture broth. The initial glucose concentration was 3 g l^{-1}. At 3.78 h the EKF software was started when the glucose concentration in the culture broth was 0.28 g l^{-1}. Thus, the feeding could be started immediately after the glucose concentration was below the set point and a starvation period between batch and fed-batch phase was therefore avoided. The initial values of model parameters given to EKF software are listed in Table 3.3.

Table 3.3 Initial values given to EKF software for fed-batch cultivation of *E. coli* K1 at a glucose set point of 0.1 g l^{-1}.

Parameters	$X(t_0)$ (g l^{-1})	$V_R(t_0)$ (l)	$S(t_0)$ (g l^{-1})	S_0 (g l^{-1})	$Y_{X/S}$ (g g^{-1})	K_m (g l^{-1})	$\mu_{max}(t_0)$ (h^{-1})
Values	0.99	1.69	0.28	100	0.30	0.01	0.40

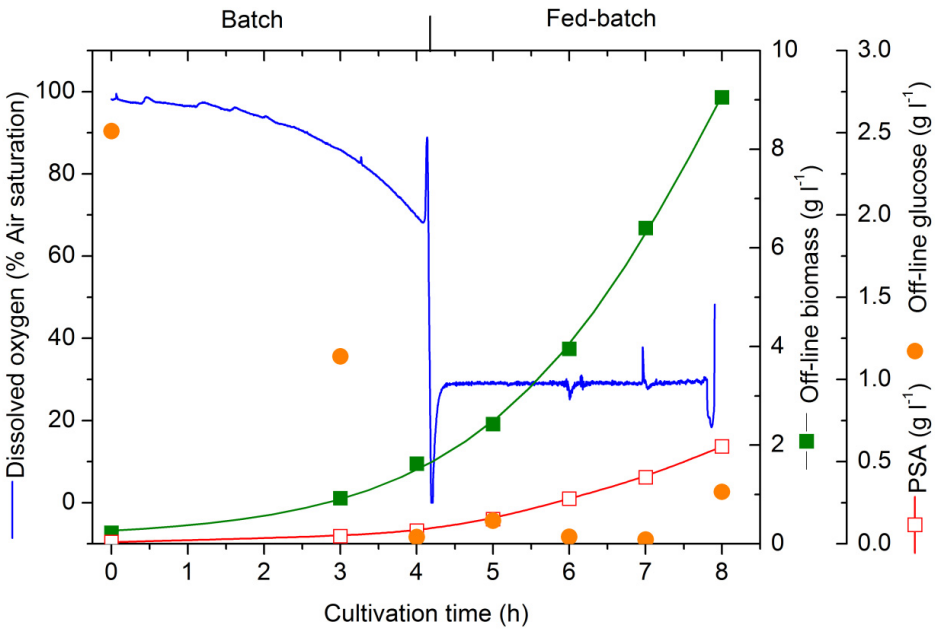

Fig. 3.9 Time profile of fed-batch cultivation at a constant glucose concentration of 0.1 g l^{-1}.

As shown in Fig. 3.9, the cell growth followed the Monod model and the dissolved oxygen concentration was kept at 30 % air saturation until 7.9 h. After that time, the dissolved oxygen concentration started to decrease because the stirrer speed was already at the maximum (1,200 rpm). Therefore, the cultivation has to be stopped at 8 h. Final biomass concentration obtained was 9.05 g l^{-1} and final PSA concentration reached 0.59 g l^{-1}. The CPR and OTR (Fig. 3.10) were kept increasing throughout the fed-batch phase.

As demonstrated in Fig. 3.11, after starting the system at 3.78 h the glucose concentration quickly reached the set point of 0.1 g l^{-1}. The EKF software switched on the feed pump after the measured glucose concentration was below 0.1 g l^{-1} (Fig. 3.10 and Fig. 3.11) and tried to control the glucose concentration at the set point. The control system was able to keep the glucose concentration at 0.1 g l^{-1} successfully during the fed-batch phase with an average value of 0.104 g l^{-1} and a standard deviation of 0.051 g l^{-1}. However, the off-line glucose concentrations were always lower than the on-line measured ones, this could be probably due to further consumption of glucose by the cells during sampling, although the samples were taken very quickly and kept on ice. The controller maintained the maximum

specific growth rate around 0.4 h^{-1} till 6 h, after that it increased to 0.49 h^{-1} and then came back to 0.4 h^{-1} at the end of the cultivation.

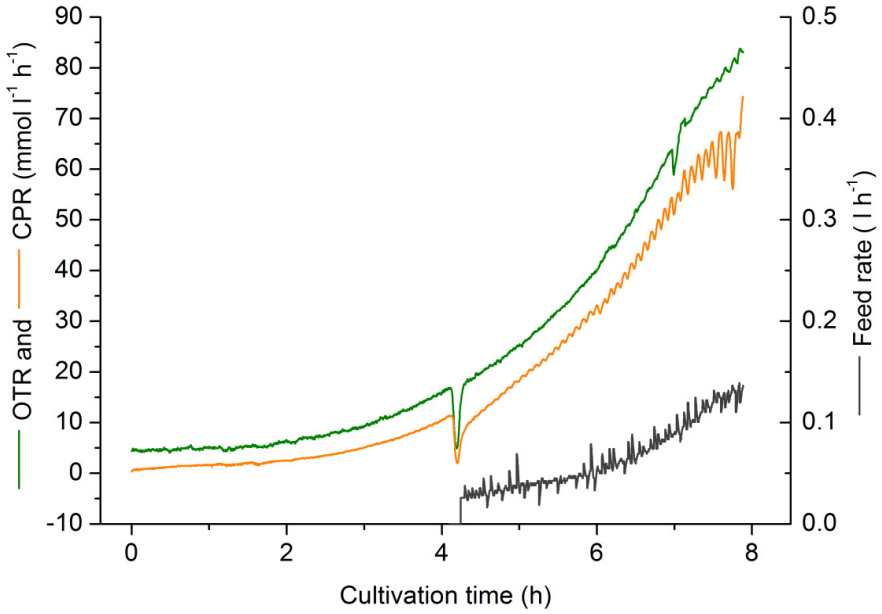

Fig.3.10 OTR, CPR and feed rate of fed-batch cultivation at a constant glucose concentration of 0.1 g l^{-1}.

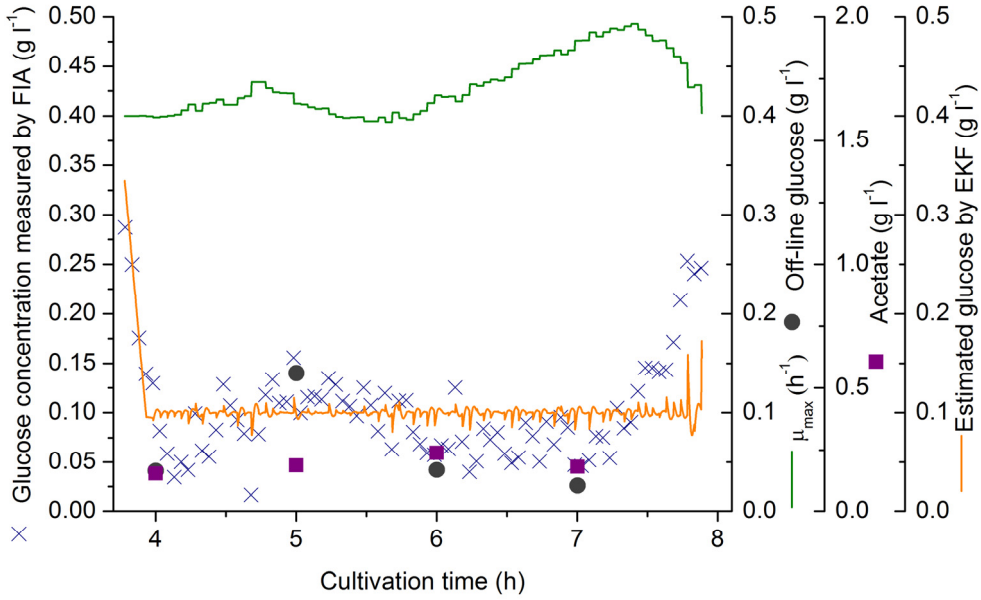

Fig.3.11 Estimated and measured glucose concentration, estimated maximum growth rate as well as acetate concentration during fed-batch cultivation of *E. coli* K1 at a glucose set point of 0.1 g l^{-1}.

During the fed-batch phase the acetate concentration was around 0.2 g l^{-1}, which was not negligible comparing to the cultivation at a constant specific growth rate of 0.25 h^{-1}, although it was still far away from the inhibitory concentration (> 2 g l^{-1}) (Lee, 1996).

Evaluating the whole process, the lower biomass and PSA concentrations and the not negligible acetate production showed that the glucose concentration set point of 0.1 g l^{-1} was not fully satisfied for PSA production. Therefore a lower glucose concentration set point of 0.05 g l^{-1} was tested.

3.4.3.2 Glucose concentration set point of 0.05 g l^{-1}

In this fed-batch experiment, a lower glucose concentration set point of 0.05 g l^{-1} was used. This set point was selected in order to minimize acetate production during the fed-batch phase. The initial glucose concentration was 5 g l^{-1}. The EKF control software was started at 4.85 h when glucose concentration in the bioreactor was 0.58 g l^{-1}. The initial values of process model parameters given to EKF software are listed in Table 3.4.

Table 3.4 Initial values given to the EKF software for fed-batch cultivation of *E. coli* K1 at a glucose set point of 0.05 g l^{-1}.

Parameters	$X(t_0)$ (g l^{-1})	$V_R(t_0)$ (l)	$S(t_0)$ (g l^{-1})	S_0 (g l^{-1})	$Y_{X/S}$ (g g^{-1})	K_m (g l^{-1})	$\mu_{max}(t_0)$ (h^{-1})
Values	2.45	1.50	0.58	100	0.375	0.01	0.32

As illustrated in Fig. 3.12, cells grew exponentially and the dissolved oxygen concentration was kept at 30 % air saturation. The final biomass which was obtained was 15.2 g l^{-1} and the final PSA concentration in the reactor was 1.35 g l^{-1}. Acetate formation was not observed during the fed-batch phase (Fig. 3.12). After 11 h, the reactor could not keep the dissolved oxygen concentration at 30 % air saturation, since the stirrer speed was already at maximum speed (1,200 rpm). Therefore the cultivation was stopped at 11.2 h. The CPR, OTR as well as flow rate of the feed solution were kept increasing in the fed-batch phase (Fig. 3.13).

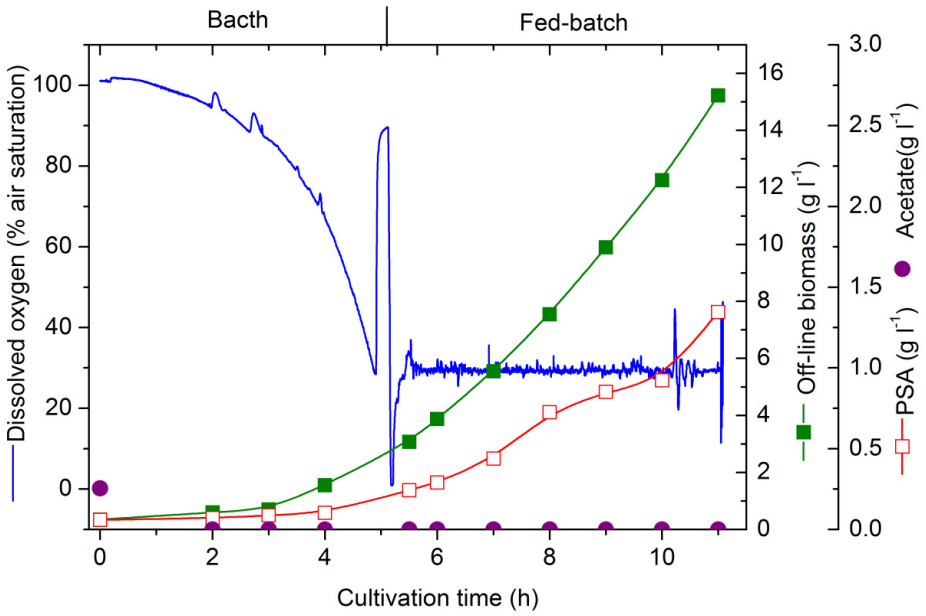

Fig.3.12 Time course of fed-batch cultivation at a constant glucose concentration of 0.05 g l^{-1}.

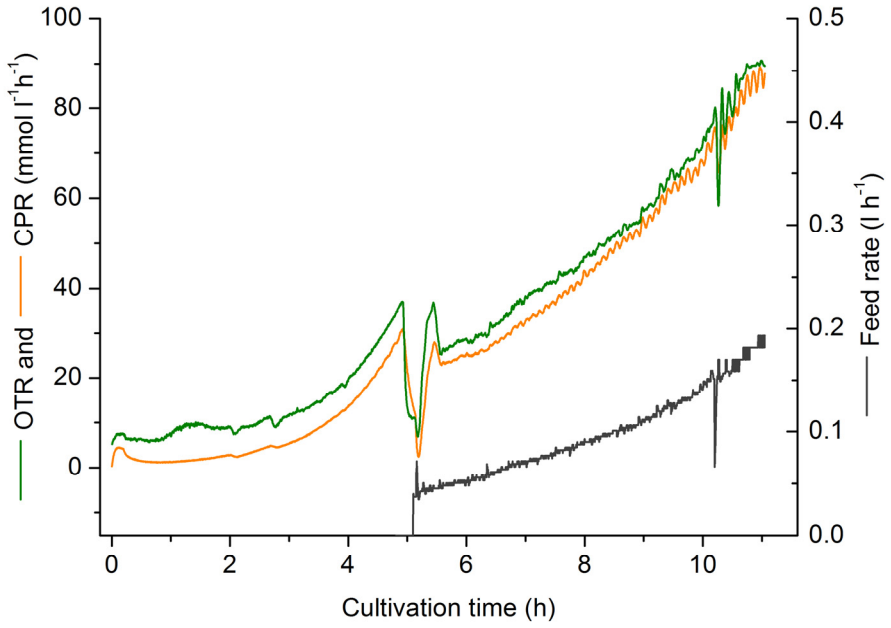

Fig.3.13 OTR, CPR and feed rate of fed-batch cultivation at a constant glucose concentration of 0.05 g l^{-1}.

After starting the EKF software at 4.85 h, the glucose concentration quickly reached the set point of 0.05 g l^{-1} (Fig. 3.14). The software switched on the feed pump immediately after

the measured glucose concentration was at the first time below 0.05 g l^{-1} (Fig. 3.13 and Fig. 3.14), and managed to control the glucose concentration at the set point. The average glucose concentration measured by FIA was 0.054 g l^{-1} with a standard deviation of 0.016 g l^{-1} during the fed-batch phase, which proved the control being successful.

The off-line glucose concentrations were always lower than the on-line measured ones, which was the same as in fed-batch cultivation at a constant glucose concentration of 0.1 g l^{-1}. The initial value of maximum specific growth rate given to the EKF software (0.32 h^{-1}) was lower than the actual value, so that the system suddenly increased the estimated growth rate to 0.38 h^{-1}. Afterwards the growth rate was decreasing very slowly throughout the feeding phase with an average value of 0.35 h^{-1} (Fig. 3.14).

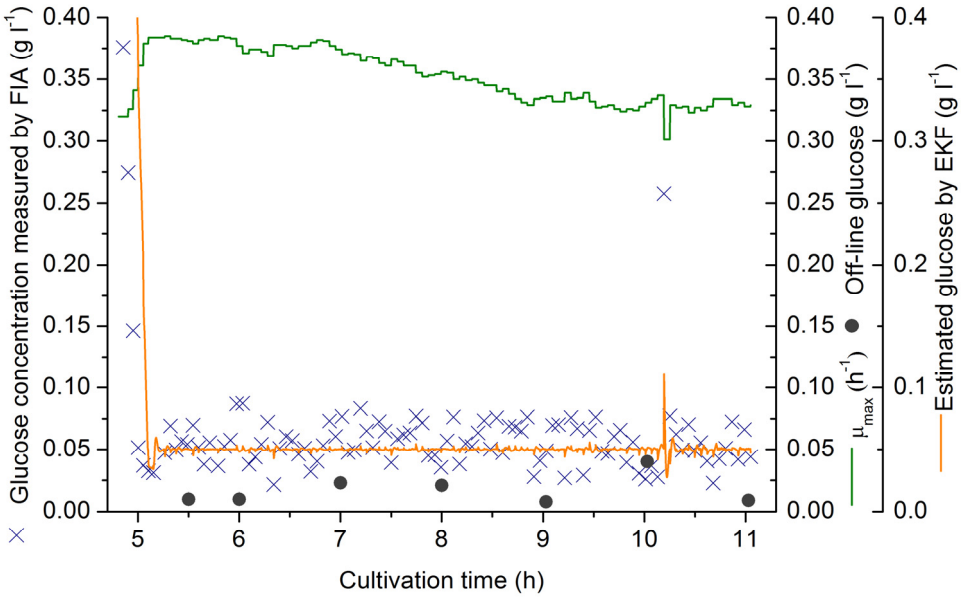

Fig.3.14 On-line, off-line measured and EKF estimated glucose concentrations as well as estimated maximum growth rate during the fed-batch at a glucose set point of 0.05 g l^{-1}.

An unusual high glucose concentration was obtained at 10.2 h (Fig. 3.14), which was most likely caused by an air bubble in the FIA system. As a consequence, the feeding rate was drastically decreased by the control system. The whole process was suddenly disturbed, as can be seen from all process variables. This effect was simply due to temporary problems in the analytical system. As soon as the analysis system stabilized again, the cultivation

process itself became stable immediately, suggesting that the whole control system was fault-tolerant in total.

Assessing the whole cultivation, at lower glucose concentration set point (0.05 g l^{-1}) the biomass concentration in the reactor reached 15.23 g l^{-1} and PSA concentration was 1.35 g l^{-1} after feeding for 6 h proved that it was more efficient than the higher glucose concentration set point (0.1 g l^{-1}).

3.4.4 Comparison of biomass and PSA productivity under different cultivation strategies

The biomass and PSA productivity under three different cultivation strategies are shown in Table 3.5 and 3.6. Compared to biomass and PSA yield on glucose ($Y_{X/S}$ and $Y_{P/S}$), fed-batch cultivations were higher than that of the batch cultivation. Since they avoided overflow metabolism (i.e. formation of acetate) and oxygen transfer limitation, the efficiency of the cultivation was significantly improved. The highest biomass yield obtained was 0.49 g g^{-1} with the highest PSA yield of 0.043 g g^{-1} in the fed-batch cultivation at a constant glucose concentration of 0.05 g l^{-1}.

Table 3.5 Comparison of biomass and PSA production in batch and fed-batch cultivations.

	μ_{esti} (h^{-1})	μ_{calc} (h^{-1})	Final Biomass concentration (g l^{-1})	Final PSA concentration (g l^{-1})	Time-space-yield of PSA (g l^{-1} h^{-1})
Batch		0.70	6.15	0.47	0.068
Fed-batch at a constant μ of 0.25 h^{-1}	μ_{esti}= 0.25	0.24	10.59	0.80	0.067
Fed-batch at a constant S of 0.1 g l^{-1}	μ_{max}= 0.43	0.46	9.05	0.59	0.074
Fed-batch at a constant S of 0.05 g l^{-1}	μ_{max}= 0.35	0.32	15.23	1.35	0.122

Table 3.6 Comparison of biomass and PSA yield on glucose in batch and fed-batch cultivations.

	$Y_{X/S}$ (g g^{-1})	$Y_{P/S}$ (g g^{-1})	$Y_{A/S}$ (g g^{-1})	PSA carbon yield ($C_{PSA}/C_{glucose}$) (%)
Batch	0.35	0.026	0.094	2.79
Fed-batch at a constant μ of 0.25 h^{-1}	0.38	0.035	0	3.71
Fed-batch at a constant S of 0.1 g l^{-1}	0.46	0.030	0.011	3.22
Fed-batch at a constant S of 0.05 g l^{-1}	0.49	0.043	0	4.63

3.5 Discussion

3.5.1 Acetate formation under different cultivation strategies

A common factor limiting the efficiency of *E. coli* cultivations is the formation of acetate. Studies in continuous cultures (Brown et al., 1985; Meyer et al., 1984) have revealed that the formation of acetate occurred when specific growth rate was above 0.35 h^{-1} in a defined medium or 0.2 h^{-1} in a complex medium.

In our previous study (Rode et al., 2008), we have cultivated *E. coli* K1 at a controlled specific growth rate of 0.35 h^{-1}. We found that the acetate production was significantly decreased (< 0.5 g l^{-1}) compared to the batch cultivation (> 1.6 g l^{-1}), but still could not be eliminated totally. In this study, we performed the fed-batch cultivation at a constant specific growth rate of 0.25 h^{-1} and could not detect any acetate accumulation during the feeding phase. This indicated that the growth rate of 0.35 h^{-1} was higher than the critical growth rate of acetate formation. While for fed-batch cultivations with a constant glucose concentration, at a growth rate of 0.32 h^{-1} there was no acetate produced during the fed-batch phase, even at a growth rate of 0.46 h^{-1} only about 0.2 g l^{-1} acetate was produced. Therefore, we assumed the threshold for acetate production varied with different cultivation strategies. The fed-batch cultivation at a constant glucose concentration gave better results than the fed-batch cultivation at a constant specific growth rate, since it provided better conditions for cell growth.

3.5.2 Comparison of biomass yield under different cultivation strategies

No acetate was observed in the fed-batch cultivation at a constant growth rate of 0.25 h^{-1}, thus a higher biomass yield was expected. However, since the efficient glucose concentration during the fed-batch phase was nearly zero, the glucose limitation might have forced the cells to use more energy for cell maintenance rather than for cell growth. This might be the main reason for the slightly different biomass yield on glucose between this cultivation (0.38 g g^{-1}) and the batch cultivation (0.35 g g^{-1}) even the PSA yield on glucose was slightly increased in the fed-batch process. This explanation was supported by the fact that the biomass yield on glucose increased in fed-batch cultivation with a constant glucose concentration of 0.1 g l^{-1} and 0.05 g l^{-1} (0.46 g g^{-1}, 0.49 g g^{-1} respectively). For fed-batch cultivation at a glucose concentration set point of 0.1 g l^{-1}, the biomass yield was a little bit lower than fed-batch cultivation at a glucose concentration set point of 0.05 g l^{-1} that might be at higher glucose set point the cells were growing too fast and around 0.2 g l^{-1} acetate was produced throughout the fed-batch phase while at lower glucose concentration set point (0.05 g l^{-1}) no acetate formation was detected. Therefore the highest biomass yield was obtained in fed-batch cultivation at a glucose concentration set point of 0.05 g l^{-1}.

3.5.3 Comparison of PSA yield under different cultivation strategies

As shown in Table 3.5 and Table 3.6, fed-batch cultivation strategies have greatly increased the PSA yield on glucose ($Y_{P/S}$). The final PSA concentration obtained from the fed-batch cultivation at a constant specific growth rate of 0.25 h^{-1} was nearly 2 times higher and at a constant glucose concentration of 0.05 g l^{-1} was nearly 3 times higher compared to that of the batch cultivation. While for the fed-batch cultivation at a constant glucose concentration of 0.1 g l^{-1} the final PSA concentration only increased 26 % compare to the batch cultivation. Comparing the two feeding strategies, the time-space-yield of fed-batch at a constant glucose concentration of 0.05 g l^{-1} was 82 % higher than the fed-batch cultivation at a constant specific growth rate of 0.25 h^{-1}. It is clear that maintain a very low glucose concentration in the reactor was more efficient for PSA production. Supposing we could extend the cultivation time by blending air with pure oxygen, a final PSA concentration up to 2 g l^{-1} should be possible.

3.5.4 Effect of specific growth rate on PSA production

It should be pointed out that the PSA yield on glucose ($Y_{P/S}$) was correlated to the specific growth rate of the cells. The relationship is plotted in Fig. 3.15. In the first place, the PSA yield on glucose increased according to the increase in the specific growth rate up to its maximum and then decreased. At extremely high specific growth rate (0.7 h^{-1}), which was obtained from the batch cultivation, the PSA yield on glucose was very low (0.026 g g^{-1}). However, at lower specific growth rate (0.24 h^{-1}) obtained from the fed-batch cultivation at a constant specific growth rate, the PSA yield was also relatively low (0.035 g g^{-1}). For the specific growth rate of 0.46 h^{-1}, the PSA yield on glucose was in between that of 0.7 h^{-1} and 0.24 h^{-1}. The maximal PSA yield on glucose (0.043 g g^{-1}) was obtained at a specific growth rate of 0.32 h^{-1} in the fed-batch cultivation at a constant glucose concentration of 0.05 g l^{-1}. These cultivation conditions were therefore considered to be the optimal conditions for PSA production in *E. coli* K1.

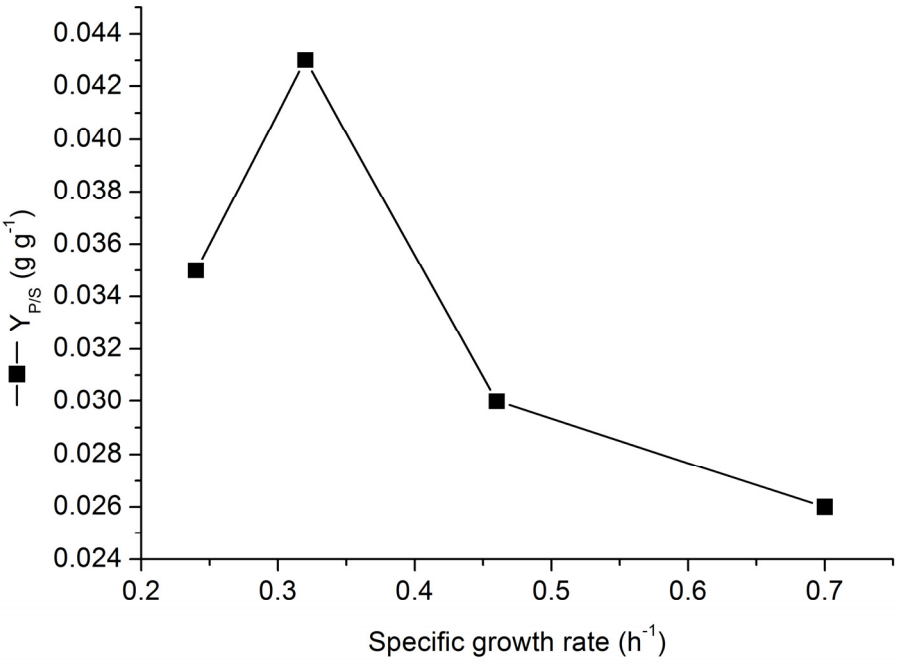

Fig. 3.15 Correlation of PSA yield to glucose at different specific growth rates.

3.6 Summary and conclusion

In this work, different cultivation strategies were used for the optimization of PSA production in *E. coli* K1. The preliminary study started with a batch cultivation and an

initial glucose concentration of 18 g l^{-1}. The results demonstrated that in the batch cultivation the cells were growing at an extremely high specific growth rate of 0.7 h^{-1} and giving a biomass yield on glucose of 0.35 g g^{-1}, PSA yield on glucose of 0.026 g g^{-1} with high amount of acetate up to 1.74 g l^{-1}.

In order to reduce acetate production, fed-batch cultivations were introduced. An exponential feeding strategy with a controlled constant specific growth rate of 0.25 h^{-1} was used. The results revealed that in the fed-batch cultivation acetate formation during the fed-batch phase was prevented. Biomass yield and PSA yield on glucose were increased to 0.38 g g^{-1} and 0.035 g g^{-1}, separately.

To overcome the glucose limitation in exponential feeding, a feedback/feedforward control system was used to keep a constant glucose concentration in the bioreactor. The system consisted of a FIA system for the on-line glucose measurement and an extended Kalman filter for the estimation and control of the bioprocess. Fed-batch cultivations were carried out at two different glucose set points 0.1 g l^{-1} and 0.05 g l^{-1}. At the glucose set point of 0.1 g l^{-1}, the biomass yield on glucose reached 0.46 g g^{-1} with PSA yield on glucose of 0.03 g g^{-1}. The specific growth rate was around 0.46 h^{-1} and non-ignorable 0.2 g l^{-1} acetate was produced throughout the fed-batch phase. While at the glucose set point of 0.05 g l^{-1}, the yield of biomass on glucose increased incredibly to 0.49 g g^{-1} and the PSA yield on glucose increased to 0.043 g g^{-1} with no detectable acetate formation during the fed-batch phase.

The cultivation experiments of *E. coli* K 1 with different strategies revealed that the PSA production was correlated to the specific growth rate of the cells. Fed-batch cultivation with a constant glucose concentration was the best cultivation condition for PSA production. The optimal specific growth rate for PSA production was 0.32 h^{-1}.

3.7 Outlook and future work

Future work could include scaling up of the fed-batch cultivation to 10 l and 30 l, blending air with pure oxygen to overcome the oxygen supply limitation, further optimization of

cultivation medium for high cell density cultivation and developing better FIA system for the on-line measuring of glucose concentration at even lower set points such as 0.01 g l^{-1}.

3.8 Acknowledgements

This work was part of the DFG research unit 548 “Polysialinsäure: Evaluation eines neuen Werkstoffs als Gerüstsubstanz für die Herstellung artifizieller Gewebe”.

4. Bench-scale production and purification of FGF-2

4.1 Introduction

4.1.1 FGF family and FGF-2

Fibroblast growth factors (FGFs) are a large family of cytokines which are widely distributed among various organisms. There are 22 members in the human FGF family and their structures are highly correlated (Ornitz and Itoh, 2001). FGFs have great affinity to heparin and they play an important role in cell proliferation, differentiation, survival and apoptosis (Böttcher and Niehrs, 2005).

1 10
Met Ala Ala Gly Ser Ile Thr Thr Leu Pro Ala Leu Pro Glu Asp Gly Gly

20 30
Ser Gly Ala Phe Pro Pro Gly His Phe Lys Asp Pro Lys Arg Leu Tyr Cys

40 50
Lys Asn Gly Gly Phe Phe Leu Arg Ile His Pro Asp Gly Arg Val Asp Gly

60
Val Arg Glu Lys Ser Asp Pro His Ile Lys Leu Gln Leu Gln Ala Glu Glu

70 80
Arg Gly Val Val Ser Ile Lys Gly Val Cys Ala Asn Arg Tyr Leu Ala Met

90 100
Lys Glu Asp Gly Arg Leu Leu Ala Ser Lys Cys Val Thr Asp Glu Cys Phe

110
Phe Phe Glu Arg Leu Glu Ser Asn Asn Tyr Asn Thr Tyr Arg Ser Arg Lys

120 130
Tyr Thr Ser Trp Tyr Val Ala Leu Lys Arg Thr Gly Gln Tyr Lys Leu Gly

140 150
Ser Lys Thr Gly Pro Gly Gln Lys Ala Ile Leu Phe Leu Pro Met Ser Ala

155
Lys Ser

Fig. 4.1 Primary sequence of human FGF-2.

FGF-2 was first isolated by Denis Gospodarowicz (1974) from pituitary and brain as a basic protein (pI of 9.6). Therefore it was named basic fibroblast growth factor (bFGF, FGF-2) and it was also the first member of the FGF family.

The FGF-2 as described in this work is a recombinant, human, non-glycosylated protein, consisting of 155 amino acids. The primary sequence of human FGF-2 is presented in Fig. 4.1.

4.1.2 Physicochemical properties

X-ray diffraction analysis revealed that FGF-2 is composed of 12 β strands connected by β turns (Eriksson et al., 1993; Eriksson et al., 1991; Zhang et al., 1991; Zhu et al., 1991). The Three-dimensional structure of FGF-2 is shown in Fig. 4.2.

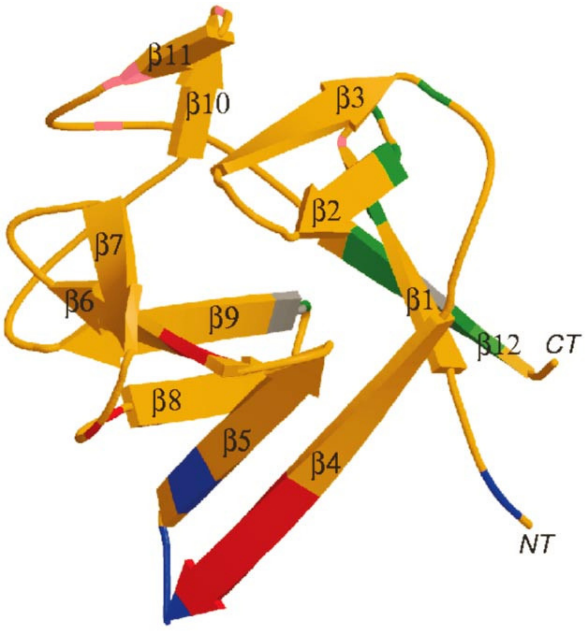

Fig. 4.2 Three-dimensional structure of FGF-2. A ribbon diagram of FGF-2 is shown and strands are labeled as β1-β12. The heparin-binding region (pink colored) includes residues in the loop between β strands 1 and 2 and in β strands 10 and 11. Residues contact with the FGFRs (fibroblast growth factor receptors) are shown in green (the region contacting Ig-domain 2 of the receptor), blue (contacting Ig-domain 3) and red (contacting the alternatively spliced region of Ig-domain 3). Amino acid residues that contact the linker region are shown in gray (Plotnikov et al., 2000). This figure has been adapted from Ornitz and Itoh (2001).

FGF-2 has two exposed cysteines (78 and 96) and two buried cysteines (34 and 101). The two exposed -SH groups can form disulfide-link when contacted with air, which makes the protein unstable (Thompson and Fiddes, 1991). Replacing the two cysteine residues (78 and 96) by serine residues can significantly improve its stability and bioactivity (Arakawa et al., 1989; Seno et al., 1988). FGF-2 only has a single tryptophan residue. The fluorescence from this tryptophan residue is completely suppressed in the properly folded protein and increases when the protein is unfolded (Shahrokh et al., 1994). Therefore, in the native protein the fluorescence emission spectrum is dominated by tyrosine fluorescence.

FGF-2 has a strong affinity to glycosaminoglycans (GAGs) such as heparin, heparin sulfate and heparan sulfate. Heparin can also protect FGF-2 from digestion by trypsin and inactivation by heat and acid (Gospodarowicz and Cheng, 1986). This feature was also utilized for the purification of FGF-2 (Garke et al., 2000; Iwane et al., 1987; Seeger and Rinas, 1996; Shing, 1988; Squires et al., 1988).

4.1.3 Biologic activity

FGF-2 is a potent mediator of cell proliferation and differentiation both *in vitro* and *in vivo* (Burgess and Maciag, 1989). It can stimulate the division of a variety of cells such as smooth muscle cells, fibroblasts, myoblasts and osteoblasts (Schweigerer, 1988). Moreover, FGF-2 can accelerate wound healing (Albertson et al., 1993; Tsuboi et al., 1992), tissue regeneration (Bikfalvi et al., 1997) and involves in the development or function of the nervous system (Baird, 1994; Logan et al., 1991), the lung (Han et al., 1992b; Sannes et al., 1992), the reproductive system (Murono et al., 1992), the skin (Halaban et al., 1992), the eye (McAvoy et al., 1991; Park and Hollenberg, 1993), the muscle and the skeleton (Fallon et al., 1994; Templeton and Hauschka, 1992) and the digestive system (Iida et al., 1994; Szabo et al., 1994).

4.1.4 Applications

4.1.4.1 Cell culture

FGF-2 was widely used in the cultivation of various cells, such as mesenchymal stem cells, embryonic stem cells (ESC), neural cells and endothelial cells. Since FGF-2 can maintain the cells in an undifferentiated state, it has been extensively used in human ESC culture

(Amit et al., 2000; Liu et al., 2006). In recent years, its application in tissue engineering has also been investigated (King et al., 2009; Macdonald et al., 2010; Marra et al., 2008; Nakamura et al., 2009; Pei et al., 2002).

4.1.4.2 Wound healing and tissue regeneration

Diabetics often have weakened wound healing, however, treating with FGF-2 could accelerate healing (Fiddes et al., 1991). FGF-2 can stimulates the healing of experimental duodenal ulcers in rats (Szabo et al., 1994) as well as diabetic foot ulcers (Bennett et al., 2003). It can also be used for the therapy of herpetic stromal keratitis (Kim et al., 2006) and reformation of periodontal tissues (Murakami et al., 1999). In addition, FGF-2 could assist the regeneration of alveolar bone in the treatment of periodontitis (Kitamura et al., 2008).

4.1.4.3 Other therapeutic potential

Chemoresistance is a main problem in cancer treatment. This resistance was regulated by acidic and basic fibroblast growth factors (Roidl et al., 2009; Song et al., 2000). Low level of suramin (inhibitor of FGFs) could reduce the FGF-induced resistance and increase the efficiency of chemotherapy (Song et al., 2001; Song et al., 2004; Xin et al., 2005; Zhang et al., 2001). Wang and Becker (1997) also reported that suppression of FGF-2 signaling can restrain tumor growth by inhibiting vascularization. FGF-2 has also been applied in the treatment of peripheral circulation and mood disorders (Beenken and Mohammadi, 2009).

4.1.5 Production and purification

Several purification processes have been established for the production of recombinant FGF-2 from *E. coli* in the past 20 years. They can be mainly classified into three types: (1) single step purification by heparin affinity chromatography (Ke et al., 1992; Squires et al., 1988). (2) combination of cation exchange column chromatography and heparin affinity chromatography (Iwane et al., 1987; Knoerzer et al., 1989; Patry et al., 1994; Seeger and Rinas, 1996; Wang et al., 2006). (3) combination of continuous bed or expanded bed chromatography and heparin affinity chromatography (Garke et al., 2000; Garke et al., 1999). However, these already existed processes have multiple disadvantages. During the first process, part of FGF-2 is lost which resulting in low protein recovery. In the second process, the used of cation exchange column chromatography has significantly improved

the protein recovery rate, but the long process time and subsequent dialysis step reduce the efficiency of the whole process. Although the use of continuous bed or expanded bed chromatography in the third process can treat cell lysate directly without separation, the binding capacity is lower or just comparable to that of cation exchange column chromatography. In addition, some authors have also produced FGF-2 from a fusion protein (Gasparian et al., 2009; Kroiher et al., 1995; Lappi et al., 1994; Lemaître et al., 1995; Sheng et al., 2003). However, extra cleavage step is needed to obtain FGF-2, which could lower down the protein yield. For these reasons, the methods described above are not cost-effective for large scale production of FGF-2.

4.1.6 Membrane adsorber technology

Membrane adsorbers have been extensively used for protein purification (Ghosh, 2002; Roper and Lightfoot, 1995; Thoemmes and Kula, 1995; Zeng and Ruckenstein, 1999). They consist of microporous or macroporous membranes which incorporate functional ligands in the inner pore surface as adsorbents. The transfer of fluid through the membrane is dominated by convective flow, while pore diffusion is prevented. That results in lower back pressure, higher flow rate, shorter resident time and higher productivity as compared to conventional chromatographic packed columns (Krause et al., 1991; Kubota et al., 1996). In this study, different membrane adsorbers were used for the efficient and cost-effective purification of FGF-2.

4.2 Bacterial strain

E. coli strain BL21(DE3) (Novagen, Darmstadt, Germany) transformed with the plasmid pET29c(+)-hFGF-2 which contains a cDNA encoding for human basic fibroblast growth factor (155 AA) was used in this study. The plasmid was constructed by the group of PD Dr. Ursula Rinas at HZI (Helmholtz Centre for Infection Research, Inhoffen Str. 7, 38124 Braunschweig) (Hoffmann et al., 2004), the FGF-2 coding sequence was previously described by Knoerzer et al. (1989). The strain was stored as a 50 % (v v^{-1}) glycerol stock at - 80 °C.

4.3 Cultivation and purification

4.3.1 Preculture and medium

A LB medium (see Appendix 6.2.2.1) supplemented with 30 µg ml^{-1} kanamycin was used as preculture medium. The preculture was incubated on a rotary shaker at 30 °C, 120 rpm for 12-14 h and then directly used to inoculate the bioreactor. A synthetic medium was prepared according to Seeger et al. (1995) and used for the fed-batch cultivation of *E. coli* BL21, as described in Appendix 6.2.2.2. The media were sterilized by autoclaving at 121 °C for 20 min except thiamine·HCl and kanamycin solution which were sterilized by filtration.

4.3.2 Bioreactor cultivation

Cultivations were carried out at 30 °C in a 2 l stirred tank bioreactor (Bio-Stat® B; B. Braun Biotech, Melsungen, Germany). The initial culture conditions were the following: initial culture volume = 1.5 l, air flow rate = 1.5 l min^{-1}, pH value = 6.9, stirrer speed = 800 rpm. The pH value was maintained at 6.9 by adding 25 % (w w^{-1}) ammonia solution. Automatic control of pH value, temperature and dissolved oxygen were done by the digital control unit of the bioreactor. The concentrations of oxygen and carbon dioxide in the exhaust gas were determined by Modularsystem S710 gas analyzer (SICK MAIHAK GmbH, Reute, Germany). All the on-line measurement data were recorded by the RISP software (real-time integrating software platform, Institute for Technical Chemistry, Leibniz University of Hannover). Antifoam reagent (Desmophen VP PU 21lK01, Bayer MaterialScience AG, Leverkusen, Germany) was added when needed. The diagram of the bioreactor system is shown in Appendix 6.4.1.

Off-line samples were taken approximately every hour and optical density was measured at 600 nm (OD_{600}) on a spectrophotometer (Uvikon 922; Kontron Instruments, Basel, Switzerland). The concentrations of biomass, glucose and acetate were determined as described in Appendix 6.3.1.

When the batch phase was finished, as indicated by a sudden increase in the dissolved oxygen concentration, the fed-batch phase was started. During the fed-batch phase, the

concentration of dissolved oxygen was kept constant at 30 % air saturation by adjusting the stirrer speed (0-1,200 rpm). A process model for keeping constant growth rate was used to control the feed flow rate. The feeding solution was placed on a balance to record the consumption of glucose over time (density of glucose feeding solution was 1.044 g cm^{-3}). Culture broth volume changes by off-line sampling were manually corrected by subtracting the sampling volume from the culture broth volume. The protein expression was induced by adding 1 mM IPTG when OD reached 15 as indicated in Fig. 4.3 and Fig. 4.5.

4.3.3 Bioprocess model

To control the fed-batch cultivation, a process model was developed based on the Monod model with limited substrate and an ideal stirred tank bioreactor (see section 3.3.4.2).

4.3.4 Fed-batch cultivations of *E. coli* BL21at different specific growth rates

Fed-batch cultivations were carried out at two different specific growth rates (0.35 h^{-1}, 0.15 h^{-1}) in order to study the effect of preinduction specific growth rate on recombinant product formation. The cells firstly grew at a constant specific growth rate-μ_{set} in the fed-batch phase until OD reached 15 and then the protein production was induced by adding 1 mM IPTG to the reactor.

4.3.4.1 Fed-batch cultivation of *E. coli* BL21 at μ_{set} = 0.35 h^{-1}

An initial glucose concentration of 4 g l^{-1} was used in the fed-batch cultivation and the overview of the production process is presented in Fig. 4.3. The initial values of model parameters given to the Neu-ork program are summarized in Table 4.1.

Table 4.1 Initial values given to the Neu-ork program for fed-batch cultivation of *E. coli* BL21 at a constant growth rate of 0.35 h^{-1}.

Parameters	$X(t_0)$ (g l^{-1})	$V_R(t_0)$ (l)	S (g l^{-1})	S_0 (g l^{-1})	$Y_{X/S}$ (g g^{-1})	K_m (g l^{-1})	μ_{set} (h^{-1})
Values	1.75	1.45	0.04	100	0.41	0.05	0.35

After unlimited growth in the batch phase (μ = 0.39 h^{-1}), as indicated by a sharp increase in dissolved oxygen concentration, the fed-batch phase was started at a specific growth rate of

μ_{calc} = 0.34 h^{-1} (μ_{set} = 0.35 h^{-1}) as shown in Fig. 4.3. The FGF-2 production was induced by adding 1 mM IPTG to the reactor at 9.2 h when OD reached 15 (Fig. 4.3). The OTR and CPR was calculated according to the equations in Appendix 6.4.3 and shown in Fig. 4.4.

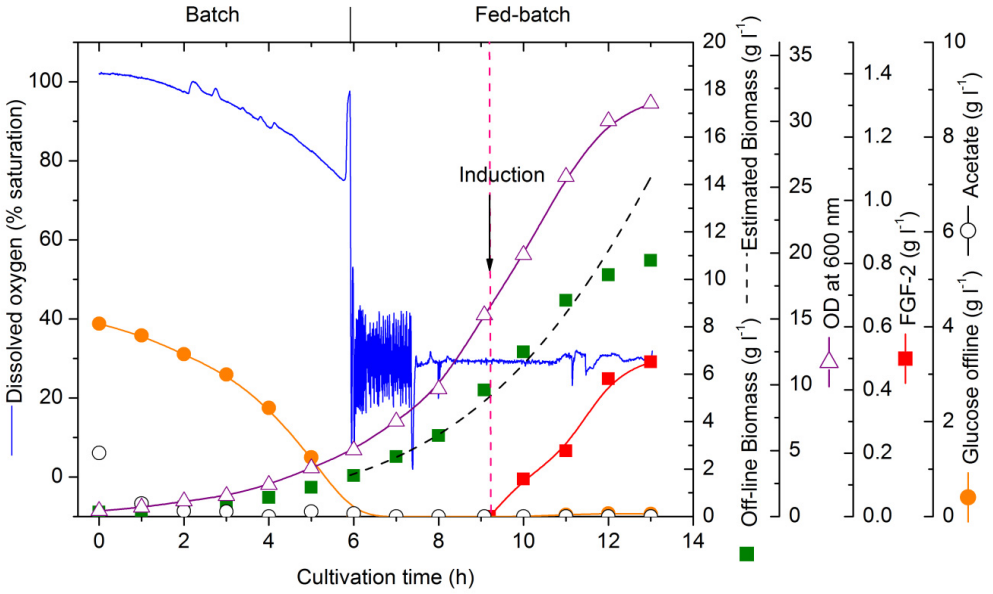

Fig. 4.3 IPTG induced FGF-2 production during Fed-batch cultivation of *E. coli* at a constant growth rate of μ_{set} = 0.35 h^{-1}. The disturbance in dissolved oxygen concentration at about 11.4 h was caused by the adding antifoam reagent.

E. coli BL21 strain was known to produce little acetate even at high growth rates (Shiloach et al., 1996). During the fed-batch phase the acetate concentrations were less than 0.15 g l^{-1} (Fig. 4.3) which were far away from the inhibitory concentration (> 2 g l^{-1}) (Lee, 1996). A high concentration of acetate (1.34 g l^{-1}) at the beginning of the cultivation came from the preculture (Fig. 4.3).

During the fed-batch phase the dissolved oxygen concentration was maintained at 30 % air saturation and glucose concentrations in the bioreactor were always near 0 g l^{-1} (Fig. 4.3). The estimated biomass values were agreed with off-line biomass values until 11 h and after that a negative deviation was observed (Fig. 4.3). OTR, CPR kept increasing until 10.8 h and feed flow rate kept increasing throughout the fed-batch phase (Fig. 4.4). Final biomass

concentration reached 10.8 g l^{-1} and final FGF-2 concentration in the reactor was 0.489 g l^{-1} (estimated as described in Appendix 6.3.3.2).

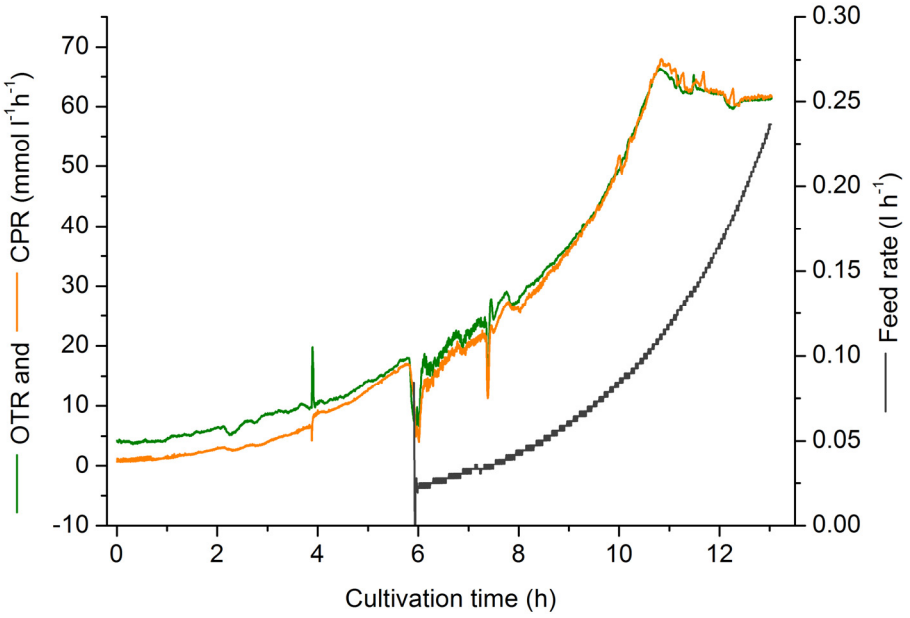

Fig. 4.4 OTR, CPR and feed rate during fed-batch cultivation of *E. coli* BL21 at a constant specific growth rate of $\mu_{set} = 0.35\ h^{-1}$.

4.3.4.2 Fed-batch cultivation of *E. coli* BL21 at $\mu_{set} = 0.15\ h^{-1}$

This fed-batch cultivation was started with an initial glucose concentration of 3.5 g l^{-1}. The process profile is presented in Fig. 4.5. The initial values of model parameters given to the Neu-ork program are listed in Table 4.2.

Table 4.2 Initial values given to the Neu-ork program for fed-batch cultivation of *E. coli* BL21 at constant growth rate of 0.15 h^{-1}.

Parameters	$X(t_0)$ (g l^{-1})	$V_R(t_0)$ (l)	S (g l^{-1})	S_0 (g l^{-1})	$Y_{X/S}$ (g g^{-1})	K_m (g l^{-1})	μ_{set} (h^{-1})
Values	1.48	1.45	0.04	100	0.40	0.05	0.15

As illustrated in Fig. 4.5, after unlimited growth in the batch phase ($\mu = 0.44\ h^{-1}$), the fed-batch phase was started at a specific growth rate of $\mu_{calc} = 0.13\ h^{-1}$ ($\mu_{set} = 0.15\ h^{-1}$). The FGF-2 production was induced by adding 1 mM IPTG to the reactor at 15.2 h when OD

reached 15 (Fig. 4.5). The OTR and CPR during the fed-batch cultivation are shown in Fig. 4.6.

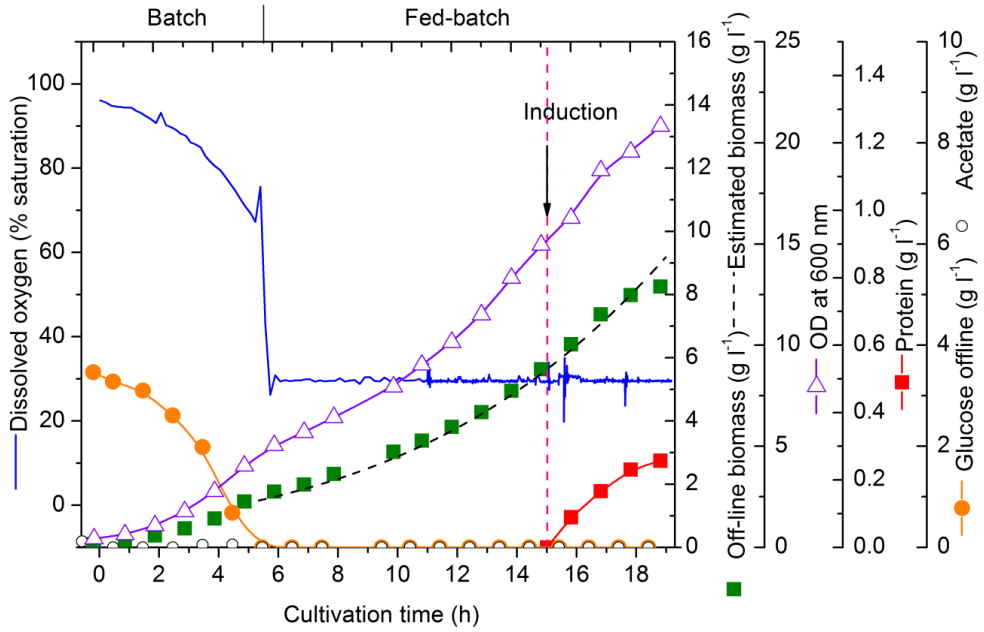

Fig. 4.5 IPTG induced FGF-2 production during Fed-batch cultivation of *E. coli* at a constant growth rate of $\mu_{set} = 0.15\ h^{-1}$.

During the fed-batch phase the dissolved oxygen concentration was maintained at 30 % air saturation and glucose concentrations in the bioreactor were always about 0 g l^{-1} (Fig. 4.5). The estimated biomass values were agreed with off-line biomass values until 18 h and after that a small negative deviation was observed (Fig. 4.5). Acetate concentrations in the fed-batch phase were always 0 g l^{-1} (Fig. 4.5). OTR, CPR and feed rate kept increasing in the fed-batch phase (Fig. 4.6). The final biomass concentration reached 8.25 g l^{-1} and final FGF-2 concentration in the reactor was 0.257 g l^{-1} (estimated as described in Appendix 6.3.3.2).

In the first 3.5 h of the fed-batch phase, the feed flow rate fluctuated between the minimum feed rate and 0 l h^{-1}(Fig. 4.6), that might because the initial biomass concentration of the fed-batch phase was too low, therefore the calculated feeding pump rate was sometimes lower than the minimum pump rate and the pump was switching between off and the

minimum pump rate. But the increase in biomass concentration raised the demand for glucose so that the feed flow rate kept increased after 9 h.

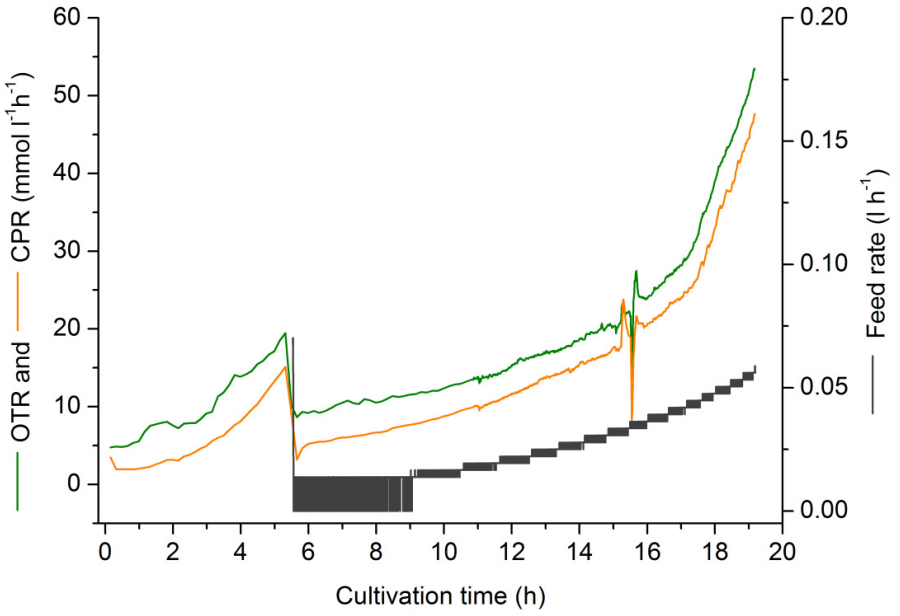

Fig. 4.6 OTR, CPR and feed rate during fed-batch cultivation of *E. coli* BL21at a constant specific growth rate of $\mu_{set} = 0.15\ h^{-1}$.

4.3.4.3 Comparison of biomass and FGF-2 production at different growth rates

At the higher specific growth rate (0.35 h^{-1}), the final biomass and FGF-2 concentrations were both higher than that at lower specific growth rate (0.15 h^{-1}) (Table 4.3). However, more soluble FGF-2 fractions (about 13 %) were obtained at the lower specific growth rate (0.15 h^{-1}) (Table 4.3). This indicated lower specific growth rate might be better for the proper folding of FGF-2.

Table 4.3 Comparison of biomass and protein production at different specific growth rates

μ_{set} (h^{-1})	Final biomass (g l^{-1})	Final FGF-2 concentration[a] (mg g^{-1} dry cell)	Soluble FGF-2 to total FGF-2[a] (%)
0.35	10.8	42	46
0.15	8.25	31	59

[a] estimated by gel densitometry.

As shown in Table 4.4, the biomass yields were nearly the same at both growth rates before induction (0.48 g g^{-1} and 0.47 g g^{-1} for μ_{set} = 0.35 h^{-1} and μ_{set} = 0.15 h^{-1}, respectively) but both decreased drastically after induction (0.28 g g^{-1}, 0.35 g g^{-1} respectively), which demonstrated that protein expression has significantly affected the cell growth. However, the biomass yield on glucose was higher at μ_{set} = 0.15 h^{-1} (0.42 g g^{-1}) indicated that the cells using glucose more efficiently.

This explanation was supported by the respiratory quotient (RQ) value (see Appendix 6.4.3), at μ_{set} = 0.35 h^{-1} the RQ value was 0.99, very close to the theoretical RQ value of glucose (RQ = 1). However, at μ_{set} = 0.15 h^{-1} the RQ value was only 0.89 which indicated the metabolic direction has changed at lower growth rate. The cells utilized oxygen but produced less carbon dioxide, in other words, they converted more glucose to biomass rather than carbon dioxide via pure metabolic oxidation.

Table 4.4 Comparison of biomass yield on glucose at different specific growth rates

μ_{set} (h^{-1})	$Y_{X/S}$ (g g^{-1})	$Y_{X/S}$ (g g^{-1}) before induction	$Y_{X/S}$ (g g^{-1}) After induction till end
0.35	0.33	0.48	0.28
0.15	0.42	0.47	0.35

Table 4.5 Comparison of protein yield on glucose and biomass at different specific growth rates

μ_{set} (h^{-1})	Yield(total protein/glucose) (g g^{-1})	Yield (Soluble protein/ glucose) (g g^{-1})	Yield (Soluble protein/ biomass) (g g^{-1})	Time-space yield of soluble protein[a] (g l^{-1} h^{-1})
0.35	0.014	0.0065	0.019	0.056
0.15	0.012	0.0070	0.018	0.038

[a] Calculated only for the production phase (after induction till end of the cultivation).

For protein yield, the yield of soluble protein on biomass was nearly the same at two different growth rates (Table 4.5). While at μ_{set} = 0.15 h^{-1} the yield of soluble protein on glucose increased a little bit comparing to that at μ_{set} = 0.35 h^{-1} (Table 4.5).

But for the time-space yield of soluble protein, at μ_{set} = 0.35 h^{-1} was 47.3 % higher than that at μ_{set} = 0.15 h^{-1}. Since the protein production rate was very high at μ_{set} = 0.35 h^{-1}, more soluble protein were produced in a given period of 4 h, although the soluble protein fractions were less than that of μ_{set} = 0.15 h^{-1}. Besides, using higher growth rate not only can save time, but also save the cost for maintaining the cultivation system and labor work. Therefore, the specific growth rate of 0.35 h^{-1} was selected to be the better condition for FGF-2 production.

4.3.4.4 Effect of specific growth rate on FGF-2 production

Specific growth rate can affect recombinant product yield, although it was quite case specific. For example, Riesenberg et al. (1990) reported that interferon alpha 1 productivity was higher when the specific growth rate was relatively low (0.15 h^{-1}) in fed-batch cutivations. While Curless et al. (1990) found that *E. coli* produced recombinant alpha consensus interferon more efficiently when the preinduction specific growth rate increased from 0.025 h^{-1} to 0.2 h^{-1}. However, Hellmuth et al. (1994) and Park et al. (1990) considered there should be an optimal cell growth rate, at which the maximum protein productivity could be obtained. Moreover, Zabriskie et al. (1987) found that there was no relationship between preinduction cell growth rate and recombinant malaria antigen productivity.

In this study, FGF-2 expression level was increased with the increase in specific growth rate (31 and 42 mg g^{-1} dry cell, for μ_{set}= 0.15 and 0.35 h^{-1}, respectively). Sandén et al. (2003) investigated the limiting factors of recombinant *β*-galactosidase production in *E. coli* at different specific growth rates. They predicted that at higher specific growth rates (e.g. 0.5 h^{-1}) the protein production was transcription limited while at lower specific growth rates (e.g. 0.1 h^{-1}) it was substrate limited. Therefore, I considered there was an optimal specific growth rate for FGF-2 production. As it was well known that at even higher specific growth rates (e.g. 0.5 h^{-1}), loss of plasmids and degradation of ribosome would reduce the protein synthetic capacity (Dong et al., 1995b), while at even lower specific growth rates (e.g. 0.05 h^{-1}), cell starvation and endogenous metabolism would also lower the productivity of recombinant protein. However, further experiments on the ribosome content, plasmid stability at different growth rates are needed to prove this hypothesis.

4.3.4.5 Comparison of cell growth rates after induction

As shown in Fig. 4.3 and 4.5, the estimated biomass concentrations were consistent with off-line biomass concentrations before induction, which demonstrated the open-loop control system was effective in controlling the specific growth rates at the set values. But after induction the off-line biomass concentrations started to deviate from the estimated biomass concentrations. This was due to the cells were not able to keep their growth on the growth rate set point since over-expression of FGF-2 imposed metabolic burden on the cells. As shown in Table 4.6, the specific growth rates after induction were drastically decreased at both growth rate set points, therefore the cells were harvested at 4 h after induction.

Table 4.6 Specific growth rates after induction at different growth rates

Cultivations	Specific growth rate after induction (h^{-1})		
	2 h after induction	3 h after induction	4 h after induction
$\mu_{set} = 0.35\ h^{-1}$	0.319	0.175	0.156
$\mu_{set} = 0.15\ h^{-1}$	0.148	0.097	0.057

4.3.5 Downstreaming and purification

Since soluble FGF-2 fraction was about 50 % (46 % and 59 %, respectively, as estimated by gel densitometry) of the total protein expressed, the downstreaming process was designed to isolate FGF-2 from the soluble protein fractions. Since the downstreaming processes for the two cultivations were the same, only the downstreaming processes of the cultivation with a constant specific growth rate of 0.35 h^{-1} are discussed here.

Part of the optimization of the downstreaming and purification process was done by my Diplom student Yangxi Zhao (2008). The purification processes described here is based on the optimized conditions. The flow chart of whole downstreaming and purification process is presented in Fig 4.7. It is clear that by using membrane adsorbers, we can produce bioactive FGF-2 in just 12 steps. The detailed downstreaming and purification processes are described in the following sections.

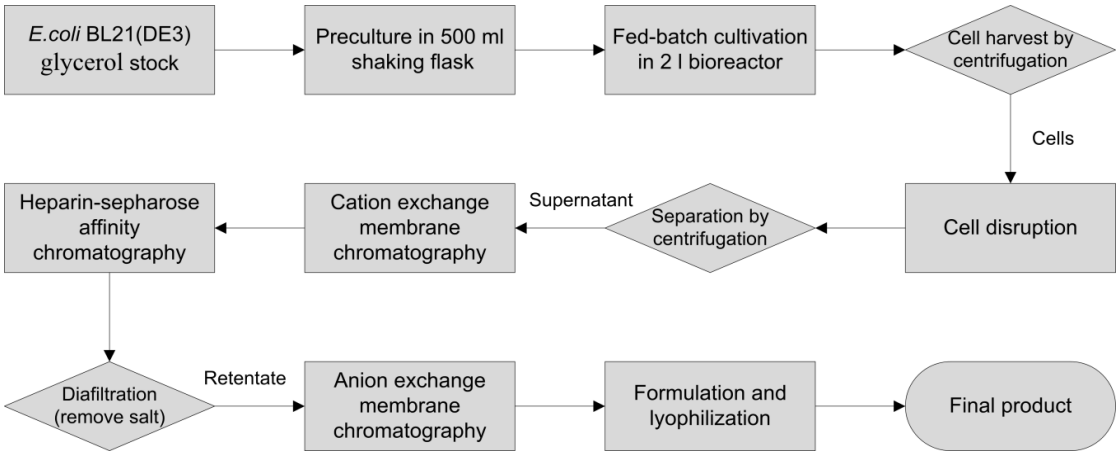

Fig. 4.7 Flow chart of the whole downstreaming and purification process for FGF-2 production.

4.3.5.1 Cell harvest

After the cultivation, 1.9 l of culture broth was distributed into 500 ml centrifuge tubes. Cells were harvested by centrifugation for 20 min at 4,000 rpm (3,345 × g) and 4 °C (Megafuge® 1.0 RS, Heraeus, Hanau, Germany). About 80 g cell pellets were collected and stored at -20 °C until used.

4.3.5.2 Cell disruption and separation

After thawing, 20 g of the cell pellets were resuspended in lysis buffer (25 mM phosphate buffer pH 7.5, 100 mM NaCl, 0.25 g l^{-1} $MgCl_2 \cdot 7H_2O$, 1 U ml^{-1} benzonase with 3 mM DTT and 1 mM EDTA) to a final volume of 100 ml. Cell suspension was fed into a high pressure homogenizer (M-110L; Microfluidics, Newton, USA). Cells were disrupted by 6 discrete passages through the interaction chamber at 620 bar (9,000 psi). The chamber was cooled by immersion in an ice/water bath. Then the cell lysate was distributed into 2 ml tubes, cell debris and insoluble protein were removed by centrifugation on an ultracentrifuge (Heraeus Fresco 17, Thermo Scientific, Germany) at 13,000 rpm (17,000 × g) and 4 °C for 1 h. About 90 ml supernatant were collected and stored at 4 °C until used.

4.3.5.3 Cation exchange membrane chromatography

45 ml supernatant was filtrated through a 0.2 µm sterile filter (Minisart® high flow; Sartorius Stedim Biotech, Göttingen, Germany) and loaded onto a strong cation exchange

membrane adsorber module (Sartobind S75; Sartorius Stedim Biotech, Göttingen, Germany) in an FPLC (fast protein liquid chromatography) system (Biologic Duo Flow; Bio-Rad, Munich, Germany). The membrane was equilibrated prior to use at room temperature with 10 ml equilibration buffer (25 mM sodium phosphate buffer pH 7.5, with 3 mM DTT and 1 mM EDTA). Sample injection was carried out via an auxiliary pump (Econo pump EP-1; Bio-Rad, Munich, Germany) at a flow rate of 1.0 ml min^{-1}. After that the membrane was washed with 15 ml of equilibration buffer at a flow rate of 1.0 ml min^{-1}. FGF-2 was eluted by elution buffer 1 (25 mM sodium phosphate buffer pH 7.5, 1 M NaCl with 3 mM DTT and 1 mM EDTA) and a linear gradient of 0-1 M NaCl as shown in Fig.4.8. All the elution fractions were pooled and stored at 4 °C until the next step. The FPLC protocol for the cation exchange membrane chromatography is described in Appendix 6.5.1.1.

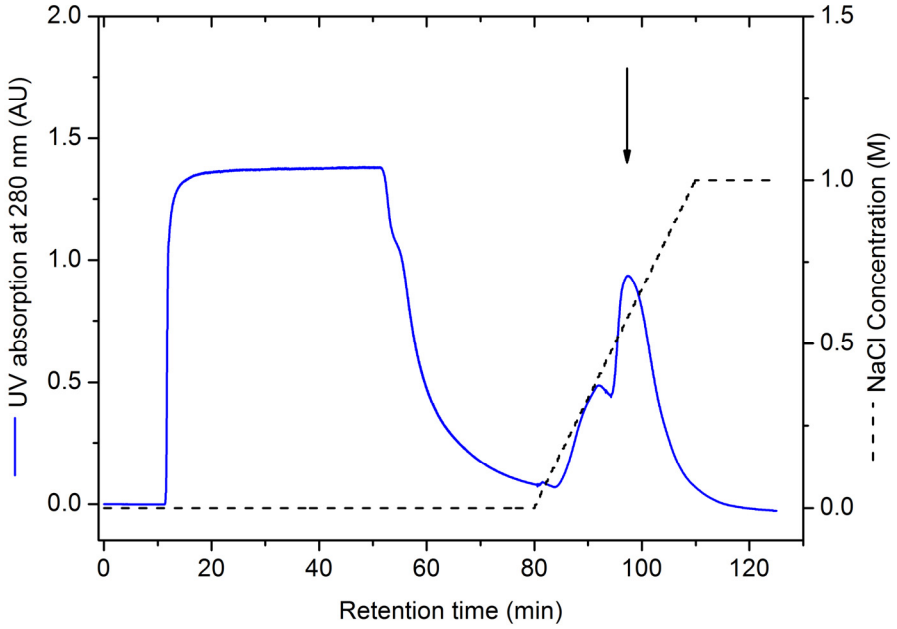

Fig.4.8 Cation exchange membrane chromatography of clarified cell lysate. Elution was carried out with a linear gradient of 0-1 M NaCl. Elution of FGF-2 occurred at about 0.5 M NaCl. The arrow indicates FGF-2 peak.

4.3.5.4 Heparin-sepharose affinity chromatography

42 ml FGF-2-containing solution collected from previous step was filtrated through the 0.2 µm sterile filter and was directly applied to a heparin-sepharose column (HiTrap Heparin HP 5 ml; GE Healthcare, Munich, Germany) in the FPLC system. The column was pre-equilibrated at room temperature with 10 ml equilibration buffer. Sample injection was carried out via the auxiliary pump at a flow rate of 1.0 ml min^{-1}. After loading the sample, the column was washed with 15 ml of equilibration buffer at a flow rate of 1.0 ml min^{-1} until a stable baseline was reached. FGF-2 was eluted by elution buffer 2 (25 mM sodium phosphate buffer pH 7.5, 2.5 M NaCl with 3 mM DTT and 1 mM EDTA) and a linear gradient of 0-2.5 M NaCl as illustrated in Fig. 4.9.

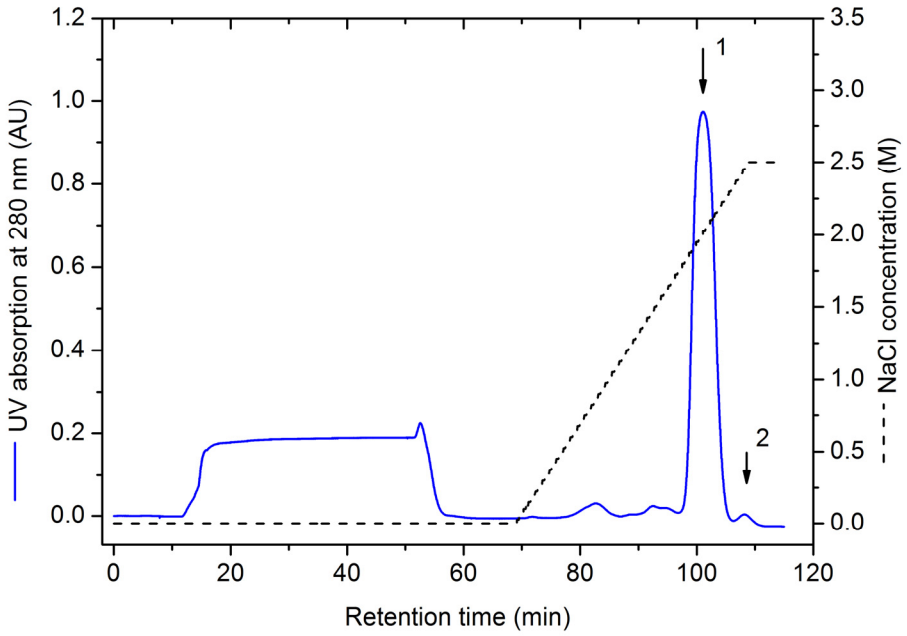

Fig.4.9 Heparin-sepharose affinity chromatography of FGF-2 containing fractions from cation exchange membrane chromatography. The arrows indicate FGF-2 peaks. Elution was carried out using a linear gradient of 0 to 2.5 M NaCl. Elution of FGF-2 occurred at 1.8 M NaCl (peak 1) and 2.2 M NaCl (peak 2).

As shown in Fig. 4.9, FGF-2 was eluted as a main peak (peak 1) and a minor peak (peak 2). SDS-PAGE and RP-HPLC analysis of both peak fractions showed that they were identically pure FGF-2 (data not shown). This was consistent with the observation of Iwane

et al. (1987) and Seeger et al. (1996), who also found two FGF-2 peaks when eluted from heparin-sepharose affinity column. Moreover, it was reported that the amino acid composition for the two peaks was also the same (Iwane et al., 1987). Therefore, both peak fractions were pooled and stored at 4 °C until the next step. The FPLC protocol for heparin-sepharose affinity chromatography is described in Appendix 6.5.1.2.

4.3.5.5 Salt removal by diafiltration

The above two steps (section 4.3.5.3 and 4.3.5.4) were repeated once due to the limited binding capacity of the cation exchange membrane module and heparin-sepharose column. All FGF-2 fractions collected from heparin affinity chromatography were pooled for the next steps.

32 ml FGF-2 solution was sterile filtrated and concentrated 20-fold using Vivaspin 20 centrifugal concentrators (MWCO 3,000 Da; Sartorius Stedim Biotech, Göttingen, Germany) on the refrigerated centrifuge at 4,000 rpm (3,345 × g) and 4 °C. Remaining salt was removed by diafiltration of concentrated FGF-2 solution against 20 volumes exchanging buffer (20 mM Tris-HCl buffer pH 7.5, with 150 mM NaCl, 3 mM DTT and 1 mM EDTA) for 2 times at 4,000 rpm (3,345 × g) and 4 °C. Finally, 25 ml retentate was collected.

4.3.5.6 Anion exchange membrane chromatography

Endotoxins are lipopolysaccharides which locate on the outer membrane of gram-negative bacteria. They can be released to the environment when the cells are destroyed and they are toxic to human beings and animals even at very low levels (Williams, 2007). Therefore endotoxins must be removed from the final product. Since FGF-2 is positively charged while endotoxins and DNAs are negatively charged at pH 7.5, it is possible to separate them by anion exchange membrane chromatography.

Prior to use, the FPLC system was washed with 2 M KOH containing 30 % ethanol followed with pyrogen-free water to remove traces of endotoxins. An anion exchange membrane adsorber module (Sartobind Q75; Sartorius Stedim Biotech, Göttingen, Germany) was washed sequentially with 0.1 M KOH containing 20 % ethanol, 1.5 M NaCl and pyrogen-free water to make it endotoxin-free (Minobe et al., 1983). Then the

membrane was equilibrated with 10 ml of exchanging buffer. 25 ml FGF-2 solution from the diafiltration step were loaded onto the membrane at a flow rate of 0.5 ml min^{-1} (Fig. 4.10) and the flow-through fractions were collected as pure FGF-2. The FPLC protocol for the anion exchange membrane chromatography is described in Appendix 6.5.1.3.

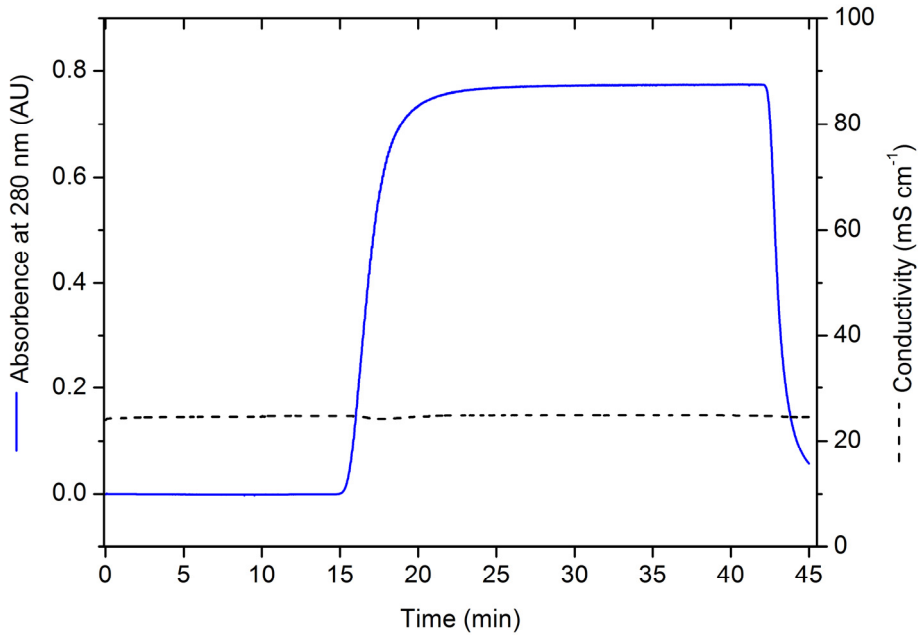

Fig. 4.10 Endotoxin removal from FGF-2 solution by anion exchange membrane chromatography. Flow through fractions were collected as pure FGF-2.

4.3.5.7 Endotoxin determination

The endotoxin content of purified FGF-2 was determined by LAL assay as described in Appendix 6.3.5. As shown in Table 4.7, the anion exchange membrane chromatography was effective in removing endotoxins from FGF-2 solution. The final endotoxin content in the purified FGF-2 was 1.425 EU ml^{-1}.

Table 4.7 Comparison of endotoxin concentrations before and after anion exchange membrane chromatography

	Endotoxin level (EU ml^{-1})	Clearance rate (%)	Protein recovery rate (%)
before	37600		
after	1.425	99.99	≥ 98

4.3.5.8 More about endotoxin

The endotoxin level is critical for the proteins to be used for cell culture or clinical applications. In the final product, the endotoxin level was reduced to a very low value (Table 4.7) by anion exchange membrane chromatography, which was acceptable even for clinical applications (< 5 EU kg^{-1} h^{-1} as specified in European Pharmacopoeia (2007)).

However, it should be pointed out, a certain amount of endotoxins could be still remained in the purified FGF-2. Since the positively charged protein can form complexes with the negatively charged endotoxins, demonstrating so-called masking of endotoxins. Moreover, the masked endotoxins can not be detected by the LAL test (Magalhães et al., 2007; Petsch and Anspach, 2000). Researches on the toxicity of protein-endotoxin complexes are inconsistent. Rogy et al. (1994) reported that protein-bound endotoxins were still toxic as free endotoxins. While Emancipator et al. (1992) found that lipoprotein-endotoxin complexes were less toxic compared to free endotoxins.

Petsch et al. (1998) reported that the masked endotoxins could be totally recovered by digesting the protein with proteinase K. Garke et al. (2000) digested purified FGF-2 with proteinase K and found an increase in endotoxin concentration afterwards. But the endotoxin level was still lower than the critical point (< 5 EU kg^{-1} h^{-1}).

4.3.5.9 FGF-2 concentration determination

The concentration of the pure FGF-2 was 1.52 mg ml^{-1} as determined by UV absorbance at 280 nm (see Appendix 6.3.3.3). The total pure FGF-2 obtained was 52.28 mg. The calculated endotoxin content was 0.0009 EU μg^{-1} protein.

4.3.5.10 FGF-2 formulation and lyophilization

A carrier-free freeze-drying formulation was developed in order to meet the requirement of transportation and long term storage of the protein. The formulation contains 1-2 mg ml^{-1} FGF-2, in 20 mM Tris-HCl buffer pH 7.5, with 150 mM NaCl, 3 mM DTT, 1 mM EDTA and 2 % (w v^{-1}) sucrose.

The formulated FGF-2 solution was sterile filtrated through the 0.2 µm filter and lyophilized (see Appendix 6.3.6). The lyophilized powder was stored at - 80 °C.

4.3.6 SDS-PAGE visualization of the downstreaming and purification process

Sodium dodecyl sulfate polyacrylamide gel electrophoresis (SDS-PAGE) is a widely used approach to separate proteins according to their molecular weights. Gel preparation and running processes were described in Appendix 6.3.4.1. The whole purification process was visualized by SDS-PAGE and shown in Fig.4.11. The gel was stained with blue silver stain solution (Candiano et al., 2004) (see Appendix 6.3.4.1.1).

As shown in Fig. 4.11, after heparin-sepharose affinity chromatography the SDS-PAGE gel demonstrated only a single band of FGF-2 (Lane 6), which indicated that our new two-step purification process was effective in FGF-2 purification. And the polishing step has no negative effect on the protein purity (Lane 7).

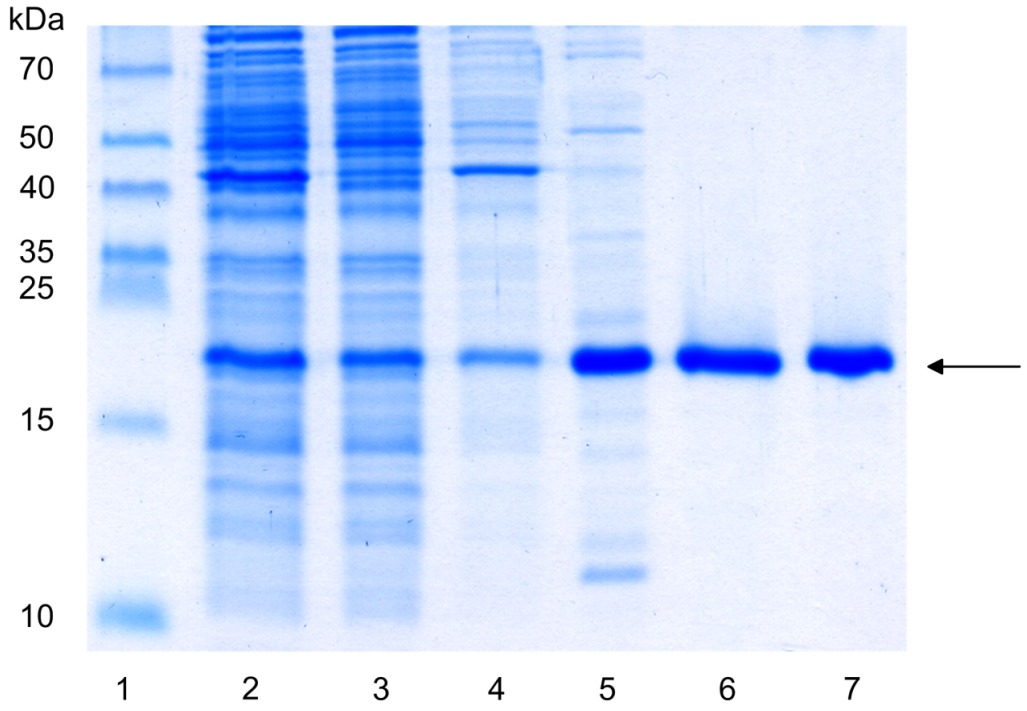

Fig.4.11 Purification of FGF-2 presented by SDS-PAGE visualized with Blue-silver stain solution. Lane 1, molecular weight marker; Lane 2, total cell lysate (dilution 1:20); Lane 3, soluble fractions of cell lysate (dilution 1:20); Lane 4, insoluble fraction of cell lysate (dilution 1:20); Lane 5, pooled fractions from cation exchange membrane chromatography (dilution 1:10); Lane 6, pooled fractions from heparin affinity chromatography (dilution 1:10); Lane 7, pooled fractions from anion exchange membrane chromatography (dilution 1:10). The arrow indicates the position of FGF-2.

4.3.7 FGF-2 recovery during the purification process

The recovery rates of FGF-2 produced at different specific growth rates (0.35 h^{-1} and 0.15 h^{-1}) during sequential purification steps are shown in Fig. 4.12 and Fig.4.13, respectively. It is obvious that in both conditions about 23 % of soluble FGF-2 were lost during the purification process. Main protein loss was occurred in the centrifugation step and cation exchange membrane chromatography step. Since cells produce more soluble protein fractions at μ_{set} = 0.15 h^{-1}, the finally FGF-2 recovery rate was 36 % while for μ_{set} = 0.35 h^{-1} the final FGF-2 recovery rate was 22 %. The FGF-2 contents were estimated by Bradford assay (see Appendix 6.3.3.1) and gel densitometry (see Appendix 6.3.3.2).

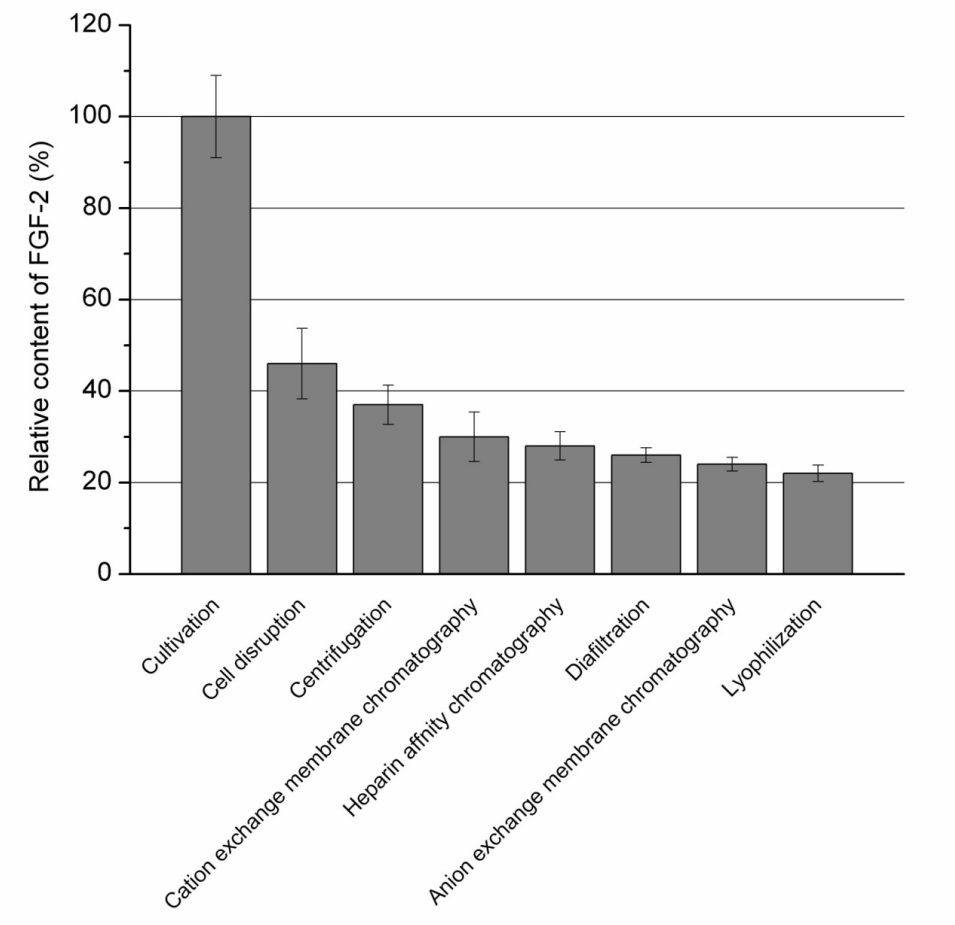

Fig.4.12 Relative contents of FGF-2 during sequential purification steps (μ_{set}= 0.35 h^{-1}). The protein contents were estimated by bradford assay and gel densitometry.

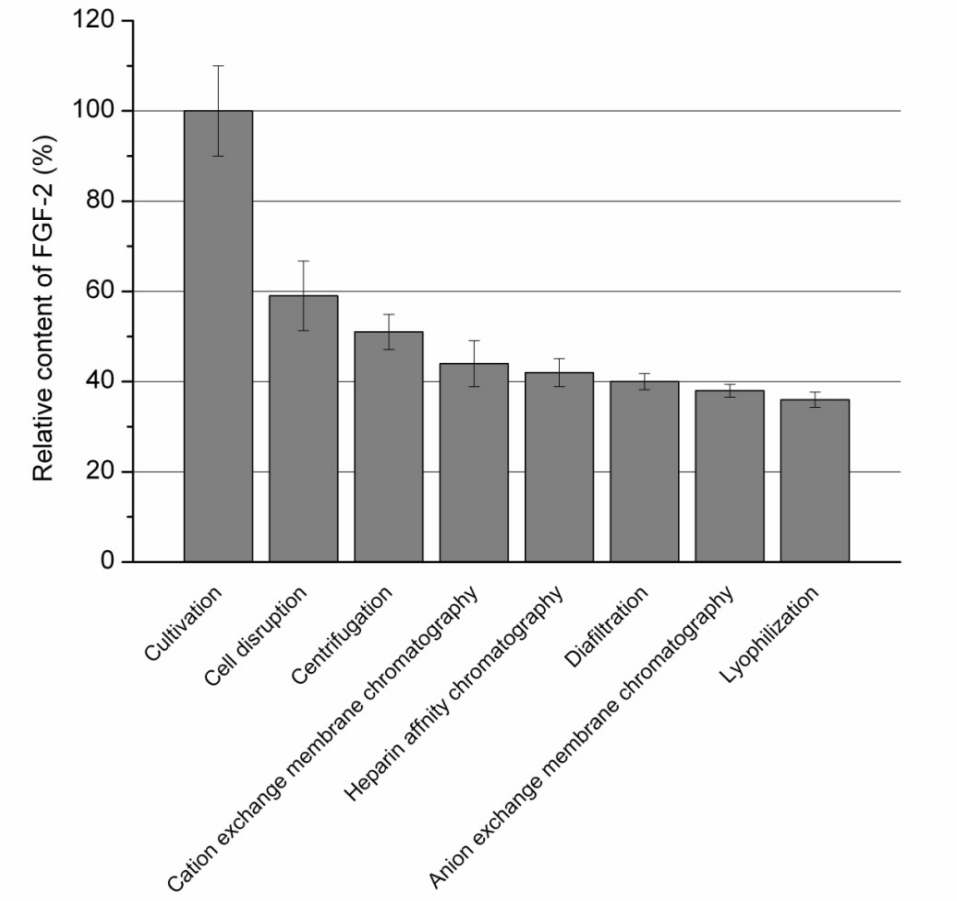

Fig.4.13 Relative contents of FGF-2 during sequential purification steps (μ_{set}= 0.15 h^{-1}). The protein contents were estimated by bradford assay and gel densitometry.

4.3.8 Improvement of the new purification process

In this study, we developed an efficient protocol for cost-effective production of FGF-2. Reusable cation exchange membrane adsorber was used in the first purification step for fast and easy binding of FGF-2. Applying the pooled elution fractions from cation exchange membrane chromatography directly onto the heparin-sepharose column without dialysis was time-saving. The diafiltration step is faster than conventional dialysis process for salt removal, with protein loss less than 2 %. Last polishing step using high efficiency anion exchange membrane adsorber to remove endotoxins and DNAs result in protein recovery $\geq$ 98 % and endotoxin level less than 0.001 EU μg^{-1} protein. The whole process yielded highly pure FGF-2 with a recovery rate of 22 % to 36 %.

4.3.9 Stabilizing of FGF-2 during the purification process

FGF-2 is unstable and easy to be oxidized when contacts with air (Thompson and Fiddes, 1991). Therefore, several methods have been used to keep FGF-2 in its reduced form during the purification process. All buffers and solutions used in the purification process were degassed by sonication to remove the oxygen dissolved in water. Moreover, DTT (Dithiothreitol) was added to all the buffers as a reducing agent.

Due to air oxidation, DTT is relative unstable (half-life 10 h, at pH 7.5, 20 °C in 0.1 M potassium phosphate buffer) and oxidized DTT gives a strong UV absorption at 283 nm (Iyer and Klee, 1973). Since proteins have a maximum absorbance at 280 nm, a small increase of oxidized DTT amount could cause great change of protein concentration measured by UV absorption. However, the life time of DTT can be extended by storage at lower temperature and the addition of the metal chelating agent EDTA which can effectively inhibit disulfide bond formation (Foster et al., 1993). Therefore, all buffers were kept at 4 °C in the fridge with 3 mM DTT and 1 mM EDTA. At these conditions, the buffers could be kept for one week with negligible oxidation of DTT.

By using the methods described above, FGF-2 was protected from oxidation and maintained its native conformation throughout the whole purification process (data not shown).

4.4 Product identification

4.4.1 MALDI-TOF MS

Matrix assisted laser desorption ionization-time of flight mass spectrometry (MALDI-TOF MS) can be used for the determination and characterization of biomolecules, including proteins, peptides, oligosaccharides, etc. This method was used to further identify the molecular weight of FGF-2. The test was performed by the group of Prof. Dr. Ulrich Martin at Hannover Medical School (MHH) and the procedure for the sample preparation and operation are described in Appendix 6.3.4.2.

Purified FGF-2 demonstrates a single peak at m/z = 17,124 which represents FGF-2 monomer and no FGF-2 dimer is detected (Fig.4.15).

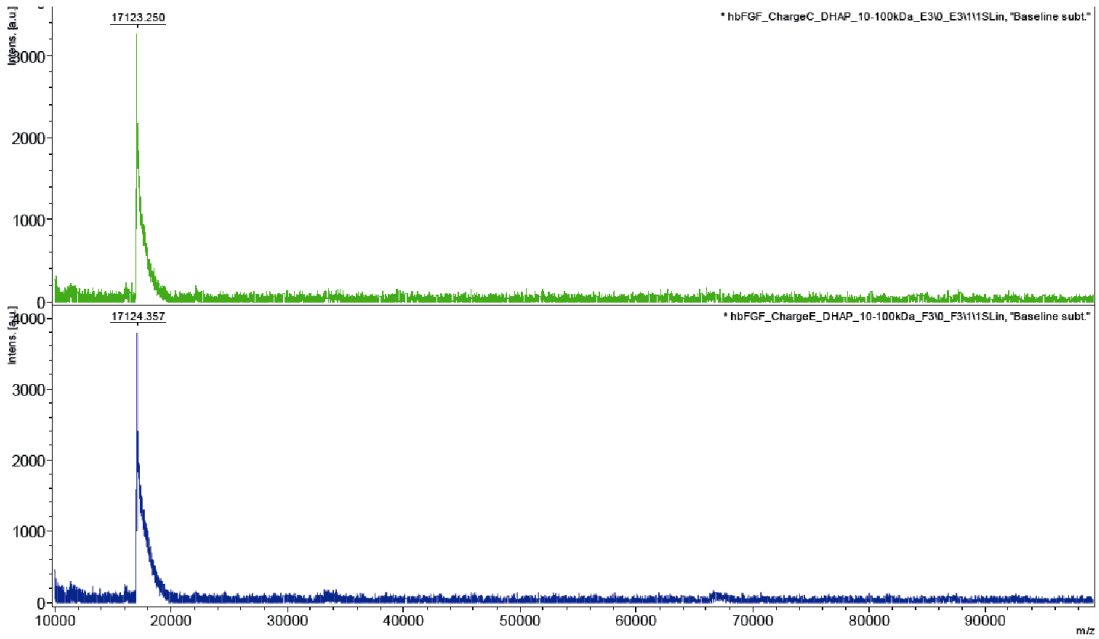

Fig. 4.15 MALDI-TOF MS of two different FGF-2 charges. In both charges, a single peak at m/z = 17,124 is observed.

4.4.2 SDS-PAGE

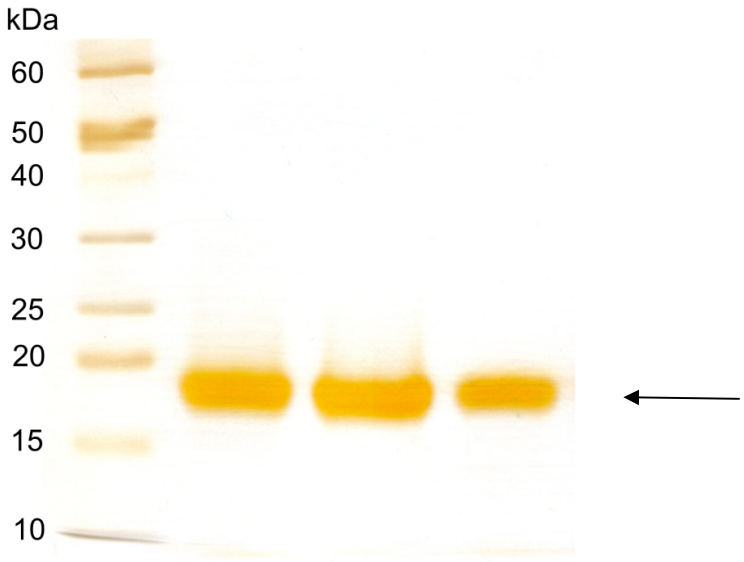

Fig. 4.14 SDS-PAGE of purified FGF-2 stained with silver. The arrow indicates the position of FGF-2.

The molecular weight of FGF-2 was identified with 12 % polyacrylamide gel using the recipe of Laemmli (1970). Gel preparation and running process were described in Appendix 6.3.4.1. Purified FGF-2 visualized with silver stain (see Appendix 6.3.4.1.2) revealed a single band at about 17 kDa (Fig. 4.14).

4.4.3 Fluorescence spectroscopy

Fluorescence spectroscopy is a fast and effective method for the evaluation of FGF-2 conformation properties. FGF-2 has only one tryptophan residue. In properly folded protein the emission of this tryptophan residue is completely suppressed and the emission spectrum is dominant by the fluorescence of tyrosine residues ($\lambda_{max} \approx 306$ nm). While unfolded FGF-2 shows a strong increase of tryptophan fluorescence ($\lambda_{max} \approx 350$ nm) together with the tyrosine fluorescence (Estape et al., 1998). The fluorescence spectrum of purified FGF-2 demonstrates an asymmetry peak at 306 nm (Fig. 4.16) which indicates the purified FGF-2 is completely folded. The analytical protocol is described in Appendix 6.3.4.4.

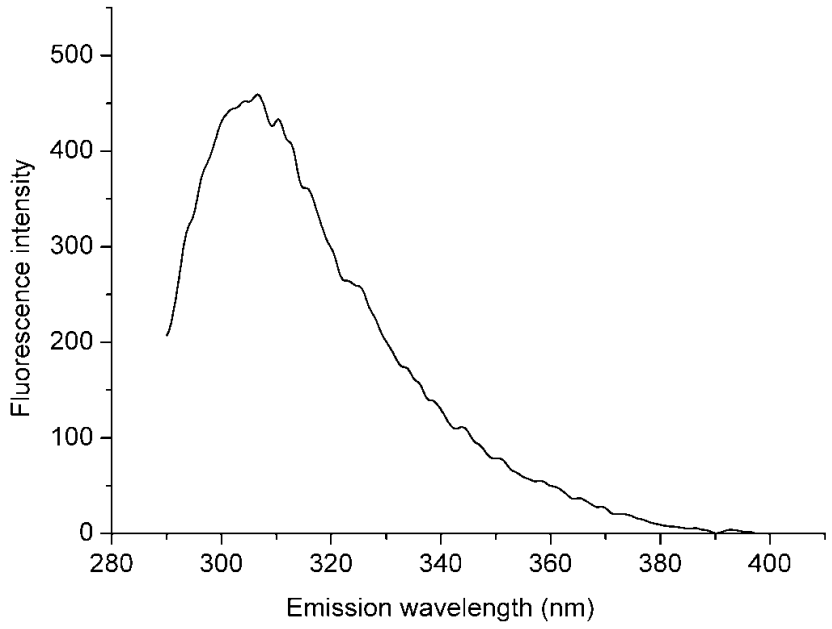

Fig.4.16 Base-line corrected fluorescence spectrum of purified FGF-2. The asymmetric peak at 306 nm indicates the properly folded state of FGF-2.

4.4.4 Western blot analysis

Western blot analysis is based on the specific binding of FGF-2 to the monoclonal anti-human-FGF-2 antibody. The procedure is described in Appendix 6.3.4.3. Western blot analysis of purified FGF-2 demonstrates a single band at about 17 kDa (Fig. 4.17).

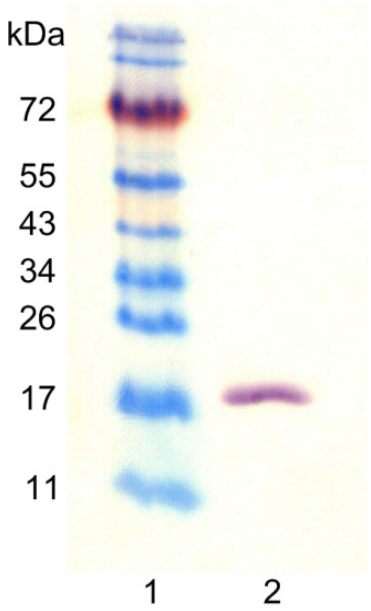

Fig.4.17 Western blot analysis of purified FGF-2. Lane 1, molecular weight marker; Lane 2, purified FGF-2.

4.4.5 RP-HPLC

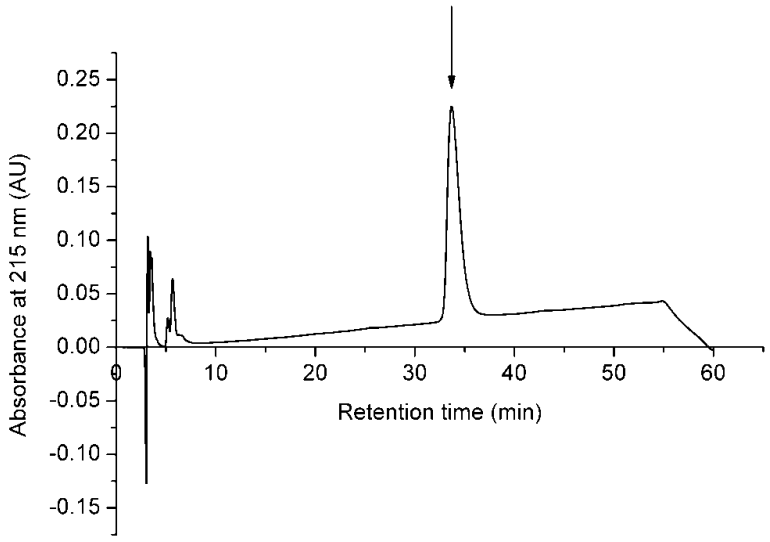

Fig.4.18 RP-HPLC analysis of purified FGF-2.

Reverse phase-high performance liquid chromatography (RP-HPLC) was used to determine the purity of purified FGF-2. The system construction and chromatography conditions are described in Appendix 6.3.4.5. The HPLC protocol is presented in Appendix 6.5.2. HPLC analysis of purified FGF-2 revealed that the protein was eluted by 34 % acetonitrile as a single peak, which was consistent with the report of Squires et al. (1988). The peak at about 5.7 min refers to DTT. The purity of FGF-2 calculated by area normalization method was 98.2 %.

4.5 Biological activity test

4.5.1 Bioactivity test performed at the TCI

The activity test was performed by Dr. Ingrida Majore and Antonina Lavrentieva at the TCI on the proliferation of mesenchymal stem cell-like cells and NIH-3T3 fibroblast cells.

4.5.1.1 Bioactivity test on mesenchymal stem cell-like cells

The biological activity of purified FGF-2 was tested using mesenchymal stem cell-like cells obtained from human umbilical cord. Mesenchymal stem cell-like cells were seeded in 24-well-plates at a density of 500 cells cm^{-2} and cultivated in αMEM (minimum essential medium, alpha modified) enriched with 1 % human serum, 10 µg ml^{-1} insulin, 5.5 µg ml^{-1} transferrin, 6.7 pg ml^{-1} sodium selenite, 2 mg ml^{-1} human albumin, 50 µg ml^{-1} gentamicin and appropriate amounts of FGF-2 varying in the range from 0 to 1 ng ml^{-1}. Medium was changed three times a week. 9 days after cell seeding, the indirect determination of the number of viable cells was performed using CellTiter-Blue® cell viability assay (Promega, Southampton, UK) according to the manufacturer's instructions. Commercially available FGF-2 (ref. 167100-18B-B, tebu-bio, Offenbach, Germany) was applied as a positive control.

The produced FGF-2 demonstrated a high activity on the proliferation of mesenchymal stem cell-like cells and gave an EC_{50} (half maximal effective concentration) of 0.13 ng ml^{-1}, while the EC_{50} of a commercially available FGF-2 was 0.21 ng ml^{-1} as shown in Fig.4.19. Our purified FGF-2 gave better results than the commercial one.

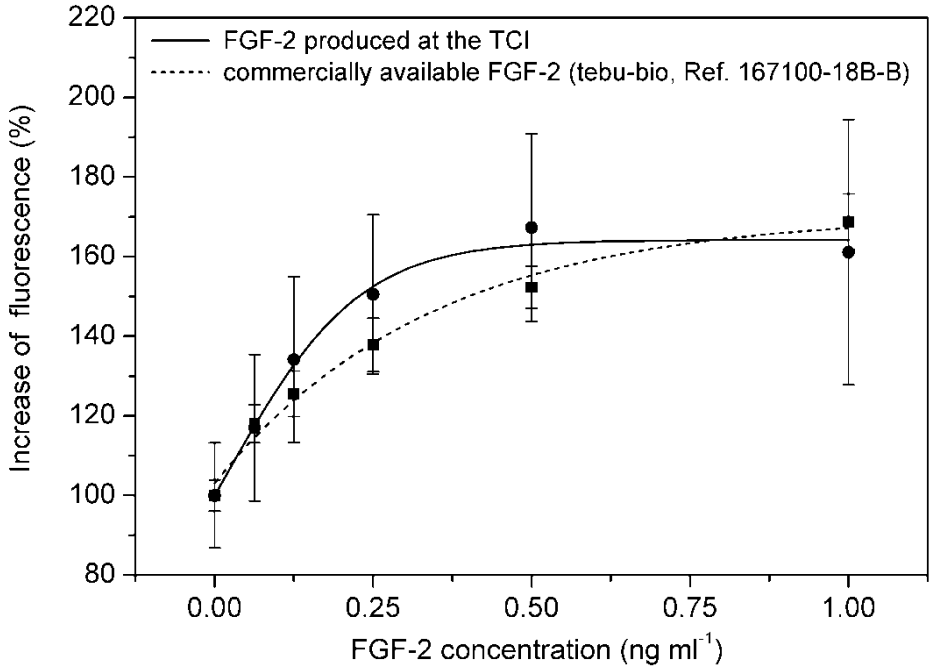

Fig. 4.19 Dose-dependent proliferation of mesenchymal stem cell-like cells in the presence of FGF-2.

4.5.1.2 Bioactivity test on NIH-3T3 cells

Biologic activity of FGF-2 was also tested by a dose-dependent cell proliferation assay on NIH-3T3 fibroblast cells (DSMZ, Deutsche Sammlung von Mikroorganismen und Zellkulturen GmbH, Braunschweig, Germany). Cells were seeded in 96-well-plates in culture medium (DMEM, Sigma-Aldrich, Taufkirchen, Germany) supplemented with 10 % (V V^{-1}) FCS (fetal calf serum) and 1 % penicillin-streptomycin (PAA Laboratories GmbH, Pasching, Austria) with an initial cell density of 4,000 cells $well^{-1}$. After seeding, cells were starved for 24 h in DMEM with 1 % FCS and then cultivated in FGF-2-containing media for 52 h. Cells cultivated in culture medium without FGF-2 served as negative control.

For the indirect estimation of cell proliferation, CellTiter-Blue® cell viability assay (Promega, Southampton, UK) was performed. The metabolic capacity of viable cells was measured as a result of the reduction of the indicator dye resazurin into highly fluorescent, pink colored resorufin (Ex 579 nm/Em 584 nm), according to the manufacturer´s

instructions (Fig. 4.20). Fluorescence measurements were performed on the Fluoroskan Ascent microplate reader (Thermo Scientific, Dreieich, Germany) and results are presented as percentage to the negative control.

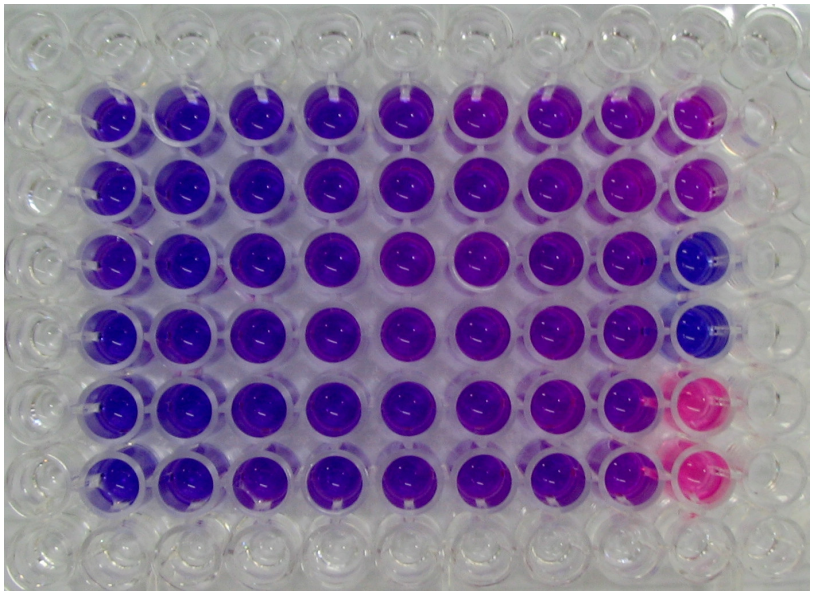

Fig. 4.20 Changing of CellTiter-Blue® reagent color after 2 h incubation at 37 °C (pink color indicates a higher rate of dye reduction because of a higher cell number).

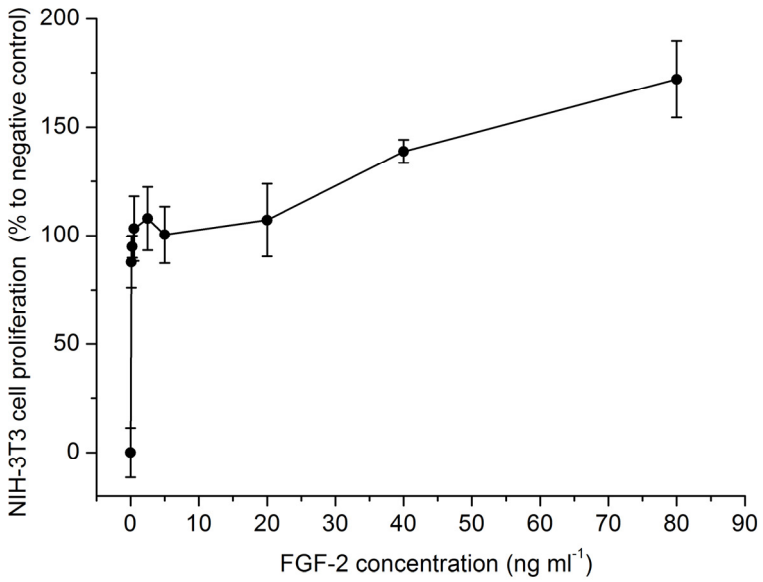

Fig.4.21 Dose-dependent proliferation of NIH-3T3 cells in the presence of FGF-2.

The adding of FGF-2 resulted in significant increase of NIH-3T3 cell division and gave an EC_{50} of 0.10 ng ml^{-1} as shown in Fig.4.21. The EC_{50} was calculated according to the method of Alexander et al. (1999). This was consistent with other reports on the mitogenic activity of recombinant FGF-2 on 3T3 fibroblast cells (Fox et al., 1988; Garke et al., 2000; Gasparian et al., 2009; Squires et al., 1988), which have an EC_{50} of 0.15 to 3 ng ml^{-1}.

4.5.2 Bioactivity test performed at MHH

In order to further test the bioactivity of purified FGF-2, the activity tests were also performed at Hannover Medical School (MHH) on a large variety of cells.

4.5.2.1 Activity test on neuronal differentiation of PC12 cells

The activity test was performed by Silvana Taubeler-Gerling, Dipl.-Biol. Maike Wesemann and PD Dr. Kirsten Haastert at the Institute of Neuroanatomy, MHH. The neuronal differentiation activity of FGF-2 was tested on PC 12 cells. A commercial FGF-2 (PeproTech Inc., Rocky Hill, USA) was used as positive control. The results are shown in Fig.4.22-Fig.4.25. The neuronal differentiation observed with purified FGF-2 was similar to the commercial FGF-2 (Fig. 4.24, Fig. 4.25).

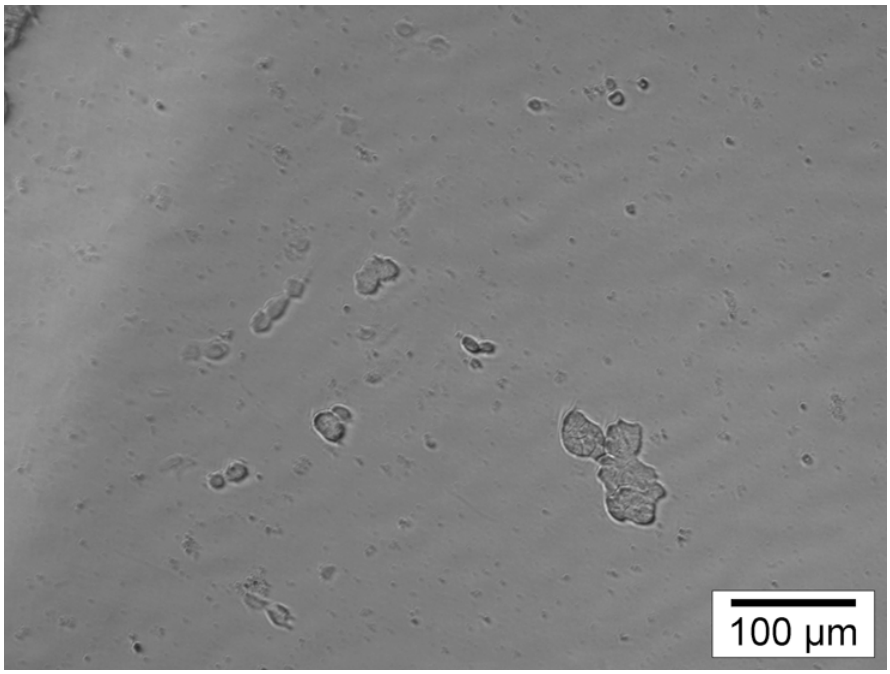

Fig. 4.22 PC 12 cells without FGF-2 in the medium were used as negative control. The cells were cultivated *in vitro* for 6 days and no neuronal differentiation was observed.

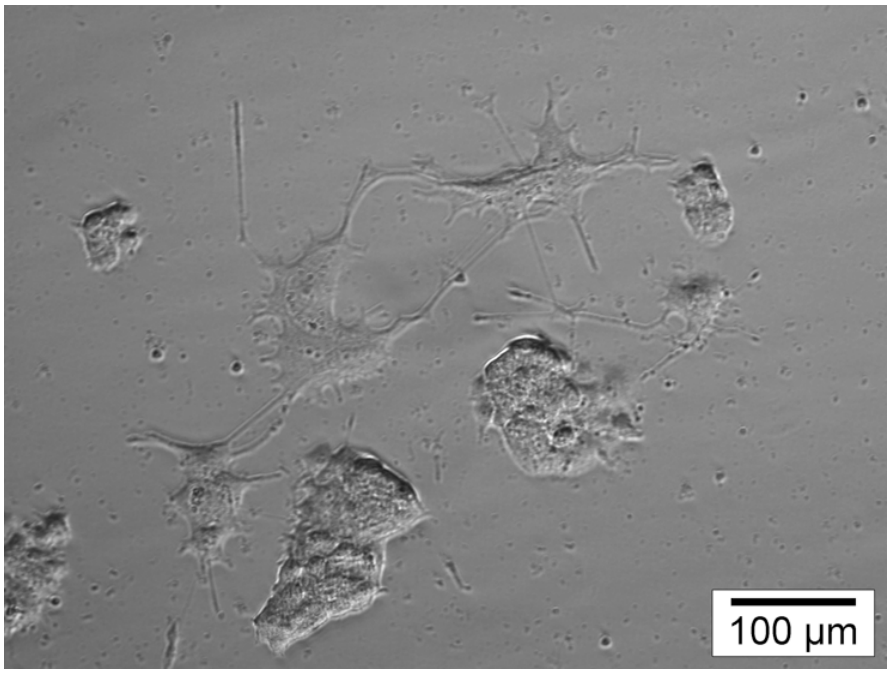

Fig. 4.23 PC 12 cells supplemented with commercial FGF-2 to a concentration of 100 ng ml^{-1} in the medium. The cells were cultivated *in vitro* for 6 days and show neuronal differentiation by protruding cell processes.

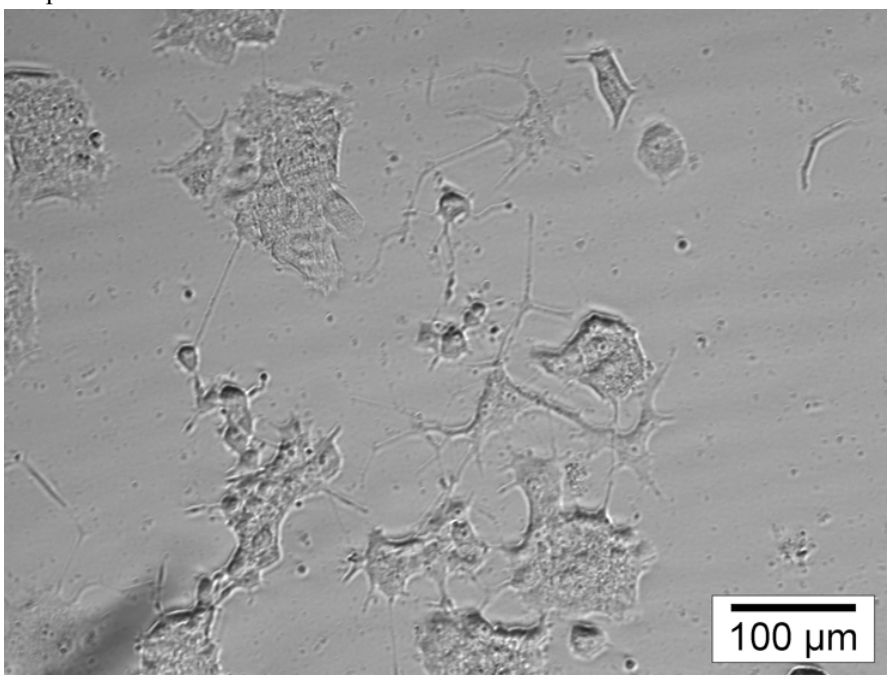

Fig. 4.24 PC 12 cells supplemented with purified FGF-2 to a concentration of 50 ng ml^{-1} in the medium. The cells were cultivated *in vitro* for 6 days and show neuronal differentiation similar to the commercial FGF-2.

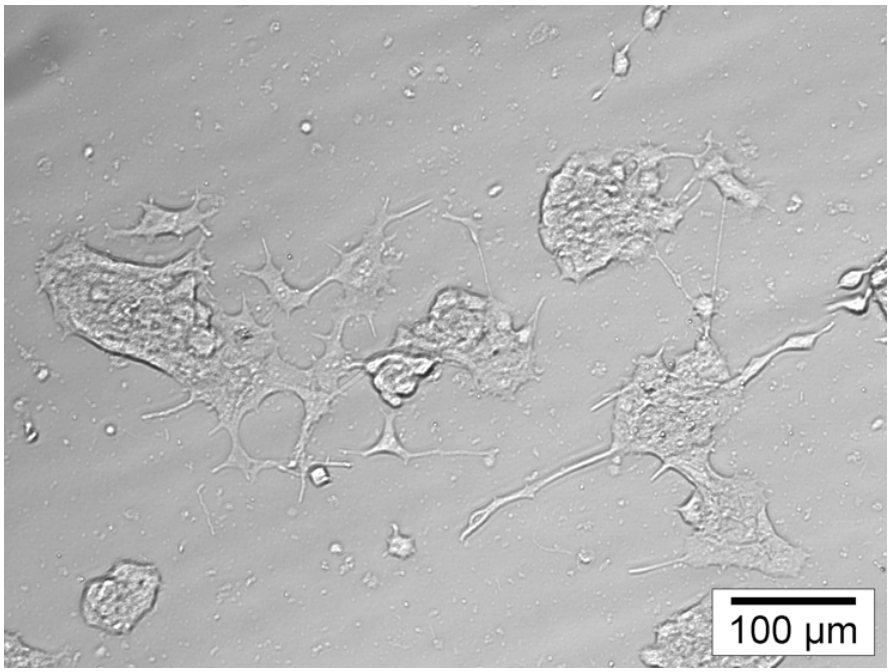

Fig. 4.25 PC 12 cells supplemented with purified FGF-2 to a concentration of 100 ng ml^{-1} in the medium. The cells were cultivated *in vitro* for 6 days and show neuronal differentiation similar to the commercial FGF-2.

4.5.2.2 Activity test on pluripotent cell culture

This activity test was performed by Susann Müller, Dr. Robert Zweigerdt and Prof. Dr. Ulrich Martin at the department of Cardiac-, Thoracic-, Transplantation and Vascular Surgery, REBIRTH-Center for Regenerative Medicine, MHH.

Pluripotent stem cells (PSC) including ESC and iPSC (induced pluripotent stem cell) are important research subjects since the mechanisms underlying cellular differentiation, expansion, and self-renewal can be studied along with differentiated tissue development and regeneration *in vitro* (Cantz and Martin, 2010; Zweigerdt, 2009). Furthermore, human PSC hold promise for cell and tissue replacement approaches to treating human diseases. The rhesus and the cynomolgus monkey are clinically relevant primate models that will likely be required to bring these clinical applications to fruition (Schwanke et al., 2006). Primates ESC share a number of properties with human ESC including their sensitivity to *in vitro* culture conditions and particularly the FGF-2 content in the medium, which is a key factor in keeping the cells pluripotent. Thus, we have applied both, primate ESC and human iPS cell lines to test the biological activity of the FGF-2 generated in this study.

Feeder-dependent culture of undifferentiated human cord blood endothelial cell-derived iPSC (Haase et al., 2009), rhesus ESC (Schwanke et al., 2006) and cynomolgus monkey ESC (MF12; (Olmer et al., 2010)) were cultured and expanded under standard hESC culture conditions (Olmer et al., 2010; Singh et al., 2010). In brief, cells were grown mitotically inactivated fibroblast in KnockOut™ DMEM supplemented with 20 % KnockOut™ serum replacement, 1 mM *L*-glutamine, 0.1 mM *ß*-mercaptoethanol, 1 % nonessential amino acid stock (all from Invitrogen, Karlsruhe, Germany), and 4 ng ml^{-1} commercial FGF-2 (positive control; R&D Systems, Wiesbaden, Germany) or respective concentration of FGF-2 generated in this study (test FGF-2) as indicated in the results.

To assess the seeding efficiency and pluripotency markers expression, cells were passaged in the respective FGF-2 concentration for 6 passages on fibroblasts and then seeded in decreasing concentration on gelatine coated plates in a 24-well format. After 4 days cells were fixed, H&E stained (hematoxylin and eosin stain) and the cell density was analysed by light microscopy.

For flow cytometry, single cell suspensions were prepared by collagenase digest. Cells were incubated in a 96 v-bottom plate with an SSEA 4 (stage-specific embryonic antigen 4) specific primary antibody (1:68, MC-813-70, Developmental Studies Hybridoma Bank University of Iowa) and corresponding isotype controls for 30 min at 4 °C. After washing, cells were incubated with a secondary antibody, Cy™3-labeled donkey anti-mouse IgG (1:200; Jackson Immunoresearch Laboratories, Suffolk, UK) for 30 min at 4 °C. The cells were analyzed using a FACSCalibur cell analyzer (BD Bioscience, Heidelberg, Germany). Data were further processed using WinMDI 2.9 software.

Primate ESC and human cord blood-derived iPSC (Haase et al., 2009) were culture for 6 passages either in purchased FGF-2 at 4 ng ml^{-1} (positive control), in our generated test FGF-2 at 2, 4 and 8 ng ml^{-1} or in FGF-free conditions (negative control). Thereafter (at passage 7) cells were seeded in decreasing concentration on gelatine coated plates in the presence of the respective FGF-2 concentration and quality and seeding efficiency was semi-quantitatively assessed 4 days later. As exemplarily shown for rhesus ESC in Fig. 4.26A, seeding efficiency and cell growth in our produced FGF-2 was at least equivalent to

the commercially available FGF-2 even at the lowest concentration tested (respective data for cynomolgus ESC and human iPSC not shown).

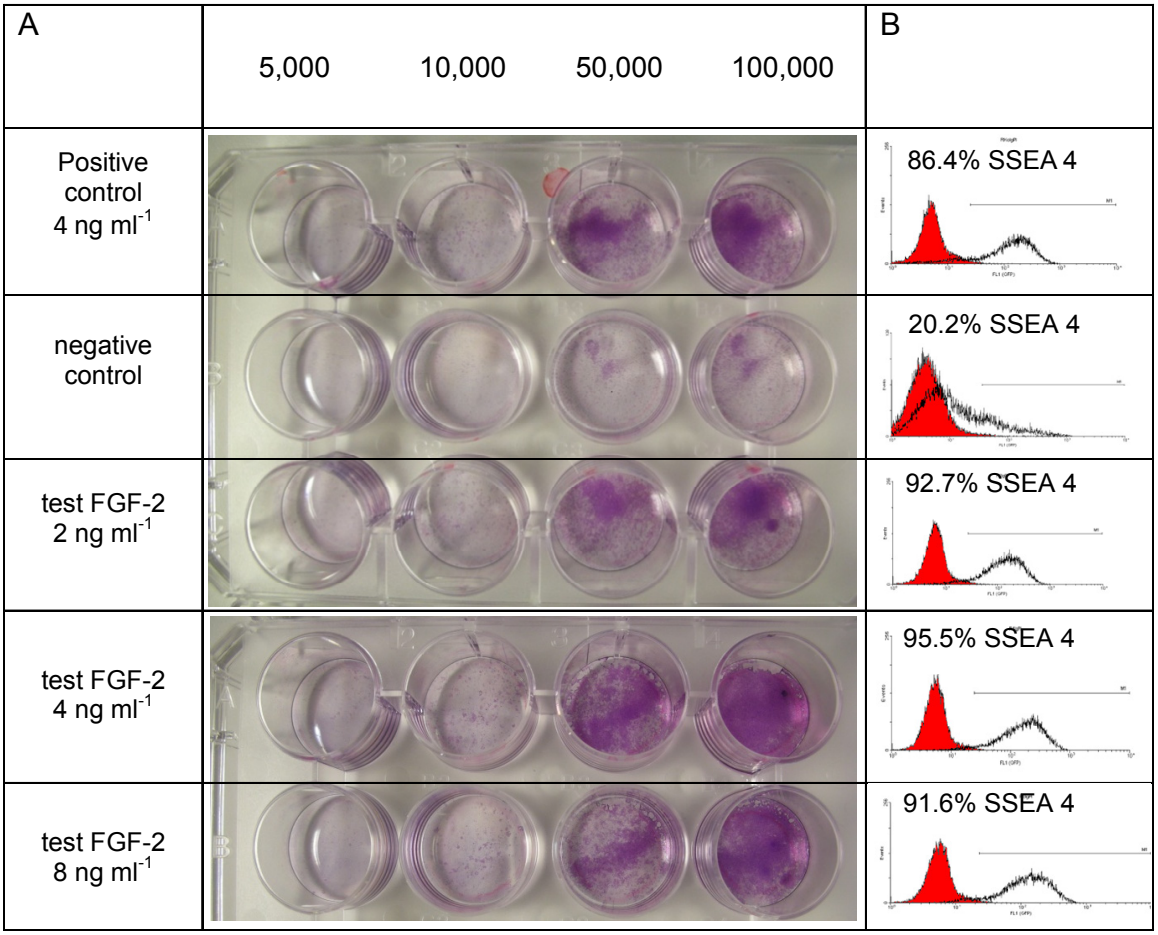

Fig. 4.26 Biological activity of FGF-2 on pluripotent cells. (A): Assessment of seeding efficiency and expansion of rhesus ESC. After 6 passages in the respective FGF-2 concentration, cells were seeded at 5-100 k cells per well and cultured for 4 days in the respective FGF-2 concentration as indicated. Thereafter, H&E staining was performed and cells were analysed by light microscopy. (B): Flow cytometry analysis (histograms) documenting the percentage of SSEA4 positive rhesus ES cells after 6 passages in the presence of the respective FGF-2 concentration. The isotype control is indicated in red.

To assess pluripotency of the cells, flow cytometry specific to the pluripotency-associated surface marker SSEA4 was performed after 6 passages in the respective FGF-2 concentration, as described above. With our test FGF-2, > 90 % of the cells were SSEA4

positive at all concentrations as compared to about 86 % positive cells observed in the control FGF-2 (Fig. 4.26B). As expected, the proportion of SSEA4 positive cells dropped to only about 20 % in the absence of the growth factor. These data strongly suggest the optimal biological activity of the generated FGF-2.

4.5.2.3 Other bioactivity tests

The bioactivity of our produced FGF-2 was also tested successfully by the group of Dr. Axel Schambach at MHH, Dr. Inga von Ahsen at the Small Animal Clinic, University of Veterinary Medicine Hannover (TiHo) and also the group of Prof. Joseph Itskovitz-Eldor at the Stem Cell Center, Faculty of Medicine, Technion (Israel Institute of Technology), Israel.

4.5.3 Comparison of bioactivity of FGF-2 produced at different growth rates

Growth rates can greatly affect many metabolic processes of *E. coli* like cell growth, acetate formation (Button, 1985; Hempfling and Mainzer, 1975; Shiloach et al., 1996). Some researches also reported it could affect the activity of produced recombinant protein (Hellmuth et al., 1994; Kazan et al., 1995). Therefore, the biological activity of FGF-2 produced at two different growth rates (0.35 and 0.15 h^{-1}) was tested and compared.

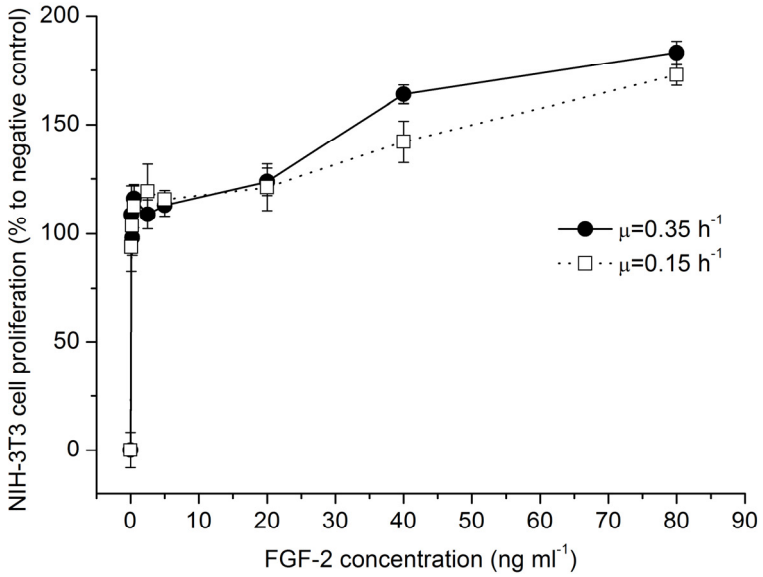

Fig. 4.27 Comparison of bioactivity of FGF-2 produced at different growth rates. Error bars indicate the standard deviation from 3 measurements.

The bioactivity tests were performed as described in section 4.5.1.2. NIH-3T3 cells proliferation at different concentration of FGF-2 is shown in Fig. 4.27. The calculated EC_{50} for FGF-2 produced at specific growth rate of 0.35 h^{-1} was 0.11 ng ml^{-1} and for 0.15 h^{-1} was 0.12 ng ml^{-1}. There seems to be no significant difference between them. That might because the purification process was designed for isolating FGF-2 from the soluble fractions which were properly folded protein, while the misfolded protein fractions (insoluble as inclusion bodies) were discarded before the purification process. Therefore, at different growth rate only the FGF-2 recovery rate was changed, the activity was the same.

4.5.4 Effect of lyophilization on the bioactivity of FGF-2

Dehydration process can lead to remarkable conformation changes of most native proteins (Wang, 2000). These conformation changes can be detected and analyzed by FTIR (Fourier transform infrared) spectroscopy (Costantino et al., 1995; Dong et al., 1995a; Luthra et al., 2007). By comparing second-derivative FTIR spectra of the protein in aqueous solution and dry state, structure damage caused by freeze-drying could be qualitatively determined.

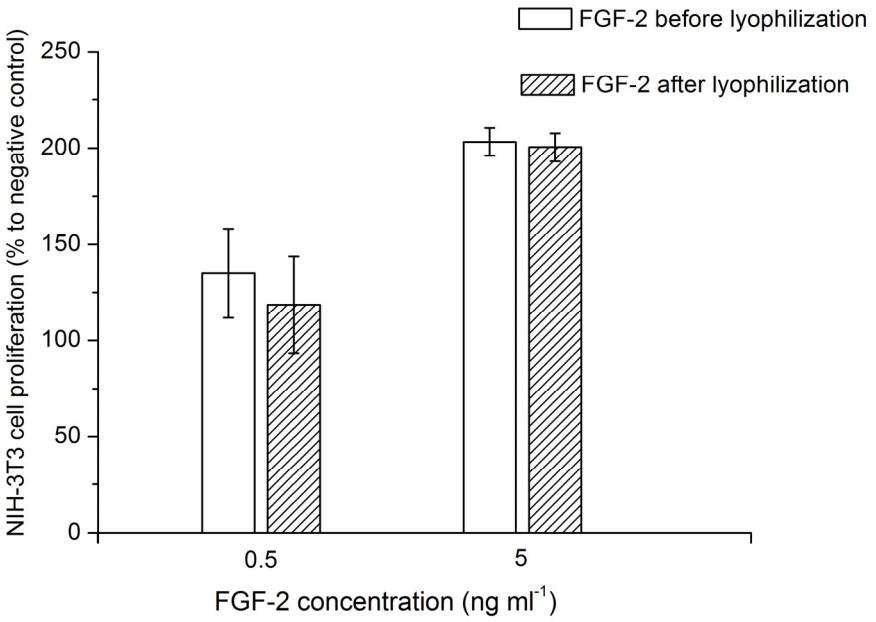

Fig.4.28 Comparison of NIH-3T3 cell proliferation in the presence of FGF-2 solution and lyophilized FGF-2. Error bars indicate the standard deviation from 3 measurements.

Prestrelski et al. (1993) investigated the conformational changes of FGF-2 when lyophilized in Tris-HCl buffer. They found moderate changes in certain bands (e.g. loss of band at 1657cm^{-1} and band broadening at 1643 cm^{-1}) after lyophilization and these changes could be prevented by adding sucrose as a stabilizer. They considered this phenomenon could be explained by the water substitute hypothesis (Carpenter and Crowe, 1989). A possible mechanism could be that sucrose can form hydrogen bonds with FGF-2 and replaced the water which was lost during drying process. Therefore, unfolding of the protein due to dehydration can be inhibited. But till now, the actual protection mechanism is still not completely revealed (Chang et al., 2005; Rey and May, 2004).

In our formulation, 2 % (w v^{-1}) sucrose was added to the FGF-2 solution (1.52 mg ml^{-1} FGF-2 in 20 mM Tris-HCl pH 7.5, with 150 mM NaCl, 3 mM DTT, 1 mM EDTA) as a cryoprotectant, which resulted in no significant change in bioactivity was observed before and after dehydration as shown in Fig. 4.28.

4.6 Preliminary stability test of lyophilized FGF-2

4.6.1 Residual water content determination

The residual water content usually determines the long-term stability of lyophilized proteins (Franks, 1992; Hatley and Franks, 1991). Water can affect protein stability by acting as reaction medium or reactant (Shalaev and Zografi, 1996). Water content of lyophilized proteins can be determined by several methods, including loss-on-drying, Karl Fischer titration, thermal gravimetric analysis (TGA), gas chromatography (GC) and NIR (near infrared).

The residual water content in lyophilized FGF-2 powder was determined by loss-on-drying method. 5 random tubes were chosen from a batch of lyophilized FGF-2. The tubes were dried at 80 °C till a constant weight was reached. The weight loss was considered to be residual water. The water content was presented as the weight of water to the weight of lyophilized powder and summarized in Table 4.8. Wu et al. (1998) have investigated the degradation of FGF-2 lyophilized with sugar and found that lyophilized FGF-2 was stable unless the water content is above 2 %. Our formulation has successfully met this

requirement with average residual water content of 1.90 % and a standard deviation of 0.17 %.

Table 4.8 Residual water contents of five random chosen lyophilized FGF-2 samples.

Tube	1	2	3	4	5	Average
Residual water content (%)	1.83	1.66	1.96	1.89	2.19	1.90 ± 0.17

4.6.2 Preliminary stability test

A stability test is used to study the quality of a pharmaceutical product under specific storage conditions over a certain time period. It could be used to study the influence of the environmental factors (e.g. temperature, humidity, agitation and light) on the quality of a drug product. From the stability test a shelf-life of the pharmaceutical product could be estimated and the best storage conditions could be identified (Mollica et al., 1978).

In this test, a multiple isothermal stability method was used. Formulated FGF-2 aliquots (1 ml) were lyophilized in 15 ml screw-caped, polypropylen centrifuge tubes according to Appendix 6.3.6. After that, 14 tubes were taken out and placed in controlled-temperature unit at 37 °C (4 tubes), 4 °C (5 tubes) and room temperature (5 tubes). At set intervals one tube was removed and kept at -80 °C until analyzed.

The quantitative measurement of FGF-2 content was performed by RP-HPLC as described in Appendix 6.3.4.5. A 0 day sample of lyophilized FGF-2 was used as reference. The results are shown in Table 4.9. It is clear that no significant change of FGF-2 content was observed during 17 days storage at 37 °C, 1 month at room temperature or 2 month at 4 °C. Moreover, no FGF-2 dimers or degradation products were detected during the HPLC analysis (data not shown). Fluorescence spectrum of all the testing samples indicated all the samples were in its native conformation (data not shown). So it could be conclude that the lyophilized FGF-2 powder was stable after 17 days storage at 37 °C, 1 month at room temperature or 2 month at 4 °C.

However, physical property changes of the lyophilized FGF-2 powder (i.e. collapse, volume decrease) were observed at all storage conditions. That might because the

lyophilized protein samples were sealed under conventional atmosphere, the moisture in the air could react with the lyophilized protein and reduce its stability. If we extend the stability test period, decreases in the FGF-2 content should be seen. Therefore, it is recommended to store lyophilized FGF-2 at -20 °C to -80 °C. Supposing we can seal the lyophilized protein under nitrogen or vacuum, the storage time might be further extended.

Table 4.9 Stability data by RP-HPLC of FGF-2 in polypropylene tubes at different temperatures.

Storage time (days)	% FGF-2 remaining[a]		
	37 °C	Room temperature	4 °C
0	100.0	100.0	100.0
4	95.4		
8	96.0	99.4	
12	97.8	106.4	104.3
17	99.3	101.8	
22		110.9	
24			106.9
29		98.8	
36			102.6
51			104.7
59			117.8

[a] Percentage compare to 0 day. Percentage was calculated based on FGF-2 peak area.

4.7 Summary and conclusion

In this work, a new production process of FGF-2 from recombinant *E. coli* was described. Effective production of FGF-2 was achieved by fed-batch cultivation of *E. coli* BL21on a defined medium. Two different specific growth rates were used (0.35 h^{-1} and 0.15 h^{-1}) and final FGF-2 expression level reached 42 and 31 mg g^{-1} dry cell, respectively. Due to the high time-space yield of soluble protein (0.056 g l^{-1} h^{-1}), the higher specific growth rate (0.35 h^{-1}) was considered to be the better condition for FGF-2 production.

The downstreaming process was performed by disrupt the cells with a high pressure homogenizer followed by centrifugation. The clarified cell lysate was purified by a new combination of cation exchange membrane chromatography and heparin-sepharose affinity

chromatography. Endotoxins and DNAs were removed by passing the protein solution through an anion exchange membrane module. Finally, purified FGF-2 was formulated with sucrose and lyophilized for long-term storage. The overall yield of purified protein was about 22 % (μ_{set} = 0.35 h^{-1}) and 36 % (μ_{set} = 0.15 h^{-1}), respectively.

The purified FGF-2 was successfully identified by MALDI-TOF MS, SDS-PAGE, Western blot analysis, Fluorescence spectroscopy and RP-HPLC. The high yield, low-cost and time saving steps make this process easy to scale up for a large-scale production.

The mitogenic activity of the final product was compared with a commercially avalible FGF-2 (ref. 167100-18B-B, tebu-bio, Offenbach, Germany) on the proliferation of mesenchymal stem cell-like cells at the TCI. The activity of purified FGF-2 (EC_{50} = 0.13 ng ml^{-1}) was even higher than the commercial one (EC_{50} = 0.21 ng ml^{-1}). Activity test of purified FGF-2 on the proliferation of NIH-3T3 fibroblast cells also showed extremely high activity (EC_{50} = 0.10 ng ml^{-1}) which was comparable to the activity of a commercially available FGF-2 on 3T3 cells (EC_{50} = 0.1-1.0 ng ml^{-1}, Recombinant human FGF-2, 155 AA, Invitrogen, Karlsruhe, Germany).

The bioactivity of purified FGF-2 was also tested successfully on neuronal differentiation of PC 12 cells as well as on keeping primate ESC and human iPSC cells pluripotent at MHH. Other activity tests performed at cooperation institutes also obtained positive results which proved it has great potential for application in cell culture.

A preliminary stability test demonstrated lyophilized FGF-2 powder has a residual water content of 1.9 %. And the freeze-dried protein was stable after 17 days storage at 37 °C, 1 month at room temperature or 2 month at 4 °C.

4.8 Outlook and future work

Future work could include the following aspects:

For FGF-2 production, different expression systems could be tested in order to get more soluble fractions or absolutely soluble FGF-2. Plasmid stability and ribosome content of the cells during fed-batch cultivation should be tested to determine the best specific growth rate

for FGF-2 production. Further fed-batch cultivation up to 10 l and 30 l could be interest for large-scale production of FGF-2.

For the downstreaming process, ultrafiltration could be tested instead of centrifugation for the separation of cell lysate.

For the lyophilization, seal the lyophilized protein in centrifuge tubes under nitrogen or vacuum environment instead of conventional air condition could further extend its storage period. Further sterile lyophilization process should be developed in order to produce sterile lyophilized FGF-2.

Prior to possible clinical applications, further long-term stability test of lyophilized FGF-2 should be performed according to FDA guidelines. And further experiments should be carried out to determine the DNA and heparin content of the final product. Since heparin can leak from the heparin-sepharose affinity column and it could inhibit blood coagulation.

4.9 Acknowledgements

This work was funded from Deutsche Forschungsgemeinschaft (DFG) for the Cluster of Excellence REBIRTH.

5. References

Acheson, A., Sunshine, J.L., Rutishauser, U., 1991. NCAM polysialic acid can regulate both cell-cell and cell-substrate interactions. J. Cell Biol. 114, 143-153.

Åkesson, M., Hagander, P., Axelsson, J.P., 1999. A probing feeding strategy for *Escherichia coli* cultures. Biotechnol. Tech. 13, 523-528.

Albertson, S., Hummel, R.P., 3rd, Breeden, M., Greenhalgh, D.G., 1993. PDGF and FGF reverse the healing impairment in protein-malnourished diabetic mice. Surgery 114, 368-372; discussion 372-363.

Alexander, B., Browse, D.J., Reading, S.J., Benjamin, I.S., 1999. A simple and accurate mathematical method for calculation of the EC50. J. Pharmacol. Toxicol. Methods 41, 55-58.

Amit, M., Carpenter, M.K., Inokuma, M.S., Chiu, C.P., Harris, C.P., Waknitz, M.A., Itskovitz-Eldor, J., Thomson, J.A., 2000. Clonally derived human embryonic stem cell lines maintain pluripotency and proliferative potential for prolonged periods of culture. Dev. Biol. 227, 271-278.

Analytic Sciences Corporation. Technical Staff, Gelb, A., 1974. Applied optimal estimation. M.I.T. Press, Cambridge, Massachusetts.

Angata, T., Varki, A., 2002. Chemical diversity in the sialic acids and related alpha-keto acids: an evolutionary perspective. Chem. Rev. 102, 439-469.

Arakawa, T., Hsu, Y.-R., Schiffer, S.G., Tsai, L.B., Curless, C., Fox, G.M., 1989. Characterization of a cysteine-free analog of recombinant human basic fibroblast growth factor. Biochem. Biophys. Res. Commun. 161, 335-341.

Aristidou, A.A., San, K.Y., Bennett, G.N., 1999. Improvement of biomass yield and recombinant gene expression in *Escherichia coli* by using fructose as the primary carbon source. Biotechnol. Prog. 15, 140-145.

Arndt, M., Hitzmann, B., 2004. Kalman filter based glucose control at small set points during fed-batch cultivation of *Saccharomyces cerevisiae*. Biotechnol. Prog. 20, 377-383.

Arndt, M., Kleist, S., Miksch, G., Friehs, K., Flaschel, E., Trierweiler, J., Hitzmann, B., 2005. A feedforward-feedback substrate controller based on a Kalman filter for a fed-batch cultivation of *Escherichia coli* producing phytase. Comput. Chem. Eng. 29, 1113-1120.

Atala, A., 2006. Recent developments in tissue engineering and regenerative medicine. Curr. Opin. Pediatr. 18, 167-171.

Böttcher, R.T., Niehrs, C., 2005. Fibroblast growth factor signaling during early vertebrate development. Endocr. Rev. 26, 63-77.

Babensee, J.E., McIntire, L.V., Mikos, A.G., 2000. Growth factor delivery for tissue engineering. Pharm. Res. 17, 497-504.

Baird, A., 1994. Fibroblast growth factors: activities and significance of non-neurotrophin neurotrophic growth factors. Curr. Opin. Neurobiol. 4, 78-86.

Barry, G.T., 1958. Colominic acid, a polymer of *N*-acetylneuraminic acid. J. Exp. Med. 107, 507-521.

Barry, G.T., Goebel, W.F., 1957. Colominic acid, a substance of bacterial origin related to sialic acid. Nature 179, 206.

Bauer, K.A., Ben-Bassat, A., Dawson, M., de la Puente, V.T., Neway, J.O., 1990. Improved expression of human interleukin-2 in high-cell-density fermentor cultures of *Escherichia coli* K-12 by a phosphotransacetylase mutant. Appl Environ Microbiol 56, 1296-1302.

Beenken, A., Mohammadi, M., 2009. The FGF family: biology, pathophysiology and therapy. Nat. Rev. Drug Discov. 8, 235-253.

Bellgardt, K.H., Kuhlmann, W., Meyer, H.D., Schügerl, K., Thoma, M., 1986. Application of an extended Kalman filter for state estimation of a yeast fermentation. Control Theory and Applications, IEE Proceedings D 133, 226-234.

Bennett, S.P., Griffiths, G.D., Schor, A.M., Leese, G.P., Schor, S.L., 2003. Growth factors in the treatment of diabetic foot ulcers. Br. J. Surg. 90, 133-146.

Benthin, S., Nielsen, J., Villadsen, J., 1992. Flow-injection analysis of micromolar concentrations of glucose and lactate in fermentation media. Anal. Chim. Acta 261, 145-153.

Berski, S., van Bergeijk, J., Schwarzer, D., Stark, Y., Kasper, C., Scheper, T., Grothe, C., Gerardy-Schahn, R., Kirschning, A., Dräger, G., 2008. Synthesis and biological evaluation of a polysialic acid-based hydrogel as enzymatically degradable scaffold material for tissue engineering. Biomacromolecules 9, 2353-2359.

Bianco, P., Robey, P.G., 2001. Stem cells in tissue engineering. Nature 414, 118-121.

Bikfalvi, A., Klein, S., Pintucci, G., Rifkin, D.B., 1997. Biological roles of fibroblast growth factor-2. Endocr. Rev. 18, 26-45.

Bittner, C., Wehnert, G., Scheper, T., 1998. In situ microscopy for on-line determination of biomass. Biotechnol. Bioeng. 60, 24-35.

Bliss, J.M., Silver, R.P., 1996. Coating the surface: a model for expression of capsular polysialic acid in *Escherichia coli* K1. Mol. Microbiol. 21, 221-231.

Brandt, J., Hitzmann, B., 1994. Knowledge-based fault detection and diagnosis in flow-injection analysis. Anal. Chim. Acta 291, 29-40.

Brown, R.G., Hwang, P.Y.C., 1992. Introduction to random signals and applied Kalman filtering, 2nd ed. J. Wiley, New York.

Brown, S., Meyer, H.-P., Fiechter, A., 1985. Continuous production of human leukocyte interferon with *Escherichia coli* and continuous cell lysis in a two stage chemostat. Appl. Microbiol. Biotechnol. 23, 5-9.

Bruses, J.L., Rutishauser, U., 2001. Roles, regulation, and mechanism of polysialic acid function during neural development. Biochimie 83, 635-643.

Burgess, W.H., Maciag, T., 1989. The Heparin-Binding (Fibroblast) Growth Factor Family of Proteins. Annu. Rev. Biochem. 58, 575-606.

Button, D.K., 1985. Kinetics of nutrient-limited transport and microbial growth. Microbiol. Rev. 49, 270-297.

Candiano, G., Bruschi, M., Musante, L., Santucci, L., Ghiggeri, G.M., Carnemolla, B., Orecchia, P., Zardi, L., Righetti, P.G., 2004. Blue silver: a very sensitive colloidal Coomassie G-250 staining for proteome analysis. Electrophoresis 25, 1327-1333.

Cantz, T., Martin, U., 2010. Induced pluripotent stem cells: characteristics and perspectives. Adv. Biochem. Eng. Biotechnol. 123, 107-126.

Carpenter, J.F., Crowe, J.H., 1989. An infrared spectroscopic study of the interactions of carbohydrates with dried proteins. Biochemistry 28, 3916-3922.

Chéruy, A., 1997. Software sensors in bioprocess engineering. J. Biotechnol. 52, 193-199.

Chang, L., Shepherd, D., Sun, J., Ouellette, D., Grant, K.L., Tang, X., Pikal, M.J., 2005. Mechanism of protein stabilization by sugars during freeze-drying and storage: Native structure preservation, specific interaction, and/or immobilization in a glassy matrix? J. Pharm. Sci. 94, 1427-1444.

Chen, L.Z., Nguang, S.K., Li, X.M., Chen, X.D., 2004. Soft sensors for on-line biomass measurements. Bioprocess Biosyst. Eng. 26, 191-195.

Costantino, H.R., Griebenow, K., Mishra, P., Langer, R., Klibanov, A.M., 1995. Fourier-transform infrared spectroscopic investigation of protein stability in the lyophilized form. Biochim. Biophys. Acta 1253, 69-74.

Council of Europe, European Pharmacopoeia Commission, 2007. European pharmacopoeia, 6th ed ed. Council of Europe, Strasbourg.

Curless, C., Pope, J., Tsai, L., 1990. Effect of preinduction specific growth rate on recombinant alpha consensus interferon synthesis in *Escherichia coli*. Biotechnol. Prog. 6, 149-152.

Cutayar, J.M., Poillon, D., 1989. High cell density culture of *E. coli* in a fed-batch system with dissolved oxygen as substrate feed indicator. Biotechnol. Lett. 11, 155-160.

de Assis, A.J., Filho, R.M., 2000. Soft sensors development for on-line bioreactor state estimation. Comput. Chem. Eng. 24, 1099-1103.

do Carmo Nicoletti, M., Jain, L., Nicoletti, M., Jain, L., Giordano, R., 2009. Computational Intelligence Techniques as Tools for Bioprocess Modelling, Optimization, Supervision and Control. In: do Carmo Nicoletti, M., Jain, L.C. (Eds.), Computational Intelligence Techniques for Bioprocess Modelling, Supervision and Control. Springer Berlin / Heidelberg, pp. 1-23.

Doelle, H., Ewings, K., Hollywood, N., 1982. Regulation of glucose metabolism in bacterial systems. In: Fiechter A. (Ed.), Microbial Reactions. Springer Berlin / Heidelberg, pp. 1-35.

Dong, A., Prestrelski, S.J., Allison, S.D., Carpenter, J.F., 1995a. Infrared spectroscopic studies of lyophilization- and temperature-induced protein aggregation. J. Pharm. Sci. 84, 415-424.

Dong, H., Nilsson, L., Kurland, C., 1995b. Gratuitous overexpression of genes in *Escherichia coli* leads to growth inhibition and ribosome destruction. J. Bacteriol. 177, 1497-1504.

Dubach, A.C., Märkl, H., 1992. Application of an extended kalman filter method for monitoring high density cultivation of *Escherichia coli*. J. Ferment. Bioeng. 73, 396-402.

El Maarouf, A., Petridis, A.K., Rutishauser, U., 2006. Use of polysialic acid in repair of the central nervous system. Proc Natl Acad Sci USA 103, 16989-16994.

Emancipator, K., Csako, G., Elin, R.J., 1992. In vitro inactivation of bacterial endotoxin by human lipoproteins and apolipoproteins. Infect. Immun. 60, 596-601.

Eriksson, A.E., Cousens, L.S., Matthews, B.W., 1993. Refinement of the structure of human basic fibroblast growth factor at 1.6 Å resolution and analysis of presumed heparin binding sites by selenate substitution. Protein Sci. 2, 1274-1284.

Eriksson, A.E., Cousens, L.S., Weaver, L.H., Matthews, B.W., 1991. Three-dimensional structure of human basic fibroblast growth factor. Proc. Natl. Acad. Sci. U. S. A. 88, 3441-3445.

Estape, D., van den Heuvel, J., Rinas, U., 1998. Susceptibility towards intramolecular disulphide-bond formation affects conformational stability and folding of human basic fibroblast growth factor. Biochem. J. 335, 343-349.

Fallon, J.F., Lopez, A., Ros, M.A., Savage, M.P., Olwin, B.B., Simandl, B.K., 1994. FGF-2: apical ectodermal ridge growth signal for chick limb development. Science 264, 104-107.

Fass, R., Clem, T.R., Shiloach, J., 1989. Use of a novel air separation system in a fed-batch fermentative culture of *Escherichia coli*. Appl. Environ. Microbiol. 55, 1305-1307.

Fiddes, J.C., Hebda, P.A., Hayward, P., Robson, M.C., Abraham, J.A., Klingbeil, C.K., 1991. Preclinical wound-healing studies with recombinant human basic fibroblast growth factor. Ann. N. Y. Acad. Sci. 638, 316-328.

Finne, J., 1982. Occurrence of unique polysialosyl carbohydrate units in glycoproteins of developing brain. J. Biol. Chem. 257, 11966-11970.

Foster, L., Thompson, S.A., Tarnowski, J.S., United States Patent No. 5217954 (Jun. 8, 1993).

Fox, G.M., Schiffer, S.G., Rohde, M.F., Tsai, L.B., Banks, A.R., Arakawa, T., 1988. Production, biological activity, and structure of recombinant basic fibroblast growth factor and an analog with cysteine replaced by serine. J. Biol. Chem. 263, 18452-18458.

Franks, F., 1992. Freeze-drying: from empiricism to predictability. The significance of glass transitions. Dev. Biol. Stand. 74, 9-18; discussion 19.

Fredrickson, A.G., Megee Iii, R.D., Tsuchiya, H.M., Perlman, D., 1970. Mathematical Models for Fermentation Processes. In: Allen, L., Geoffrey, G., Sima, S. (Eds.), Adv. Appl. Microbiol. Academic Press, pp. 419-465.

Garke, G., Deckwer, W.D., Anspach, F.B., 2000. Preparative two-step purification of recombinant human basic fibroblast growth factor from high-cell-density cultivation of *Escherichia coli*. J. Chromatogr. B Biomed. Sci. Appl. 737, 25-38.

Garke, G., Radtschenko, I., Anspach, F.B., 1999. Continuous-bed chromatography for the analysis and purification of recombinant human basic fibroblast growth factor. J. Chromatogr. A 857, 137-144.

Garn, M., Gisin, M., Thommen, C., Cevey, P., 1989. A flow injection analysis system for fermentation monitoring and control. Biotechnol. Bioeng. 34, 423-428.

Gasparian, M.E., Elistratov, P.A., Drize, N.I., Nifontova, I.N., Dolgikh, D.A., Kirpichnikov, M.P., 2009. Overexpression in *Escherichia coli* and purification of human fibroblast growth factor (FGF-2). Biochemistry (Mosc.) 74, 221-225.

Ghosh, R., 2002. Protein separation using membrane chromatography: opportunities and challenges. J. Chromatogr. A 952, 13-27.

Ghoul, M., Dardenne, M., Fonteix, C., Marc, A., 1991. Extended Kalman Filtering technique for the on-line control of OKT3 hybridoma cultures. Biotechnol. Tech. 5, 367-370.

Gnoth, S., Jenzsch, M., Simutis, R., Lübbert, A., 2008. Control of cultivation processes for recombinant protein production: a review. Bioprocess Biosyst. Eng. 31, 21-39.

González-Clemente, C., Luengo, J.M., Rodríguez-Aparicio, L.B., Ferrero, M.A., Reglero, A., 1990. High production of polysialic acid [Neu5Ac alpha(2-8)-Neu5Ac alpha(2-9)]n by *Escherichia coli* K92 grown in a chemically defined medium. Regulation of temperature. Biol. Chem. Hoppe. Seyler 371, 1101-1106.

Gospodarowicz, D., 1974. Localisation of a fibroblast growth factor and its effect alone and with hydrocortisone on 3T3 cell growth. Nature 249, 123-127.

Gospodarowicz, D., Cheng, J., 1986. Heparin protects basic and acidic FGF from inactivation. J. Cell. Physiol. 128, 475-484.

Gregoriadis , G., Fernandes , A., Mital, M., McCormack, B., 2000. Polysialic acids: potential in improving the stability and pharmacokinetics of proteins and other therapeutics. Cell. Mol. Life Sci. 57, 1964-1969.

Gregoriadis, G., McCormack, B., Wang, Z., Lifely, R., 1993. Polysialic acids: potential in drug delivery. FEBS Lett. 315, 271-276.

Gunsalus, I.C., Stanier, R.Y., Orston, L.N., Sokatch, J.R., 1960. The Bacteria; a treatise on structure and function. Academic Press, New York,.

Haase, A., Olmer, R., Schwanke, K., Wunderlich, S., Merkert, S., Hess, C., Zweigerdt, R., Gruh, I., Meyer, J., Wagner, S., Maier, L.S., Han, D.W., Glage, S., Miller, K., Fischer, P., Scholer, H.R., Martin, U., 2009. Generation of induced pluripotent stem cells from human cord blood. Cell Stem Cell 5, 434-441.

Haile, Y., Haastert, K., Cesnulevicius, K., Stummeyer, K., Timmer, M., Berski, S., Dräger, G., Gerardy-Schahn, R., Grothe, C., 2007. Culturing of glial and neuronal cells on polysialic acid. Biomaterials 28, 1163-1173.

Halaban, R., Fan, B., Ahn, J., Funasaka, Y., Gitay-Goren, H., Neufeld, G., 1992. Growth factors, receptor kinases, and protein tyrosine phosphatases in normal and malignant melanocytes. J Immunother (1991) 12, 154-161.

Han, K., Lim, H.C., Hong, J., 1992a. Acetic acid formation in *Escherichia coli* fermentation. Biotechnol. Bioeng. 39, 663-671.

Han, R.N., Liu, J., Tanswell, A.K., Post, M., 1992b. Expression of basic fibroblast growth factor and receptor: immunolocalization studies in developing rat fetal lung. Pediatr. Res. 31, 435-440.

Hatley, R.H.M., Franks, F., 1991. Applications of DSC in the development of improved freeze-drying processes for labile biologicals. J. Therm. Anal. Calorim. 37, 1905-1914.

Hellmuth, K., Korz, D.J., Sanders, E.A., Deckwer, W.D., 1994. Effect of growth rate on stability and gene expression of recombinant plasmids during continuous and high cell density cultivation of *Escherichia coli* TG1. J. Biotechnol. 32, 289-298.

Hempfling, W.P., Mainzer, S.E., 1975. Effects of varying the carbon source limiting growth on yield and maintenance characteristics of *Escherichia coli* in continuous culture. J. Bacteriol. 123, 1076-1087.

Hilaly, A.K., Karim, M.N., Linden, J.C., 1994. Use of an Extended Kalman Filter and development of an automated system for xylose fermentation by a recombinant *Escherichia coli*. J. Ind. Microbiol. Biotechnol. 13, 83-89.

Hitzmann, B., Broxtermann, O., Cha, Y.L., Sobieh, O., Stärk, E., Scheper, T., 2000. The control of glucose concentration during yeast fed-batch cultivation using a fast measurement complemented by an extended Kalman filter. Bioprocess Biosyst. Eng. 23, 337-341.

Hitzmann, B., Gomersall, R., Brandt, J., van Putten, A., 1996. An expert system for the supervision of a multichannel flow injection analysis system. In: Kim, R.R., Ashok, M., Weichang Z. (Ed.), Biosensor and Chemical Sensor Technology. American Chemical Society, pp. 133-143.

Hitzmann, B., Löhn, A., Arndt, M., Ulber, R., Müller, C., 1997. A new evaluation technique for FIA measurements: projective reference evaluation. Anal. Chim. Acta 348, 161-166.

Hitzmann, B., Löhn, A., Reinecke, M., Schulze, B., Scheper, T., 1995. The automation of immun-FIA-systems. Anal. Chim. Acta 313, 55-62.

Hoffmann, F., Heuvel, J.v.d., Zidek, N., Rinas, U., 2004. Minimizing inclusion body formation during recombinant protein production in *Escherichia coli* at bench and pilot plant scale. Enzyme Microb. Technol. 34, 235-241.

Holms, W.H., 1986. The central metabolic pathways of *Escherichia coli*: relationship between flux and control at a branch point, efficiency of conversion to biomass, and excretion of acetate. Curr. Top. Cell. Regul. 28, 59-105.

Honda, H., Sugiyama, H., Saito, I., Kobayashi, T., 1998. High cell density culture of *Rhodococcus rhodochrous* by pH-stat feeding and dibenzothiophene degradation. J. Ferment. Bioeng. 85, 334-338.

Horn, U., Strittmatter, W., Krebber, A., Knupfer, U., Kujau, M., Wenderoth, R., Muller, K., Matzku, S., Pluckthun, A., Riesenberg, D., 1996. High volumetric yields of functional dimeric miniantibodies in *Escherichia coli*, using an optimized expression vector and high-cell-density fermentation under non-limited growth conditions. Appl. Microbiol. Biotechnol. 46, 524-532.

Hutmacher, D.W., 2001. Scaffold design and fabrication technologies for engineering tissues state of the art and future perspectives. J. Biomater. Sci. Polym. Ed. 12, 107-124.

Ifkovits, J.L., Burdick, J.A., 2007. Review: photopolymerizable and degradable biomaterials for tissue engineering applications. Tissue Eng. 13, 2369-2385.

Iida, S., Katoh, O., Tokunaga, A., Terada, M., 1994. Expression of fibroblast growth factor gene family and its receptor gene family in the human upper gastrointestinal tract. Biochem. Biophys. Res. Commun. 199, 1113-1119.

Iwane, M., Kurokawa, T., Sasada, R., Seno, M., Nakagawa, S., Igarashi, K., 1987. Expression of cDNA encoding human basic fibroblast growth factor in *E. coli*. Biochem. Biophys. Res. Commun. 146, 470-477.

Iyer, K.S., Klee, W.A., 1973. Direct spectrophotometric measurement of the rate of reduction of disulfide bonds. The reactivity of the disulfide bonds of bovine -lactalbumin. J. Biol. Chem. 248, 707-710.

Jacobs, O.L.R., 1993. Introduction to control theory, 2nd ed. Oxford University Press, Oxford ; New York.

Jenzsch, M., Gnoth, S., Beck, M., Kleinschmidt, M., Simutis, R., Lübbert, A., 2006. Open-loop control of the biomass concentration within the growth phase of recombinant protein production processes. J. Biotechnol. 127, 84-94.

Joeris, K., Frerichs, J.-G., Konstantinov, K., Scheper, T., 2002. *In-situ* microscopy: Online process monitoring of mammalian cell cultures. Cytotechnology 38, 129-134.

Johnson, A., 1987. The control of fed-batch fermentation processes--A survey. Automatica 23, 691-705.

Kalman, R.E., 1960. A new approach to linear filtering and prediction problems. Transactions of the ASME-Journal of Basic Engineering, 35-45.

Kapre, S.V., Shaligram, U., United States Patent No. 20100086974 (Apr. 8, 2010).

Kazan, D., Çamurdan, A., Hortaçsu, A., 1995. The effect of glucose concentration on the growth rate and some intracellular components of a recombinant *E. coli* culture. Process Biochem. 30, 269-273.

Ke, L.D., Karaganis, A.G., Shain, S.A., 1992. A rapid, two-step method for high-yield purification of recombinant rat acidic and basic fibroblast growth factors. Protein Expr. Purif. 3, 497-507.

Kelm, S., Schauer, R., 1997. Sialic acids in molecular and cellular interactions. Int. Rev. Cytol. 175, 137-240.

Kim, B., Lee, S., Kaistha, S.D., Rouse, B.T., 2006. Application of FGF-2 to modulate herpetic stromal keratitis. Curr. Eye Res. 31, 1021-1028.

King, W.J., Jongpaiboonkit, L., Murphy, W.L., 2009. Influence of FGF2 and PEG hydrogel matrix properties on hMSC viability and spreading. J. Biomed. Mater. Res. Part A 93A, 1110-1123.

Kitamura, M., Nakashima, K., Kowashi, Y., Fujii, T., Shimauchi, H., Sasano, T., Furuuchi, T., Fukuda, M., Noguchi, T., Shibutani, T., Iwayama, Y., Takashiba, S., Kurihara, H., Ninomiya, M., Kido, J., Nagata, T., Hamachi, T., Maeda, K., Hara, Y., Izumi, Y., Hirofuji, T., Imai, E., Omae, M., Watanuki, M., Murakami, S., 2008. Periodontal tissue regeneration using fibroblast growth factor-2: randomized controlled phase II clinical trial. PLoS One 3, e2611.

Kleist, S., Miksch, G., Hitzmann, B., Arndt, M., Friehs, K., Flaschel, E., 2003. Optimization of the extracellular production of a bacterial phytase with *Escherichia coli* by using different fed-batch fermentation strategies. Appl. Microbiol. Biotechnol. 61, 456-462.

Kleman, G.L., Chalmers, J.J., Luli, G.W., Strohl, W.R., 1991. A predictive and feedback control algorithm maintains a constant glucose concentration in fed-batch fermentations. Appl. Environ. Microbiol. 57, 910-917.

Klockow, C., Hüll, D., Hitzmann, B., 2008. Model based substrate set point control of yeast cultivation processes based on FIA measurements. Anal. Chim. Acta 623, 30-37.

Knoerzer, W., Binder, H.P., Schneider, K., Gruss, P., McCarthy, J.E., Risau, W., 1989. Expression of synthetic genes encoding bovine and human basic fibroblast growth factors (bFGFs) in *Escherichia coli*. Gene 75, 21-30.

Koh, B.T., Nakashimada, U., Pfeiffer, M., Yap, M.G.S., 1992. Comparison of acetate inhibition on growth of host and recombinant *E. col*i K12 strains. Biotechnol. Lett. 14, 1115-1118.

Koh, C.J., Atala, A., 2004. Tissue engineering, stem cells, and cloning: opportunities for regenerative medicine. J. Am. Soc. Nephrol. 15, 1113-1125.

Konstantinov, K., Kishimoto, M., Seki, T., Yoshida, T., 1990. A balanced DO-stat and its application to the control of acetic acid excretion by recombinant *Escherichia coli*. Biotechnol. Bioeng. 36, 750-758.

Konstantinov, K.B., Yoshida, T., 1992. Knowledge-based control of fermentation processes. Biotechnol. Bioeng. 39, 479-486.

Kopp, R.E., Orford, R.J., 1963. Linear regression applied to system identification for adaptive control systems. AIAA Journal 1, 2300-2306.

Korz, D.J., Rinas, U., Hellmuth, K., Sanders, E.A., Deckwer, W.D., 1995. Simple fed-batch technique for high cell density cultivation of *Escherichia coli*. J. Biotechnol. 39, 59-65.

Krause, S., Kroner, K.H., Deckwer, W.D., 1991. Comparison of affinity membranes and conventional affinity matrices with regard to protein purification. Biotechnol. Tech. 5, 199-204.

Kroiher, M., Raffioni, S., Steele, R.E., 1995. Single step purification of biologically active recombinant rat basic fibroblast growth factor by immobilized metal affinity chromatography. Biochim. Biophys. Acta 1250, 29-34.

Kubota, N., Miura, S., Saito, K., Sugita, K., Watanabe, K., Sugo, T., 1996. Comparison of protein adsorption by anion-exchange interaction onto porous hollow-fiber membrane and gel bead-packed bed. J. Membr. Sci. 117, 135-142.

Kumar, M.A., Thakur, M.S., Senthuran, A., Senthuran, V., Karanth, N.G., Hatti-Kaul, R., Mattiasson, B., 2001. An automated flow injection analysis system for on-line monitoring of glucose and *L*-lactate during lactic acid fermentation in a recycle bioreactor. World J. Microbiol. Biotechnol. 17, 23-29.

Laemmli, U.K., 1970. Cleavage of structural proteins during the assembly of the head of bacteriophage T4. Nature 227, 680-685.

Lanza, R.P., Langer, R.S., Vacanti, J., 2007. Principles of tissue engineering, 3rd ed. Elsevier Academic Press, Amsterdam ; Boston.

Lappi, D.A., Ying, W., Barthelemy, I., Martineau, D., Prieto, I., Benatti, L., Soria, M., Baird, A., 1994. Expression and activities of a recombinant basic fibroblast growth factor-saporin fusion protein. J. Biol. Chem. 269, 12552-12558.

Lee, J.H., Ricker, N.L., 1994. Extended Kalman filter based nonlinear model predictive control. Ind. Eng. Chem. Res. 33, 1530-1541.

Lee, S.J., 2000. Cytokine delivery and tissue engineering. Yonsei Med. J. 41, 704-719.

Lee, S.Y., 1996. High cell-density culture of *Escherichia coli*. Trends Biotechnol. 14, 98-105.

Lee, S.Y., Chang, H.N., 1993. High cell density cultivation of *Escherichia coli* W using sucrose as a carbon source. Biotechnol. Lett. 15, 971-974.

Lemaître, G., Laaroubi, K., Soulet, L., Barritault, D., Miskulin, M., 1995. Production and purification of active FGF2 via recombinant fusion protein. Biochimie 77, 162-166.

Leo, A.J., Grande, D.A., 2006. Mesenchymal stem cells in tissue engineering. Cells Tissues Organs 183, 112-122.

Lindemann, C., Marose, S., Nielsen, H.O., Scheper, T., 1998. 2-Dimensional fluorescence spectroscopy for on-line bioprocess monitoring. Sens. Actuators, B 51, 273-277.

Liu, J.-L., Wu, J.-R., Shen, F.-D., Yu, D.-F., zhang, Q., Zhan, X.-b., 2010. A new strategy to enhance polysialic acid production by controlling sorbitol concentration in cultivation of *Escherichia coli* K235. Afr. J. Biotechnol. 9, 2422-2426.

Liu, W., 1999. An extended Kalman filter and neural network cascade fault diagnosis strategy for the glutamic acid fermentation process. Artif. Intell. Eng. 13, 131-140.

Liu, Y., Song, Z., Zhao, Y., Qin, H., Cai, J., Zhang, H., Yu, T., Jiang, S., Wang, G., Ding, M., Deng, H., 2006. A novel chemical-defined medium with bFGF and N2B27 supplements supports undifferentiated growth in human embryonic stem cells. Biochem. Biophys. Res. Commun. 346, 131-139.

Logan, A., Frautschy, S.A., Baird, A., 1991. Basic fibroblast growth factor and central nervous system injury. Ann. N. Y. Acad. Sci. 638, 474-476.

Luthra, S., Kalonia, D.S., Pikal, M.J., 2007. Effect of hydration on the secondary structure of lyophilized proteins as measured by fourier transform infrared (FTIR) spectroscopy. J. Pharm. Sci. 96, 2910-2921.

Märkl, H., Zenneck, C., Dubach, A.C., Ogbonna, J.C., 1993. Cultivation of *Escherichia coli* to high cell densities in a dialysis reactor. Appl. Microbiol. Biotechnol. 39, 48-52.

Ma, P.X., Elisseeff, J.H., 2006. Scaffolding in tissue engineering. Taylor & Francis, Boca Raton.

Macdonald, M.L., Rodriguez, N.M., Shah, N.J., Hammond, P.T., 2010. Characterization of Tunable FGF-2 Releasing Polyelectrolyte Multilayers. Biomacromolecules 11, 2053-2059.

Magalhães, P.O., Lopes, A.M., Mazzola, P.G., Rangel-Yagui, C., Penna, T.C., Pessoa, A., Jr., 2007. Methods of endotoxin removal from biological preparations: a review. J. Pharm. Pharm. Sci. 10, 388-404.

Majewski, R.A., Domach, M.M., 1990. Simple constrained-optimization view of acetate overflow in *E. coli*. Biotechnol. Bioeng. 35, 732-738.

Male, K.B., Gartu, P.O., Kamen, A.A., Luong, J.H.T., 1997. On-line monitoring of glucose in mammalian cell culture using a flow injection analysis (FIA) mediated biosensor. Biotechnol. Bioeng. 55, 497-504.

Marose, S., Lindemann, C., Scheper, T., 1998. Two-dimensional fluorescence spectroscopy: a new tool for on-line bioprocess monitoring. Biotechnol. Prog. 14, 63-74.

Marose, S., Lindemann, C., Ulber, R., Scheper, T., 1999. Optical sensor systems for bioprocess monitoring. Trends Biotechnol. 17, 30-34.

Marra, K.G., Defail, A.J., Clavijo-Alvarez, J.A., Badylak, S.F., Taieb, A., Schipper, B., Bennett, J., Rubin, J.P., 2008. FGF-2 enhances vascularization for adipose tissue engineering. Plast. Reconstr. Surg. 121, 1153-1164.

Maybeck, P.S., 1979. Stochastic models, estimation and control. Academic Press, New York.

McAvoy, J.W., Chamberlain, C.G., de Iongh, R.U., Richardson, N.A., Lovicu, F.J., 1991. The role of fibroblast growth factor in eye lens development. Ann. N. Y. Acad. Sci. 638, 256-274.

McGuire, E.J., Binkley, S.B., 1964. The Structure and Chemistry of Colominic Acid. Biochemistry (Mosc.) 3, 247-251.

Meinhold, R.J., Singpurwalla, N.D., 1983. Understanding the Kalman Filter. Am. Stat. 37, 123-127.

Meyer, H.-P., Leist, C., Fiechter, A., 1984. Acetate formation in continuous culture of *Escherichia coli* K12 D1 on defined and complex media. J. Biotechnol. 1, 355-358.

Minobe, S., Sato, T., Tosa, T., Chibata, I., 1983. Characteristics of immobilized histamine for pyrogen adsorption. J. Chromatogr. 262, 193-198.

Mizanur, R.M., Pohl, N.L., 2008. Bacterial CMP-sialic acid synthetases: production, properties, and applications. Appl Microbiol Biotechnol 80, 757-765.

Mollica, J.A., Ahuja, S., Cohen, J., 1978. Stability of pharmaceuticals. J. Pharm. Sci. 67, 443-465.

Monod, J., 1949. The Growth of Bacterial Cultures. Annu. Rev. Microbiol. 3, 371-394.

Moreno, C., Lifely, M.R., Esdaile, J., 1985. Immunity and protection of mice against *Neisseria meningitidis* group B by vaccination, using polysaccharide complexed with outer membrane proteins: a comparison with purified B polysaccharide. Infect. Immun. 47, 527-533.

Mori, H., Yano, T., Kobayashi, T., Shimizu, S., 1979. High density cultivation of biomass in fed-batch system with DO-stat. J. Chem. Eng. Jpn. 12, 313-319.

Moxon, E.R., Kroll, J.S., 1990. The role of bacterial polysaccharide capsules as virulence factors. Curr. Top. Microbiol. Immunol. 150, 65-85.

Murakami, S., Takayama, S., Ikezawa, K., Sltimabukuro, Y., Kitamura, M., Nozaki, T., Terashima, A., Asano, T., Okada, H., 1999. Regeneration of periodontal tissues by basic fibroblast growth factor. J. Periodontal Res. 34, 425-430.

Murono, E.P., Washburn, A.L., Goforth, D.P., Wu, N., 1992. Evidence for basic fibroblast growth factor receptors in cultured immature Leydig cells. Mol. Cell. Endocrinol. 88, 39-45.

Náhlík, J., Burianec, Z., 1988. On-line parameter and state estimation of continuous cultivation by extended Kalman filter. Appl. Microbiol. Biotechnol. 28, 128-134.

Nakamura, S., Kanatani, Y., Kishimoto, S., Nakamura, S.-i., Ohno, C., Horio, T., Masanori, F., Hattori, H., Tanaka, Y., Kiyosawa, T., Maehara, T., Ishihara, M., 2009. Controlled release of FGF-2 using fragmin/protamine microparticles and effect on neovascularization. J. Biomed. Mater. Res. Part A 91A, 814-823.

Nakano, K., Rischke, M., Sato, S., Märkl, H., 1997. Influence of acetic acid on the growth of *Escherichia coli* K12 during high-cell-density cultivation in a dialysis reactor. Appl. Microbiol. Biotechnol. 48, 597-601.

Olmer, R., Haase, A., Merkert, S., Cui, W., Palecek, J., Ran, C., Kirschning, A., Scheper, T., Glage, S., Miller, K., Curnow, E.C., Hayes, E.S., Martin, U., 2010. Long term expansion of undifferentiated human iPS and ES cells in suspension culture using a defined medium. Stem Cell Res. 5, 51-64.

Ornitz, D.M., Itoh, N., 2001. Fibroblast growth factors. Genome Biol. 2, REVIEWS3005.3001-3005.3012.

Orskov, F., Sharma, V., Orskov, I., 1984. Influence of growth temperature on the development of *Escherichia coli* polysaccharide K antigens. J. Gen. Microbiol. 130, 2681-2684.

Paalme, T., Tiisma, K., Kahru, A., Vanatalu, K., Vilu, R., 1990. Glucose-limited fed-batch cultivation of *Escherichia coli* with computer-controlled fixed growth rate. Biotechnol. Bioeng. 35, 312-319.

Park, C.M., Hollenberg, M.J., 1993. Growth factor-induced retinal regeneration *in vivo*. Int. Rev. Cytol. 146, 49-74.

Park, S., Ryu, D.D.Y., Kim, J.Y., 1990. Effect of cell growth rate on the performance of a two-stage continuous culture system in a recombinant *Escherichia coli* fermentation. Biotechnol. Bioeng. 36, 493-505.

Patry, V., Bugler, B., Amalric, F., Prom, J.-C., Prats, H., 1994. Purification and characterization of the 210-amino acid recombinant basic fibroblast growth factor form (FGF-2). FEBS Lett. 349, 23-28.

Pei, M., Seidel, J., Vunjak-Novakovic, G., Freed, L.E., 2002. Growth factors for sequential cellular de- and re-differentiation in tissue engineering. Biochem. Biophys. Res. Commun. 294, 149-154.

Pelkonen, S., Hayrinen, J., Finne, J., 1988. Polyacrylamide gel electrophoresis of the capsular polysaccharides of *Escherichia coli* K1 and other bacteria. J. Bacteriol. 170, 2646-2653.

Petsch, D., Anspach, F.B., 2000. Endotoxin removal from protein solutions. J. Biotechnol. 76, 97-119.

Petsch, D., Deckwer, W.D., Anspach, F.B., 1998. Proteinase K digestion of proteins improves detection of bacterial endotoxins by the *Limulus* amebocyte lysate assay: application for endotoxin removal from cationic proteins. Anal. Biochem. 259, 42-47.

Plotnikov, A.N., Hubbard, S.R., Schlessinger, J., Mohammadi, M., 2000. Crystal structures of two FGF-FGFR complexes reveal the determinants of ligand-receptor specificity. Cell 101, 413-424.

Polak, J.M., Bishop, A.E., 2006. Stem cells and tissue engineering: past, present, and future. Ann. N. Y. Acad. Sci. 1068, 352-366.

Prestrelski, S.J., Tedeschi, N., Arakawa, T., Carpenter, J.F., 1993. Dehydration-induced conformational transitions in proteins and their inhibition by stabilizers. Biophys. J. 65, 661-671.

Reif, K., Unbehauen, R., 1999. The extended Kalman filter as an exponential observer for nonlinear systems. IEEE Trans. Signal Processing 47, 2324-2328.

Rey, L., May, J.C., 2004. Freeze-drying/lyophilization of pharmaceutical and biological products, 2nd ed. Marcel Dekker, New York.

Riesenberg, D., 1991. High-cell-density cultivation of *Escherichia coli*. Curr. Opin. Biotechnol. 2, 380-384.

Riesenberg, D., Guthke, R., 1999. High-cell-density cultivation of microorganisms. Appl. Microbiol. Biotechnol. 51, 422-430.

Riesenberg, D., Menzel, K., Schulz, V., Schumann, K., Veith, G., Zuber, G., Knorre, W.A., 1990. High cell density fermentation of recombinant *Escherichia coli* expressing human interferon alpha 1. Appl. Microbiol. Biotechnol. 34, 77-82.

Rinas, U., Kracke-Helm, H.-A., Schügerl, K., 1989. Glucose as a substrate in recombinant strain fermentation technology. Appl. Microbiol. Biotechnol. 31, 163-167.

Rode, B., Endres, C., Ran, C., Stahl, F., Beutel, S., Kasper, C., Galuska, S., Geyer, R., Muhlenhoff, M., Gerardy-Schahn, R., Scheper, T., 2008. Large-scale production and homogenous purification of long chain polysialic acids from *E. coli* K1. J. Biotechnol. 135, 202-209.

Rodríguez-Aparicio, L.B., Reglero, A., Ortiz, A.I., Luengo, J.M., 1988. Effect of physical and chemical conditions on the production of colominic acid by *Escherichia coli* in a defined medium. Appl. Microbiol. Biotechnol. 27, 474-483.

Rogy, M.A., Moldawer, L.L., Oldenburg, H.S., Thompson, W.A., Montegut, W.J., Stackpole, S.A., Kumar, A., Palladino, M.A., Marra, M.N., Lowry, S.F., 1994. Anti-endotoxin therapy in primate bacteremia with HA-1A and BPI. Ann. Surg. 220, 77-85.

Rohr, T.E., Troy, F.A., 1980. Structure and biosynthesis of surface polymers containing polysialic acid in *Escherichia coli*. J. Biol. Chem. 255, 2332-2342.

Roidl, A., Berger, H.-J., Kumar, S., Bange, J., Knyazev, P., Ullrich, A., 2009. Resistance to Chemotherapy Is Associated with Fibroblast Growth Factor Receptor 4 Up-Regulation. Clin. Cancer Res. 15, 2058-2066.

Roper, D.K., Lightfoot, E.N., 1995. Separation of biomolecules using adsorptive membranes. J. Chromatogr. A 702, 3-26.

Rosenberg, A., 1995. Biology of the sialic acids. Plenum Press, New York.

Růžička, J., Hansen, E.H., 1975. Flow injection analyses: Part I. A new concept of fast continuous flow analysis. Anal. Chim. Acta 78, 145-157.

Růžička, J., Hansen, E.H., 1988. Flow injection analysis, 2nd ed. J. Wiley, New York.

Sakamoto, S., Iijima, M., Matsuzawa, H., Ohta, T., 1994. Production of thermophilic protease by glucose-controlled fed-batch culture of recombinant *Escherichia coli*. J. Ferment. Bioeng. 78, 304-309.

Sandén, A.M., Prytz, I., Tubulekas, I., Forberg, C., Le, H., Hektor, A., Neubauer, P., Pragai, Z., Harwood, C., Ward, A., Picon, A., De Mattos, J.T., Postma, P., Farewell, A., Nystrom, T., Reeh, S., Pedersen, S., Larsson, G., 2003. Limiting factors in *Escherichia coli* fed-batch production of recombinant proteins. Biotechnol. Bioeng. 81, 158-166.

Sannes, P.L., Burch, K.K., Khosla, J., 1992. Immunohistochemical localization of epidermal growth factor and acidic and basic fibroblast growth factors in postnatal developing and adult rat lungs. Am. J. Respir. Cell Mol. Biol. 7, 230-237.

Schügerl, K., 2001. Progress in monitoring, modeling and control of bioprocesses during the last 20 years. J. Biotechnol. 85, 149-173.

Schügerl, K., Brandes, L., Dullau, T., Holzhauer-Rieger, K., Hotop, S., Hübner, U., Wu, X., Zhou, W., 1991. Fermentation monitoring and control by on-line flow injection and liquid chromatography. Anal. Chim. Acta 249, 87-100.

Schügerl, K., Brandes, L., Wu, X., Bode, J., Il Ree, J., Brandt, J., Hitzmann, B., 1993. Monitoring and control of recombinant protein production. Anal. Chim. Acta 279, 3-16.

Schügerl, K., Hitzmann, B., Jurgens, H., Kullick, T., Ulber, R., Weigal, B., 1996. Challenges in integrating biosensors and FIA for on-line monitoring and control. Trends Biotechnol. 14, 21-31.

Schauer, R., 1982. Sialic acids, chemistry, metabolism, and function. Springer-Verlag, Wien ; New York.

Schauer, R., 1985. Sialic acids and their role as biological masks. Trends Biochem. Sci. 10, 357-360.

Schauer, R., 2009. Sialic acids as regulators of molecular and cellular interactions. Curr. Opin. Struct. Biol. 19, 507-514.

Schauer, R., Tipson, R.S., Derek, H., 1982. Chemistry, Metabolism, and Biological Functions of Sialic Acids. In: Horton, D. (Ed.), Adv. Carbohydr. Chem. Biochem. Academic Press, pp. 131-234.

Schwanke, K., Wunderlich, S., Reppel, M., Winkler, M.E., Matzkies, M., Groos, S., Itskovitz-Eldor, J., Simon, A.R., Hescheler, J., Haverich, A., Martin, U., 2006. Generation and characterization of functional cardiomyocytes from rhesus monkey embryonic stem cells. Stem Cells 24, 1423-1432.

Schweigerer, L., 1988. Basic fibroblast growth factor and its relation to angiogenesis in normal and neoplastic tissue. Klin. Wochenschr. 66, 340-345.

Seeger, A., Rinas, U., 1996. Two-step chromatographic procedure for purification of basic fibroblast growth factor from recombinant *Escherichia coli* and characterization of the equilibrium parameters of adsorption. J. Chromatogr. A 746, 17-24.

Seeger, A., Schneppe, B., McCarthy, J.E.G., Deckwer, W.-D., Rinas, U., 1995. Comparison of temperature- and isopropyl-*β*-thiogalacto-pyranoside-induced synthesis of basic fibroblast growth factor in high-cell-density cultures of recombinant *Escherichia coli*. Enzyme Microb. Technol. 17, 947-953.

Seno, M., Sasada, R., Iwane, M., Sudo, K., Kurokawa, T., Ito, K., Igarashi, K., 1988. Stabilizing basic fibroblast growth factor using protein engineering. Biochem. Biophys. Res. Commun. 151, 701-708.

Shahrokh, Z., Eberlein, G., Wang, Y.J., 1994. Probing the conformation of protein (bFGF) precipitates by fluorescence spectroscopy. J. Pharm. Biomed. Anal. 12, 1035-1041.

Shalaev, E.Y., Zografi, G., 1996. How does residual water affect the solid-state degradation of drugs in the amorphous state? J. Pharm. Sci. 85, 1137-1141.

Sheng, Z., Chang, S.-B., Chirico, W.J., 2003. Expression and purification of a biologically active basic fibroblast growth factor fusion protein. Protein Expr. Purif. 27, 267-271.

Shieh, S.-J., Vacanti, J., 2005. State-of-the-art tissue engineering: From tissue engineering to organ building. Surgery 137, 1-7.

Shiloach, J., Kaufman, J., Guillard, A.S., Fass, R., 1996. Effect of glucose supply strategy on acetate accumulation, growth, and recombinant protein production by *Escherichia coli* BL21 (λDE3) and *Escherichia coli* JM109. Biotechnol. Bioeng. 49, 421-428.

Shimizu, N., Fukuzono, S., Fujimori, K., Nishimura, N., Odawara, Y., 1988. Fed-batch cultures of recombinant *Escherichia coli* with inhibitory substance concentration monitoring. J. Ferment. Technol. 66, 187-191.

Shing, Y., 1988. Heparin-copper biaffinity chromatography of fibroblast growth factors. J. Biol. Chem. 263, 9059-9062.

Simutis, R., Havlik, I., Lübbert, A., 1992. A fuzzy-supported Extended Kalman Filter: a new approach to state estimation and prediction exemplified by alcohol formation in beer brewing. J. Biotechnol. 24, 211-234.

Singh, H., Mok, P., Balakrishnan, T., Rahmat, S.N., Zweigerdt, R., 2010. Up-scaling single cell-inoculated suspension culture of human embryonic stem cells. Stem Cell Res. 4, 165-179.

Skalak, R., Fox, C.F., 1988. Tissue engineering : proceedings of a workshop, held at Granlibakken, Lake Tahoe, California, February 26-29, 1988. Liss, New York.

Song, S., Wientjes, M.G., Gan, Y., Au, J.L., 2000. Fibroblast growth factors: an epigenetic mechanism of broad spectrum resistance to anticancer drugs. Proc. Natl. Acad. Sci. U. S. A. 97, 8658-8663.

Song, S., Wientjes, M.G., Walsh, C., Au, J.L., 2001. Nontoxic doses of suramin enhance activity of paclitaxel against lung metastases. Cancer Res. 61, 6145-6150.

Song, S., Yu, B., Wei, Y., Wientjes, M.G., Au, J.L., 2004. Low-dose suramin enhanced paclitaxel activity in chemotherapy-naive and paclitaxel-pretreated human breast xenograft tumors. Clin. Cancer Res. 10, 6058-6065.

Sorenson, H.W., 1985. Kalman filtering : theory and application. IEEE Press, New York.

Squires, C.H., Childs, J., Eisenberg, S.P., Polverini, P.J., Sommer, A., 1988. Production and characterization of human basic fibroblast growth factor from *Escherichia coli*. J. Biol. Chem. 263, 16297-16302.

Stark, Y., Bruns, S., Stahl, F., Kasper, C., Wesemann, M., Grothe, C., Scheper, T., 2008. A study on polysialic acid as a biomaterial for cell culture applications. J. Biomed. Mater. Res. A 85, 1-13.

Steenbergen, S.M., Vimr, E.R., 2008. Biosynthesis of the *Escherichia coli* K1 group 2 polysialic acid capsule occurs within a protected cytoplasmic compartment. Mol. Microbiol. 68, 1252-1267.

Steinhaus, S., Stark, Y., Bruns, S., Haile, Y., Scheper, T., Grothe, C., Behrens, P., 2010. Polysialic acid immobilized on silanized glass surfaces: a test case for its use as a biomaterial for nerve regeneration. J. Mater. Sci. Mater. Med. 21, 1371-1378.

Stephanopoulos, G., Park, S., 1991. Bioreactor State Estimation. In: Rehm, H.-J., Reed, G. (Ed.), Biotechnology Set, 2nd ed. Wiley-VCH Verlag GmbH, pp. 225-249.

Stephanopoulos, G., San, K.-Y., 1983. On-line estimation of time-varying parameters. Application to biochemical reactors. In: Halme, A. (Ed.), Modelling and control of biotechnical processes : proceedings of the First IFAC Workshop, Helsinki, Finland, August 17-19, 1982. Pergamon Press, Oxford ; New York, pp. 195–200.

Steube, K., Spohn, U., 1994. On-line monitoring of intracellular enzyme activities with flow-injection analysis. Anal. Chim. Acta 287, 235-246.

Stewart, K.K., 1981. Flow-injection analysis: A review of its early history. Talanta 28, 789-797.

Stock, U.A., Vacanti, J.P., 2001. Tissue engineering: current state and prospects. Annu. Rev. Med. 52, 443-451.

Sugimoto, T., Tsuge, T., Tanaka, K., Ishizaki, A., 1999. Control of acetic acid concentration by pH-stat continuous substrate feeding in heterotrophic culture phase of two-stage cultivation of Alcaligenes eutrophus for production of P(3HB) from CO_2, H_2, and O_2 under non-explosive conditions. Biotechnol. Bioeng. 62, 625-631.

Szabo, S., Folkman, J., Vattay, P., Morales, R.E., Pinkus, G.S., Kato, K., 1994. Accelerated healing of duodenal ulcers by oral administration of a mutein of basic fibroblast growth factor in rats. Gastroenterology 106, 1106-1111.

Templeton, T.J., Hauschka, S.D., 1992. FGF-mediated aspects of skeletal muscle growth and differentiation are controlled by a high affinity receptor, FGFR1. Dev. Biol. 154, 169-181.

Thoemmes, J., Kula, M.R., 1995. Membrane chromatography - an integrative concept in the downstream processing of proteins. Biotechnol. Prog. 11, 357-367.

Thompson, S.A., Fiddes, J.C., 1991. Chemical characterization of the cysteines of basic fibroblast growth factor. Ann. N. Y. Acad. Sci. 638, 78-88.

Trojanowicz, M., 2000. Flow injection analysis : instrumentation and applications. World Scientific, Singapore ; River Edge, NJ.

Tsuboi, R., Shi, C.M., Rifkin, D.B., Ogawa, H., 1992. A wound healing model using healing-impaired diabetic mice. J. Dermatol. 19, 673-675.

Tsuchiya, H.M., Fredrickson, A.G., Aris, R., Thomas B. D., John W. Hoopes, J., Theodore, V., 1966. Dynamics of Microbial Cell Populations. In: Thomas B. D. (Ed.), Advances in Chemical Engineering. Academic Press, pp. 125-206.

Turner, C., Gregory, M.E., Thornhill, N.F., 1994a. Closed-loop control of fed-batch cultures of recombinant *Escherichia coli* using on-line HPLC. Biotechnol. Bioeng. 44, 819-829.

Turner, C., Gregory, M.E., Turner, M.K., 1994b. A study of the effect of specific growth rate and acetate on recombinant protein production of *Escherichia coli* JM107. Biotechnol. Lett. 16, 891-896.

Umoh, E.F., Putten, A.B.v., Schügerl, K., 1996. Simultaneous on-line monitoring of glucose and total malto sugar in fermentation processes using an FIA system. J. Chem. Technol. Biotechnol. 67, 276-280.

Valero, F., Lafuente, J., Poch, M., Solà, C., Araujo, A.N., Lima, J.L.F.C., 1990. On-line fermentation monitoring using flow injection analysis. Biotechnol. Bioeng. 36, 647-651.

Van Putten, A.B., Spitzenberger, F., Kretzmer, G., Hitzmann, B., Dors, M., Simutis, R., Schügerl, K., 1996. Improvement of the production of subtilisin Carlsberg alkaline protease by *Bacillus*

licheniformis by on-line process monitoring and control in a stirred tank reactor. J. Biotechnol. 49, 83-93.

Van Putten, A.B., Spitzenberger, F., Kretzmer, G., Hitzmann, B., Schügerl, K., 1995. On-line and off-line monitoring of the production of alkaline serine protease by *Bacillus licheniformis*. Anal. Chim. Acta 317, 247-258.

Vimr, E.R., Kalivoda, K.A., Deszo, E.L., Steenbergen, S.M., 2004. Diversity of microbial sialic acid metabolism. Microbiol. Mol. Biol. Rev. 68, 132-153.

Wang, H.Y., Lawless, R.J., Lin, J.E., 1988. Use of membrane oxygenator to increase oxygen transfer capacity of a bioreactor. Process Biochem. 23, 23-27.

Wang, J., Hong, A., Ren, J.S., Sun, F.Y., Shi, Y.J., Liu, K., Xie, Q.L., Dai, Y., Li, Z.Y., Chen, Y., 2006. Biochemical properties of C78SC96S rhFGF-2: a double point-mutated rhFGF-2 increases obviously its activity. J. Biotechnol. 121, 442-447.

Wang, W., 2000. Lyophilization and development of solid protein pharmaceuticals. Int. J. Pharm. 203, 1-60.

Wang, Y., Becker, D., 1997. Antisense targeting of basic fibroblast growth factor and fibroblast growth factor receptor-1 in human melanomas blocks intratumoral angiogenesis and tumor growth. Nat. Med. 3, 887-893.

Weigel, B., Hitzmann, B., Kretzmer, G., Schügerl, K., Huwig, A., Giffhorn, F., 1996. Analysis of various sugars by means of immobilized enzyme coupled flow injection analysis. J. Biotechnol. 50, 93-106.

Weuster-Botz, D., Kelle, R., Frantzen, M., Wandrey, C., 1997. Substrate controlled fed-batch production of *L*-Lysine with *Corynebacterium glutamicum*. Biotechnol. Prog. 13, 387-393.

Whitfield, C., 2006. Biosynthesis and assembly of capsular polysaccharides in *Escherichia coli*. Annu. Rev. Biochem. 75, 39-68.

Williams, K.L., 2007. Endotoxins : pyrogens, LAL testing and depyrogenation, 3rd ed. Informa Healthcare, New York.

Wilson, D.I., Agarwal, M., Rippin, D.W.T., 1998. Experiences implementing the extended Kalman filter on an industrial batch reactor. Comput. Chem. Eng. 22, 1653-1672.

Wlaschin, K.F., Hu, W.S., 2006. Fedbatch culture and dynamic nutrient feeding. Adv. Biochem. Eng. Biotechnol. 101, 43-74.

Wu, S., Leung, D., Vemuri, S., Shah, D., Yang, B., Wang, J., 1998. Degradation mechanism of lyophilized basic Fibroblast Growth Factor (bFGF) protein in sugar formulation. Pharm. Sci. 1 (Suppl.), S-539.

Xin, Y., Lyness, G., Chen, D., Song, S., Wientjes, M.G., Au, J.L., 2005. Low dose suramin as a chemosensitizer of bladder cancer to mitomycin C. J. Urol. 174, 322-327.

Yang, F.-C., Maa, D.-W., 1998. Fed-batch culture of yeast *Saccharomyces cerevisiae* with a DO-stat method by a fuzzy controller. Bioprocess Biosyst. Eng. 18, 79-82.

Yang, S., Leong, K.F., Du, Z., Chua, C.K., 2001. The design of scaffolds for use in tissue engineering. Part I. Traditional factors. Tissue Eng. 7, 679-689.

Yang, S., Leong, K.F., Du, Z., Chua, C.K., 2002. The design of scaffolds for use in tissue engineering. Part II. Rapid prototyping techniques. Tissue Eng. 8, 1-11.

Yangxi, Z., 2008. Diplom Thesis, Leibniz University of Hannover.

Yano, T., Kurokawa, M., Nishizawa, Y., 1991. Optimum substrate feed rate in fed-batch culture with the DO-stat method. J. Ferment. Bioeng. 71, 345-349.

Yee, L., Blanch, H.W., 1992. Recombinant protein expression in high cell density fed-batch cultures of *Escherichia coli*. Biotechnology. (N. Y.) 10, 1550-1556.

Zabriskie, D.W., Wareheim, D.A., Polansky, M.J., 1987. Effects of fermentation feeding strategies prior to induction of expression of a recombinant malaria antigen in *Escherichia coli*. J. Ind. Microbiol. Biotechnol. 2, 87-95.

Zeng, X., Ruckenstein, E., 1999. Membrane Chromatography: Preparation and Applications to Protein Separation. Biotechnol. Prog. 15, 1003-1019.

Zhan, X., Zhu, L., Wu, J., Zhen, Z., Jia, W., 2002. Production of polysialic acid from fed-batch fermentation with pH control. Biochem. Eng. J. 11, 201-204.

Zhang, J., Su, W.W., 2002. Estimation of intracellular phosphate content in plant cell cultures using an extended Kalman filter. J. Biosci. Bioeng. 94, 8-14.

Zhang, J.D., Cousens, L.S., Barr, P.J., Sprang, S.R., 1991. Three-dimensional structure of human basic fibroblast growth factor, a structural homolog of interleukin 1 beta. Proc. Natl. Acad. Sci. U. S. A. 88, 3446-3450.

Zhang, Y., Song, S., Yang, F., Au, J.L., Wientjes, M.G., 2001. Nontoxic doses of suramin enhance activity of doxorubicin in prostate tumors. J. Pharmacol. Exp. Ther. 299, 426-433.

Zhu, X., Komiya, H., Chirino, A., Faham, S., Fox, G.M., Arakawa, T., Hsu, B.T., Rees, D.C., 1991. Three-dimensional structures of acidic and basic fibroblast growth factors. Science 251, 90-93.

Zweigerdt, R., 2009. Large scale production of stem cells and their derivatives. Adv. Biochem. Eng. Biotechnol. 114, 201-235.

6. Appendix

6.1 Chemicals and buffers

6.1.1 Chemicals

All chemicals and reagents were purchased from Sigma-Aldrich (Taufkirchen, Germany) unless specified elsewhere. Deionized, pyrogen-free water was obtained from an ARIUM UF 611 water system (Sartorius Stedim Biotech, Göttingen, Germany).

6.1.2 Buffers and solutions

6.1.2.1 Buffers for FGF-2 purification

All buffers for FGF-2 purification are filtrated with 0.2 µm filters and then degassed by sonication for 30 min. After that the buffers are stored in the refrigerator at 4 °C until used.

Lysis buffer, 25 mM phosphate buffer pH 7.5 and 100 mM NaCl

Dissolve 0.1298 g $NaH_2PO_4 \cdot H_2O$, 0.5764 g Na_2HPO_4, 1.17 g NaCl, 0.0744 g EDTA disodium salt dihydrate, 0.0926 g DTT, 0.05 g $MgCl_2 \cdot 7H_2O$ and 200 U of benzonase in 200 ml deionized water.

Equilibration buffer, 25 mM phosphate buffer pH 7.5

Dissolve 0.6491 g $NaH_2PO_4 \cdot H_2O$, 2.8821 g Na_2HPO_4, 0.4628 g DTT and 0.3722 g EDTA disodium salt dihydrate in 1000 ml deionized water.

Elution buffer 1, 25 mM phosphate buffer pH 7.5 + 1 M NaCl

Dissolve 0.3245 g $NaH_2PO_4 \cdot H_2O$, 1.4411 g Na_2HPO_4, 0.2314 g DTT, 0.1861 g EDTA disodium salt dihydrate and 29.25 g NaCl in 500 ml deionized water.

Elution buffer 2, 25 mM phosphate buffer pH 7.5 + 2.5 M NaCl

Dissolve 0.3245 g $NaH_2PO_4 \cdot H_2O$, 1.4411 g Na_2HPO_4, 0.2314 g DTT, 0.1861 g EDTA disodium salt dihydrate and 73.125 g NaCl in 500 ml deionized water.

Exchanging buffer, 20 mM Tris-HCl pH 7.5 and 150 mM NaCl

Dissolve 1.2114 g Tris base in 100 ml of deionized water and adjust to the desired pH with concentrated HCl. Add 4.3875 g NaCl and 0.2314 g DTT, 0.1861 g EDTA disodium salt dihydrate. Mix and add deionized water to 500 ml.

6.1.2.2 Buffers and solutions for SDS-PAGE and stain

Sample loading buffer

Bromphenolblue buffer consists of 20 mM Tris-HCl pH 6.8, 2 mM EDTA, 5 % (v v^{-1}) SDS and 0.02 % (w v^{-1}) bromphenolblue. The sample loading buffer comprises of bromphenolblue buffer, 2-mecaptoethanol and 55 % (v v^{-1}) glycerol with a volume ratio of 3:1:1.

Running buffer (1× TGS buffer)

SDS-PAGE running buffer consists of 25 mM Tris base, 192 mM glycine and 0.1 % (w v^{-1}) SDS, pH 8.3.

Silver destaining-fix solution

Silver destaining-fix solution consists of 80 ml acetic acid, 400 ml ethanol and 400 ml deionized water.

Farmers Reducer solution

Dissolve 0.1 g sodium thiosulfate and 0.1 g potassium ferricyanide in 100 ml deionized water.

6.1.2.3 Buffers for western blot analysis

Transfer buffer

Transfer buffer comprises of 25 mM Tris base, 192 mM glycine and 10 % (v v^{-1}) ethanol, pH 8.3.

TBS buffer

TBS buffer consists of 25 mM Tris-HCl pH 7.4 and 150 mM NaCl.

TBST buffer

TBST buffer consists of 25 mM Tris-HCl pH 7.4, 150 mM NaCl and 0.5 % (v v^{-1}) Tween 20.

Block buffer

Block buffer comprises of 25 mM Tris-HCl pH 7.4, 150 mM NaCl, 2 % (w v^{-1}) BSA and 0.5 % (v v^{-1}) Tween 20.

AP (alkaline phosphatase) buffer (10×)

AP buffer consists of 100 mM Tris, pH 9.5.

Color-Development-Reagent

Color-Development-Reagent comprises of 25 ml AP-buffer and 500 µl BCIP (5-bromo-4-chloro-3 indolylphosphate)/NBT (nitroblue tetrazolium) substrate.

6.2 Media

6.2.1 Medium for cultivating *E. coli* K1

6.2.1.1 Preculture medium

The complex medium consists of 10 g l^{-1} yeast extract and 10 g l^{-1} tryptone.

6.2.1.2 Reactor cultivation medium

The composition of the synthetic medium for batch and feed solution were given in Table 6.1.

Table 6.1 Medium composition for reactor cultivation of *E. coli* K1

Components	Batch medium	Feed solution
Glucose	18[a] / 5 g l^{-1}	100 g l^{-1}
K_2HPO_4	6.665 g l^{-1}	
KH_2PO_4	0.25 g l^{-1}	
NaCl	1.2 g l^{-1}	
K_2SO_4	1.1 g l^{-1}	
$(NH_4)_2SO_4$	10 g l^{-1}	27.5 g l^{-1}
$MgSO_4 \cdot 7H_2O$	0.15 g l^{-1}	1.5 g l^{-1}
$FeSO_4 \cdot 7H_2O$	0.001 g l^{-1}	0.01 g l^{-1}
$CuSO_4 \cdot 5H_2O$	0.001 g l^{-1}	0.01 g l^{-1}
$CaCl_2 \cdot 2H_2O$	0.013 g l^{-1}	0.026 g l^{-1}

[a] For batch cultivation only

6.2.2 Medium for cultivating *E. coli* BL21

6.2.2.1 Preculture medium

The Luria-Bertani (LB) medium contains 10 g l^{-1} of tryptone, 10 g l^{-1}NaCl and 5 g l^{-1} of yeast extract.

6.2.2.2 Reactor cultivation medium

A synthetic medium is prepared with the following components (Table 6.2).

Table 6.2 Composition of medium and feed solution for reactor cultivation of *E. coli* BL21

Components	Batch medium	Feed solution
Glucose	4.0 g l^{-1}	100 g l^{-1}
KH_2PO_4	13.3 g l^{-1}	
$(NH_4)_2HPO_4$	4.0 g l^{-1}	
$MgSO_4 \cdot 7H_2O$	1.2 g l^{-1}	10 g l^{-1}
Citric acid	1.7 g l^{-1}	
$Na_2EDTA \cdot 2H_2O$	14.1 mg l^{-1}	13 mg l^{-1}
$CoCl_2 \cdot 6H_2O$	2.5 mg l^{-1}	4.0 mg l^{-1}
$MnSO_4 \cdot H_2O$	12.8 mg l^{-1}	20.1 mg l^{-1}

$CuSO_4 \cdot 5H_2O$	2.2 mg l^{-1}	3.4 mg l^{-1}
H_3BO_3	3.0 mg l^{-1}	4.7 mg l^{-1}
$Na_2MoO_4 \cdot 2H_2O$	2.1 mg l^{-1}	4.0 mg l^{-1}
$Zn(CH_3COO)_2 \cdot 2H_2O$	33.8 mg l^{-1}	16.0 mg l^{-1}
Fe(III)citrate	100.8 mg l^{-1}	40.0 mg l^{-1}
Thiamine·HCl	4.5 mg l^{-1}	4.5 mg l^{-1}
Antifoam	0.1 ml l^{-1}	
Kanamycin	20 mg l^{-1}	20 mg l^{-1}

6.3 Methods

6.3.1 Off-line parameters determination

6.3.1.1 Dry cell weight determination

Dry cell weights (DCW) were determined approximately every hour by centrifuging (17,000 × g, 3 min) 2 ml aliquots of the culture broth collected in pre-weighted tubes. Then the pellets were washed with deionized water and dried for 24 h at 80 °C. The dry cell weights were determined afterwards gravimetrically.

6.3.1.2 Glucose determination

The off-line glucose concentration was measured roughly every hour using an YSI 2700 select biochemistry analyzer (Yellow Springs Instruments, Ohio, USA). In order to get more precise measurements in the fed-batch phase, the off-line glucose concentrations were determined by RQflex® 2 reflectometer (Merck KGaA, Darmstadt, Germany), with test strips (Glucose-test, 1-100 mg l^{-1}; Merck KGaA, Darmstadt, Germany).

6.3.1.3 Acetate determination

Acetate concentrations were determined by a gas chromatography (Shimadzu GC-14B; Shimadzu, Duisburg, Germany) equipped with a flame ionization detector. 6 standard acetate concentrations (0.05 g l^{-1}, 0.1 g l^{-1}, 0.5 g l^{-1}, 1.0 g l^{-1}, 2.5 g l^{-1} and 5.0 g l^{-1}) were used and n-propanol was used as the internal standard. The amount of acetate in the samples was calculated by the Shimadzu Class VP™ chromatography software version 4.2 (Shimadzu, Duisburg, Germany).

6.3.2 Polysialic acid quantification

A modified thiobarbituric acid (TBA) method was used for the quantification of PSA. In the first step, 50 µl sample was hydrolyzed by 200 µl of 50 mM H_3PO_4 and incubated at 70 °C for 18 h, followed by neutralization with 100 µl 0.1 M NaOH. The oxidation of sialic acid residues was performed by adding 100 µl periodic acid (0.2 M) in 0.5 % (v v^{-1}) H_3PO_4. The oxidation was stopped by adding 500 µl $NaAsO_2$ solution (0.38 M) in 2 % (v v^{-1}) H_2SO_4 after 30 min of incubation at 37 °C. Finally, 500 µl thiobarbituric acid solution (0.2 M) in 1.2 % (v v^{-1}) NaOH was added to the sample and heated to 95 °C for 13 min. The pink dye was extracted by cyclohexanone and diluted to a proper range. The absorption was measured at 549 nm and PSA content were calculated from the standard curve.

6.3.3 FGF-2 quantification

6.3.3.1 Bradford assay

10 µl of the samples and different concentrations of BSA (bovine serum albumin) standards (1000 µg ml^{-1}, 750 µg ml^{-1}, 500 µg ml^{-1}, 250 µg ml^{-1}, 200 µg ml^{-1}, 100 µg ml^{-1} and 50 µg ml^{-1}) were added to a 96-well plate and mixed with 300 µl of Bradford-reagent (0.1 g l^{-1} Coomassie-brilliant-blue G250, 50 ml l^{-1} ethanol (96 %), 100 ml l^{-1} phosphoric acid (85 %)). Then the plate was shaken for 30 s and incubated at 37 °C for 10 min. Afterwards the absorption was measured at 595 nm. Protein concentrations were calculated from the BSA standard curve.

6.3.3.2 Gel-densitometry

SDS-PAGE gels were stained with blue silver stain solution over night, and then gels were destained in water for 16 h until a clear background was reached (Fig. 6.1). Afterwards, gels were scanned on a HP scanjet 2000 scanner. Gel-pro® Analyzer 6.0 software (Media Cybernetics, Marlow, UK) was used for gel image analysis to determine the total integration optical density (IOD) of the protein bands. Purified FGF-2 (750 µg ml^{-1}, 500 µg ml^{-1}, 250 µg ml^{-1}, 200 µg ml^{-1}, 100 µg ml^{-1}) were used as standards and a linear correlation between the FGF-2 concentration and IOD was obtained (Fig. 6.2). FGF-2 concentrations in the samples were calculated from the standard curve.

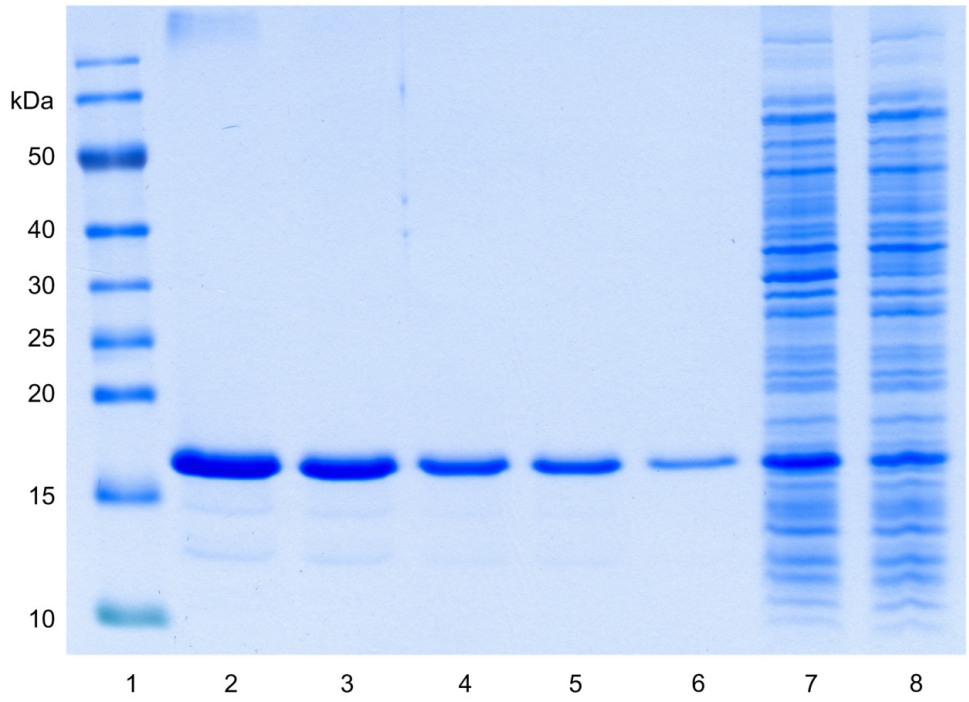

Fig. 6.1 Typical SDS-PAGE gel for quantitative estimation of FGF-2 concentrations. Lane 1, Molecular weight marker; Lane 2-6, Purified FGF-2 as standards: 750 µg ml^{-1}, 500 µg ml^{-1}, 250 µg ml^{-1}, 200 µg ml^{-1}, 100 µg ml^{-1}; Lane 7, total cell lysate (dilution 1:16); Lane 8, soluble fraction of cell lysate (dilution 1:16).

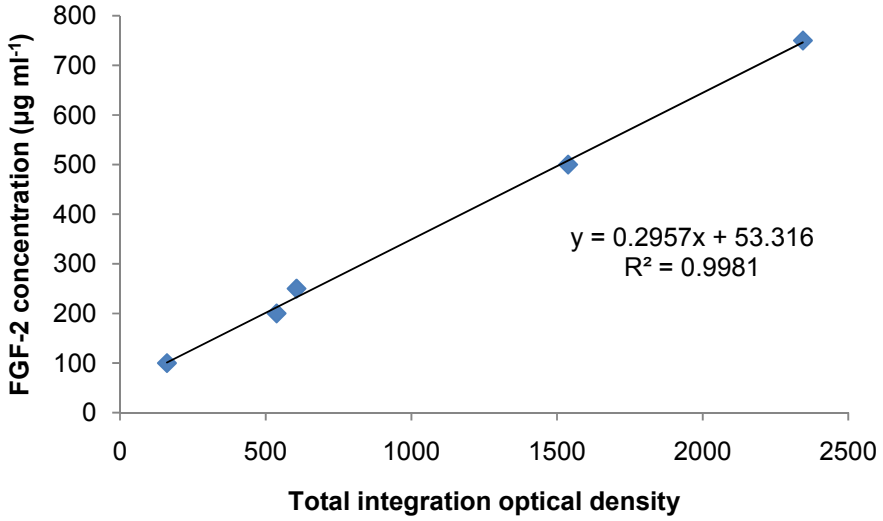

Fig. 6.2 Typical calibration curve of FGF-2 concentration against total integration optical density. The amount of FGF-2 in the samples were calculated from the curve.

6.3.3.3 UV absorbance at 280 nm

The concentration of purified FGF-2 was determined by measuring UV absorbance at 280 nm on a UV-Vis spectrophotometer (Cary 50, Varian Deutschland GmbH, Darmstadt, Germany) with a quartz cuvette (Type 6040-UV, Hellma GmbH, Müllheim, Germany). 15,930 M^{-1} cm^{-1} was used as the molar extinction coefficient. This value was calculated from the FGF-2 amino acid sequence on the ExPASy website using the ProtParam program (http://www.expasy.org/tools/protparam.html).

6.3.4 FGF-2 identification

6.3.4.1 SDS-PAGE

1. Carefully clean the glass plates and assembling the casting stands following the Mini-PROTEAN® Tetra (Bio-Rad, Munich, Germany) instruction manual.

2. Mix solutions for separating gels as shown in Table 6.3 and pour the mixture into the plates.

Table 6.3 Recipe for SDS-PAGE gel preparation.

Components	Separating gel (12 %)	Stacking gel (6 %)
Acrylamid/Bisacrylamid-solution (37.5:1)	3.0 ml	0.75 ml
1.5 M Tris-HCl pH 8.8	2.5 ml	--
1.5 M Tris-HCl pH 6.8	--	1.25 ml
1% (w v^{-1}) SDS solution	1 ml	0.52 ml
Deionized H_2O	1.76 ml	2.46 ml
25% (w v^{-1}) APS	20 µl	10 µl
TEMED	20 µl	10 µl

3. Overlay the gel with deionized water and allow gel to polymerize, remove the water afterwards.

4. Preparing the stacking gel according to Table 6.3. Insert a comb and pour the stacking gel into the casting stands, let the gel to polymerize.

5. Preapre samples by mixing sample with sample loading buffer and boiling the mixture at 95 °C for 10 min.

6. Assemble the electrophoresis cell and fill the cells with running buffer.

7. Load samples to the wells and run the gels at constant voltage of 100 V for stacking gel and 200 V for separating gel until the tracking dye reached the bottom of the gel.

8. Stain the gel with blue-silver stain solution or with silver stain.

6.3.4.1.1 Blue-silver stain

The blue-silver stain solution consists of 0.12 % Coomassie Brilliant Blue G-250 (w v^{-1}), 10 % ammonium sulphate (w v^{-1}), 10 % orthophosphoric acid (v v^{-1}) and 20 % Methanol (v v^{-1}). The stain protocol is listed below.

1. Wash the gel with deionized water for 10 min, repeat 3 times.

2. Incubate the gel in Blue-silver stain solution for 4 h or overnight.

3. Wash the gel with deionized water for 30 min.

4. Destain the gel with deionized water till a clear background is reached.

6.3.4.1.2 Silver stain

All operations are completed on a rotary shaker.

1. Incubate the gel in silver destain-fix solution for 30 min.

2. Wash the gel with deionized water for 2 times.

3. Incubate the gel in Farmers Reducer solution for 2.5 min.

4. Wash gel with deionized water for 5 min. Repeat this step till the gel is colorless.

5. Incubate the gel in 0.1 % (m v^{-1}) silver nitrate solution for 30 min.

6. Wash the gel with deionized water for 30 s, repeat once.

7. Rinse the gel with 5 % (m v^{-1}) Na_2CO_3 solution.

8. Put the gel in 100 ml 5 % (m v^{-1}) Na_2CO_3 solution with 400 µl formaldehyde. Wait until yellow-brown bands appear.

9. Incubate the gel in 5 % (v v^{-1}) acetic acid for 10 min to stop the stain.

6.3.4.2 MALDI-TOF MS

The measurement of MALDI-TOF MS of FGF-2 was done by the group of Prof. Dr. Ulrich Martin at MHH, and the procedures were as follows: 1µl of sample solution was mixed with 1 µl 0.1 % TFA (Trifluoroacetic acid) for acidifying. Then samples were applied onto AnchorChip MSP 600/96 targets (Bruker Daltonik GmbH, Bremen, Germany) using α-Cyano-4-hydroxycinnamic acid (HCCA) and 2,5-dihydroxyacetophenone (2,5-DHAP) (Bruker Daltonik GmbH, Bremen, Germany) as matrixes. For HCCA sample preparation, 0.6 µl HCCA solution (2 mg ml^{-1}) was overlaid on 1 µl of sample and dried by air; for 2,5-DHAP sample preparation, 1 µl 2 % (w v^{-1}) TFA and 1 µl 2,5-DHAP solution (7.6 mg ml^{-1}) was overlaid on 1 µl of sample and dried by air. Two different mass measure zones were used, 1-10 kDa using HCCA as the matrix and 10-100 kDa using 2,5-DHAP as the matrix. Mass spectra reported by HCCA preparation were the results from 100-300 laser shots and by 2,5-DHAP preparation were the results from 2000 laser shots. MS measurements were performed on a Bruker Microflex LT system (Bruker Daltonik GmbH, Bremen, Germany) with FlexAnalysis 3.0 software (Bruker Daltonik GmbH, Bremen, Germany). Spectra were acquired in linear mode and mass-calibrated data acquisition methods were used.

6.3.4.3 Western blot analysis

Western blot analysis was accomplished by transferring protein to a polyvinylidenefluoride (PVDF) membrane using a Criterion Blotter (Bio-Rad, Munich, Germany) according to the manufacturer's instructions. A monoclonal anti-human-FGF-2 antibody (Sigma-Aldrich, Taufkirchen, Germany) was used in a 1:5000 dilution. Immunoreactive bands were visualized by alkaline phosphatase-conjugated Goat Anti-mouse IgG (H+L) (Bio-Rad, Munich, Germany) followed with nitro blue tetrazolium/5-bromo-4-chloro-3-indolyl phosphate (NBT/BCIP) chromogenic substrates.

The operation procedures are listed below:

1. Assembling the gel into the blotting cassettes according to the instructions of the manufacturer.

2. Put an ice block in the tank and fill it with transfer buffer. Then place the tank on a magnetic stirrer plate and stir at medium speed.

3. Transfer the proteins at 100 V for 50 min.

4. Blocking the membrane with block buffer for 1 h on a shaker.

5. After blocking, without washing put the membrane in block buffer with the primary antibody in a 1:5000 dilution, incubating for 1 h on the shaker.

6. Wash the membrane for 5 min with block buffer, repeat 3 times.

7. Incubate the membrane for 1 h in TBST buffer with the secondary antibody in a 1:3000 dilution.

8. Wash the membrane for 3× 5 min with TBST buffer and then 2 times with TBS buffer.

9. Wash the membrane with AP buffer for 5 min.

10. Incubate the membrane with Color-Development-Reagent, and wait for the bands to appear.

6.3.4.4 Fluorescence spectroscopy

Fluorescence emission spectrum of FGF-2 were obtained with a HITACHI F-4500 fluorescence spectrophotometer (HITACHI, Krefeld, Germany) using a quartz cuvette (Type 104.002F-QS; Hellma GmbH, Müllheim, Germany). Spectrum was obtained using 280 nm as excitation wavelength, 10 nm slit widths and a scan speed of 240 nm min^{-1}. 500 µl of purified FGF-2 sample was load to the cuvette after adjusting its concentration to about 0.1 mg ml^{-1}.

6.3.4.5 RP-HPLC

The RP-HPLC system (Merck-Hitachi La Chrome, Darmstadt, Germany) consists of an L-7100 pump, L-7200 autosampler, D-7000 Interface Module, L-7455 diode array detector and L-7350 column oven. 20 µl of sample was applied to a C4 column (4.6 mm × 250 mm, Macherey-Nagel, Düren, Germany), equilibrated by water containing 0.1 % trifluoroacetic

acid (TFA). FGF-2 was eluted by a linear gradient of 0 - 50 % acetonitrile containing 0.1 % TFA (1 % acetonitrile min^{-1}; flow rate 1 ml min^{-1}). Column was at the room temperature and absorbance was monitored at 215 nm by the detector. The protocol is described in Appendix 6.5.2.

6.3.5 Endotoxin assay

Endotoxin content of purified FGF-2 was determined using *Limulus* amebocyte lysate (LAL) assay. The test was carried out using an Endosafe®-PTS™ system (Charles River laboratories, Kisslegg, Germany) with a cartridge ranging from 0.1-10 EU ml^{-1} and following the manufacturer's instructions.

6.3.6 Lyophilization

Lyophilization was performed on a laboratory freezing dryer (Alpha 1-4, Martin Christ GmbH, Osterode am Harz, Germany). The formulated FGF-2 aliquots (2 ml in screw-caped tubes) were frozen at a speed of 20 °C h^{-1} to -25 °C and then transferred to -80 °C freezer frozen overnight. Primary drying was performed at a shelf temperature of -25 °C for 24 h, with a vacuum level less than 0.12 mbar and a condenser temperature of -60 °C. Second drying was carried out at a shelf temperature of + 25 °C for 12 h, the vacuum level was less than 0.06 mbar and the condenser temperature was the same as in the primary drying. Finally, the lyophilized protein was sealed under conventional atmosphere and stored.

6.4 Bioreactor system construction and calculation

6.4.1 Bioreactor system for fed-batch cultivation at a controlled constant specific growth rate

The system consists of a 2 l bioreactor with digital control unit (Bio-Stat® B), an exhaust gas analyzer for measuring oxygen and carbon dioxide content in the off-gas, a PC running Neu-ork program for calculating the feeding pump rate and a peristaltic feeding pump. A diagram of the entire system could be found in Fig. 6.3. A photo of the system is shown in Fig. 6.4.

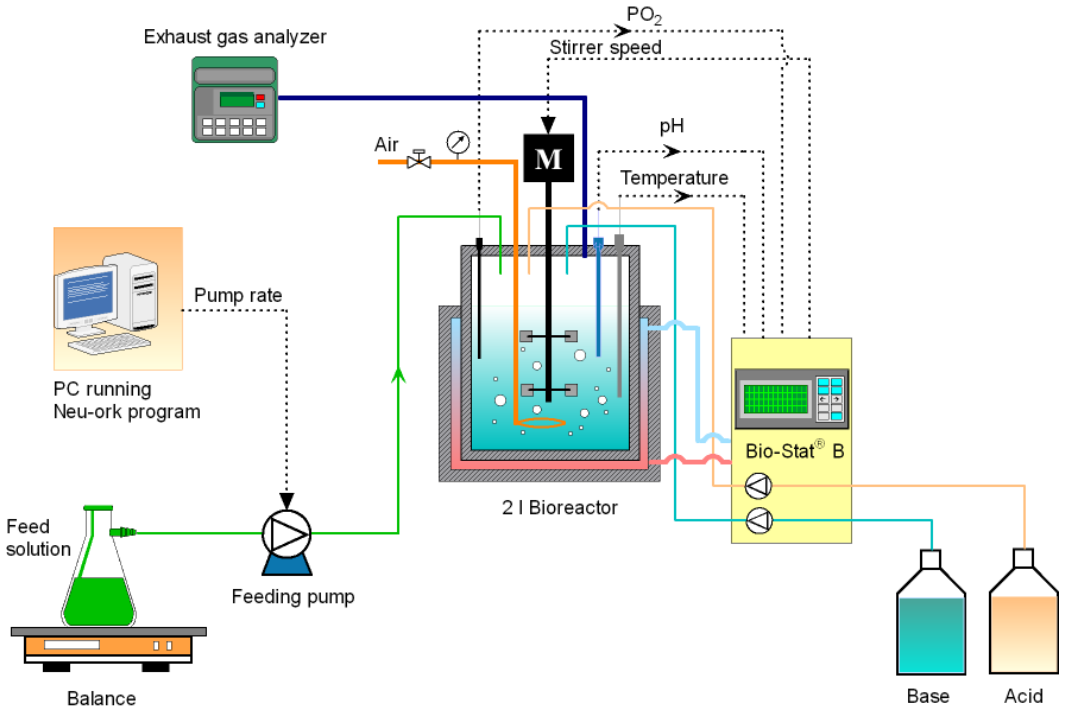

Fig. 6.3 Diagram of bioreactor and various controls of fed-batch cultivation at a constant specific growth rate.

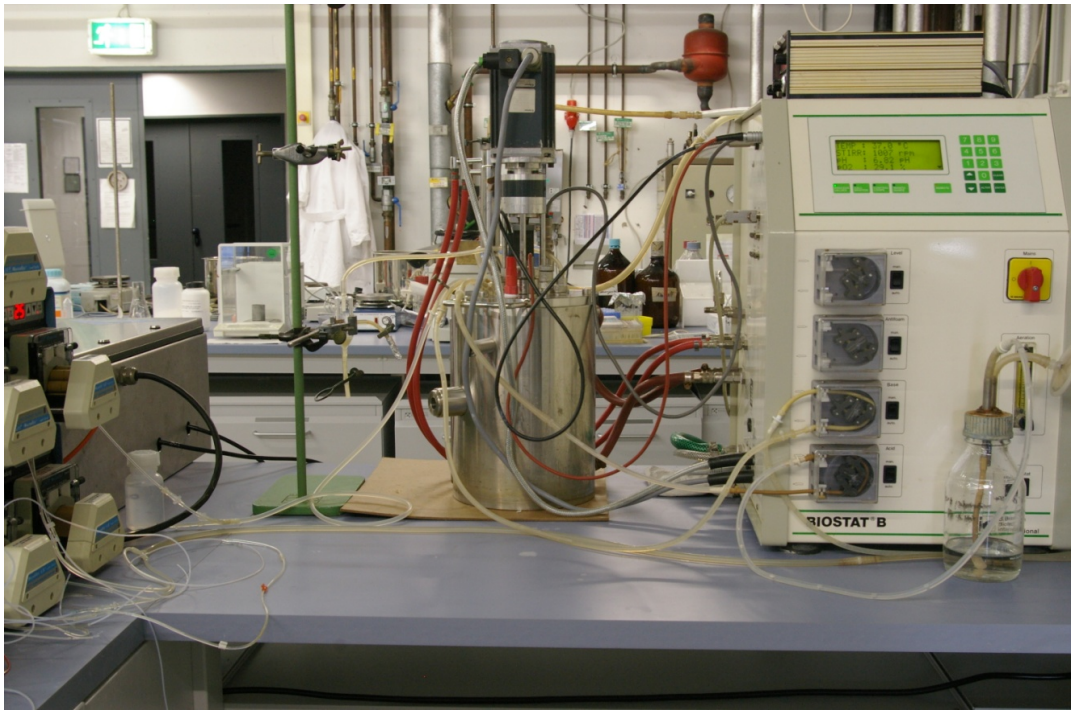

Fig. 6.4 Photo of the bioreactor system for fed-batch cultivation at a constant specific growth rate.

6.4.2 Bioreactor system for fed-batch cultivation at a constant glucose concentration

The cultivation system consists of a 2 l bioreactor with digital control unit (Bio-Stat® B), an exhaust gas analyzer for measuring oxygen and carbon dioxide content in the off-gas, a FIA system for the on-line measurement of glucose concentration, a PC running EKF (extended Kalman filter) software for estimating state variables and calculating the pump rate and a peristaltic feeding pump. A diagram of the whole system is shown in Fig. 6.5. A diagram explains the FIA system could be found in Fig. 6.6 and a screen shot of CAFCA software during glucose measurement is in Fig. 6.7. A diagram of EKF is presented in Fig. 6.8 and a screen shot of EKF software during fed-batch cultivation is shown in Fig. 6.9. A photo of the whole cultivation system is shown in Fig. 6.10.

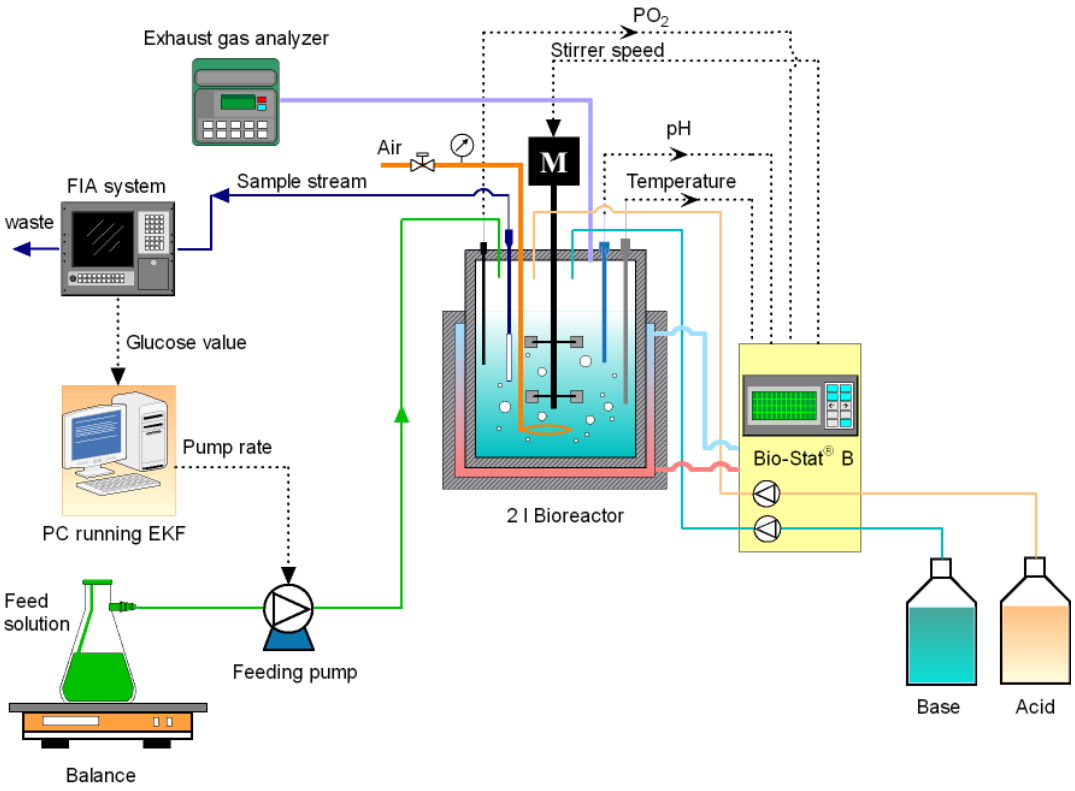

Fig. 6.5 Diagram of bioreactor and various controls of fed-batch cultivation at a constant glucose concentration.

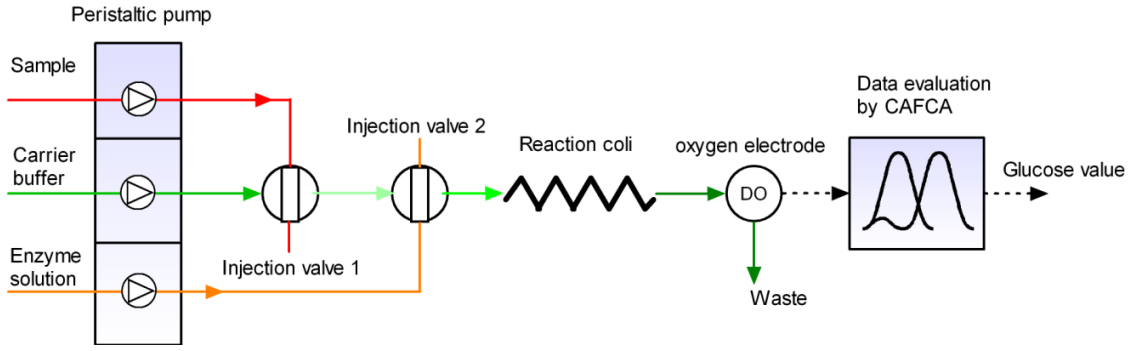

Fig. 6.6 Diagram of the FIA system.

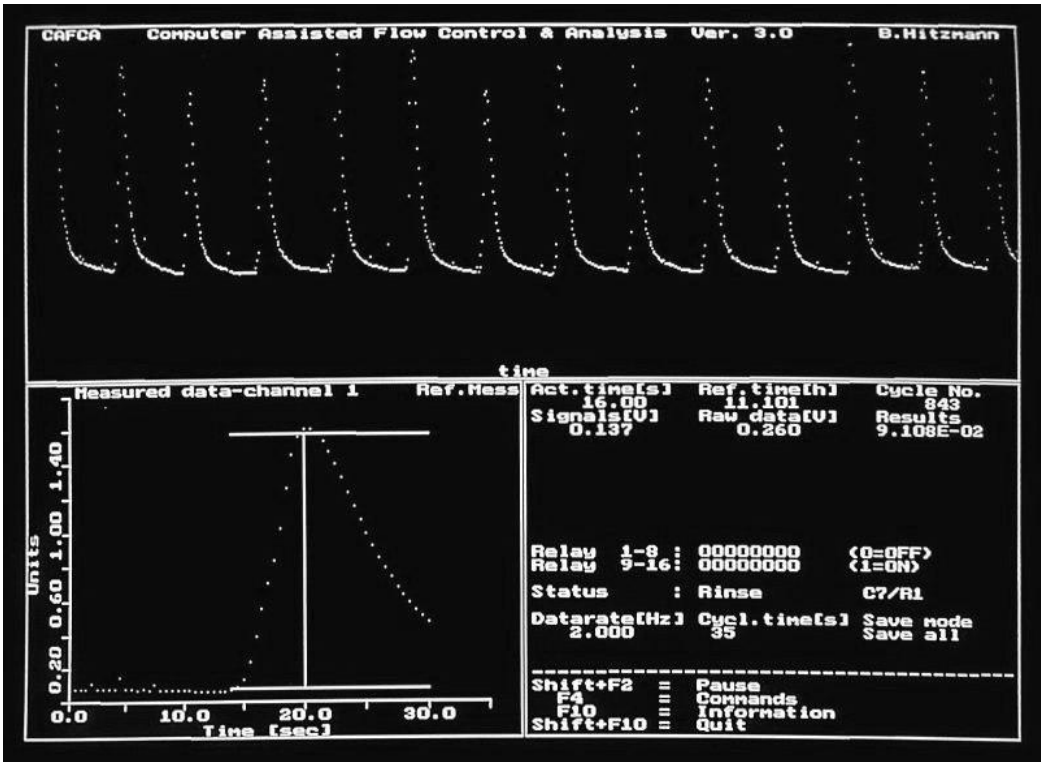

Fig. 6.7 Screen shot of CAFCA software during glucose measurement.

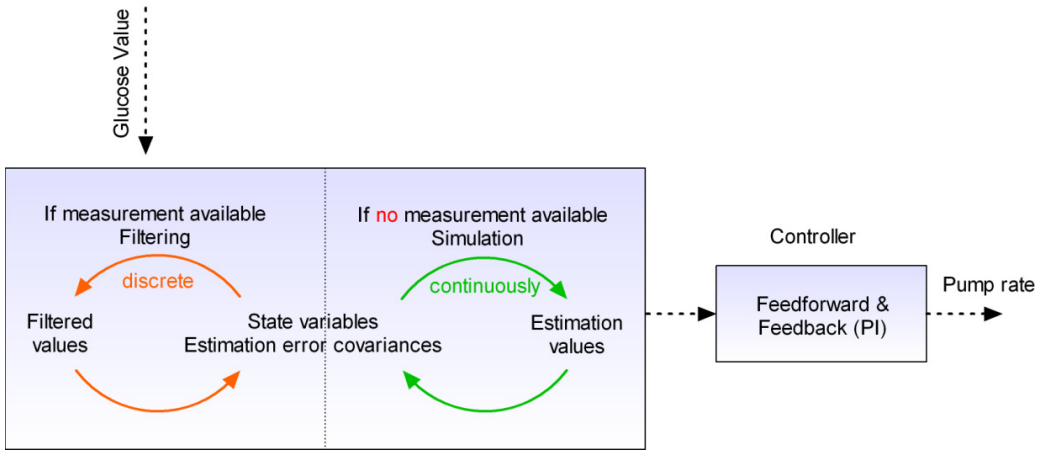

Fig. 6.8 Diagram of extended Kalman filter (EKF).

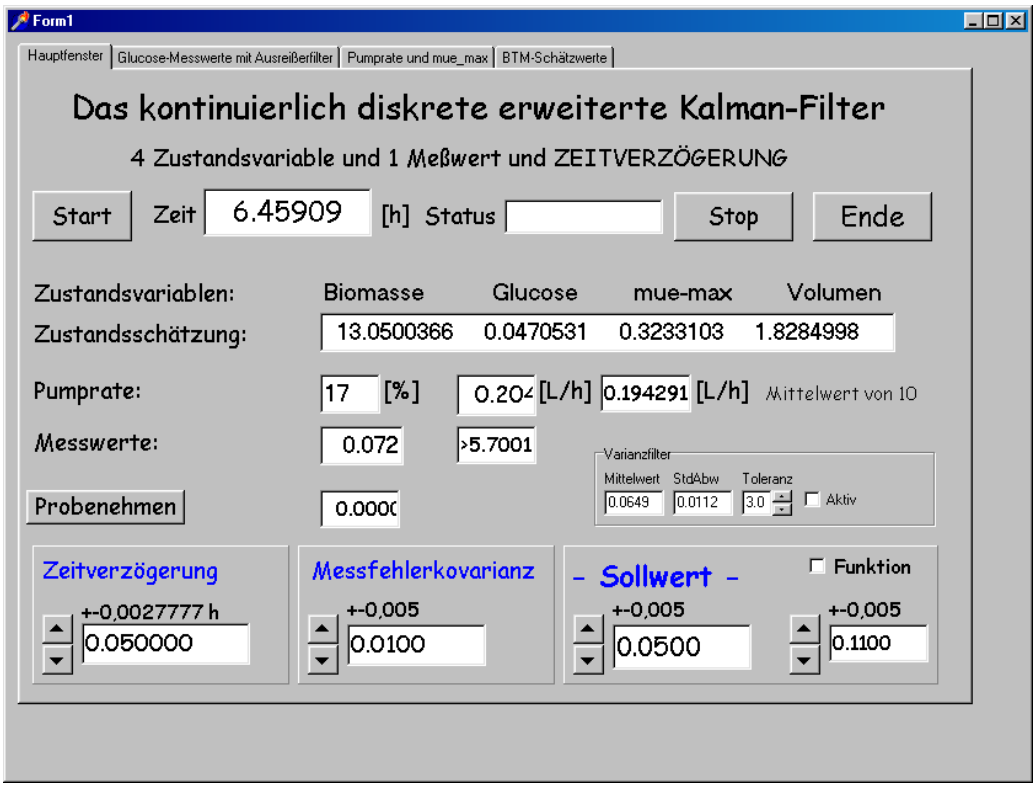

Fig. 6.9 Screen shot of EKF software during fed-batch cultivation.

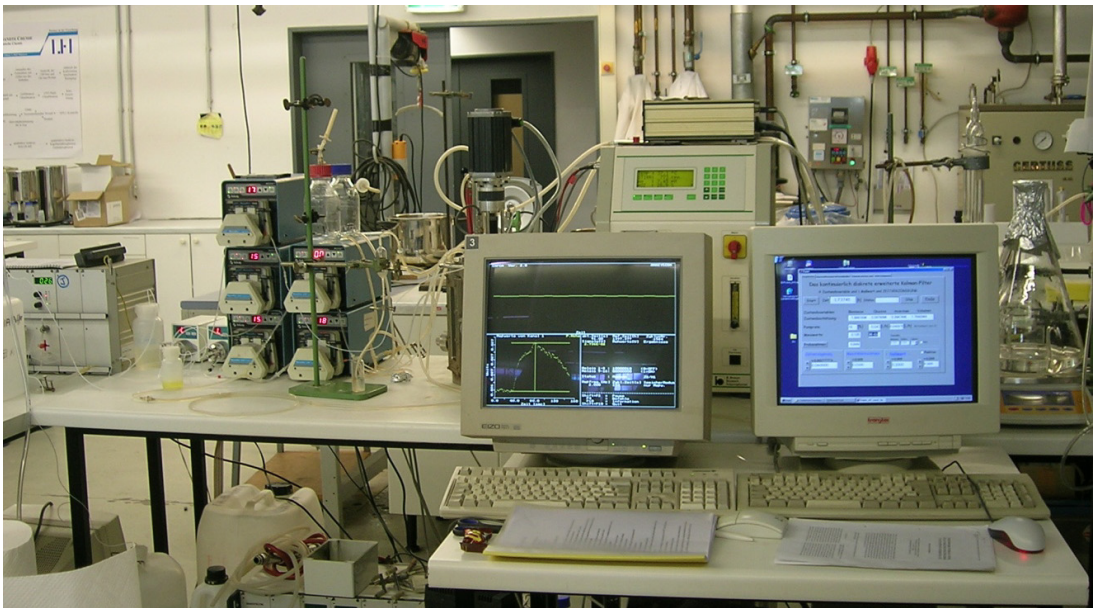

Fig. 6.10 Photo of the whole cultivation system for fed-batch cultivation at a constant glucose concentration.

6.4.3 Calculations of bioreactor cultivation

OTR (oxygen transfer rate)

$$OTR = \frac{M_{O_2} \cdot F^{in}}{V_R(t) \cdot V_M} \left(x_{O_2}^{in}(t) - x_{O_2}^{out}(t) \cdot \frac{1 - x_{O_2}^{in}(t) - x_{CO_2}^{in}(t)}{1 - x_{O_2}^{out}(t) - x_{CO_2}^{out}(t)} \right)$$

CPR (carbon production rate)

$$CPR = \frac{M_{CO_2} \cdot F^{in}}{V_R(t) \cdot V_M} \left(x_{CO_2}^{out}(t) \cdot \frac{1 - x_{O_2}^{in}(t) - x_{CO_2}^{in}(t)}{1 - x_{O_2}^{out}(t) - x_{CO_2}^{out}(t)} - x_{CO_2}^{in}(t) \right)$$

RQ (respiratory quotient)

$$RQ = \frac{CPR}{OTR}$$

Here,

M_{O_2}- molecular weight of oxygen (g mol^{-1});

M_{CO_2}- molecular weight of carbon dioxide (g mol^{-1});

F^{in}- the volumetric inlet air flow at standard conditions (l h^{-1});

$V_R(t)$- the working volume of the bioreactor (l);

V_M- the molar volume of ideal gas at standard conditions (l h^{-1});

$x_{O_2}^{in}(t)$- the molar fractions of oxygen in the inlet air (mol mol^{-1});

$x_{CO_2}^{in}(t)$- the molar fractions of carbon dioxide in the inlet air (mol mol^{-1});

$x_{O_2}^{out}(t)$- the molar fractions of oxygen in the outlet air (mol mol^{-1});

$x_{CO_2}^{out}(t)$- the molar fractions of carbon dioxide in the outlet air (mol mol^{-1});

6.5 Chromatography protocols

6.5.1 FPLC protocols

6.5.1.1 Protocol for cation exchange membrane chromatography

Step	Time (min)	System status	Parameter		Volume / Flow rate
1	0:00	Zero baseline	UV detector, 280 nm		
2	0:00	Isocratic flow	A: Buffer A	100 %	Volume: 10 ml Flow rate : 1 ml min^{-1}
			B: Buffer B	0 %	
3	10:00	Load / Inject sample	Load sample/ Direct inject	Econo pump/ Auto inject valve	Volume: 40 ml Flow rate : 1 ml min^{-1}
4	50:00	Isocratic flow	A: Buffer A	100 %	Volume: 30 ml Flow rate : 1 ml min^{-1}
			B: Buffer B	0 %	
5	80:00	Linear gradient	A: Buffer A	100 % → 0 %	Volume: 30 ml Flow rate : 1 ml min^{-1}
			B: Buffer B	0 % → 100 %	
6	110:00	Isocratic flow	A: Buffer A	0 %	Volume: 15 ml Flow rate : 1 ml min^{-1}
			B: Buffer B	100 %	
7	125:00	End of protocol			

Here, Buffer A: Equilibration buffer

Buffer B: Elution buffer 1

6.5.1.2 Protocol for heparin-sepharose affinity chromatography

Step	Time (min)	System status	Parameter		Volume / Flow rate
1	0:00	Zero baseline	UV detector, 280 nm		
2	0:00	Isocratic flow	A: Buffer A	100 %	Volume: 10 ml Flow rate : 1 ml min^{-1}
			B: Buffer B	0 %	
3	10:00	Load /Inject sample	Load sample/ Direct inject	Econo pump/ Auto inject valve	Volume: 40 ml Flow rate : 1 ml min^{-1}
4	50:00	Isocratic flow	A: Buffer A	100 %	Volume: 15 ml Flow rate : 1 ml min^{-1}
			B: Buffer B	0 %	
5	65:00	Linear gradient	A: Buffer A	100 % → 0 %	Volume: 40 ml Flow rate : 1 ml min^{-1}
			B: Buffer B	0 % → 100 %	
6	105:00	Isocratic flow	A: Buffer A	0 %	Volume: 10 ml Flow rate : 1 ml min^{-1}
			B: Buffer B	100 %	
7	115:00	End of protocol			

Here, Buffer A: Equilibration buffer

Buffer B: Elution buffer 2

6.5.1.3 Protocol for anion exchange membrane chromatography (Endotoxin removal)

Step	Time (min)	System status	Parameter		Volume / Flow rate
1	0:00	Zero baseline	UV detector, 280 nm		
2	0:00	Isocratic flow	A: Buffer A	100 %	Volume: 10 ml Flow rate : 1 ml min^{-1}
3	10:00	Load / Inject sample	Load sample/ Direct inject	Econo pump/ Auto inject valve	Volume: 25 ml Flow rate : 0.5 ml min^{-1}
4	60:00	Isocratic flow	A: Buffer A	100 %	Volume: 10 ml Flow rate : 1 ml min^{-1}
5	70:00	End of protocol			

Here, Buffer A: Exchanging buffer

6.5.2 RP-HPLC protocol

Step	Time (min)	System status	Parameter		Volume / Flow rate
1	0:00	Inject sample	Autosampler		20 µl
2	0:00	Linear gradient	A: Eluent A	100 % → 50 %	Flow rate : 1 ml min^{-1}
			B: Eluent B	0 % → 50 %	
3	0:50	Linear gradient	A: Eluent A	50 % → 100 %	Flow rate : 1 ml min^{-1}
			B: Eluent B	50 % → 0 %	
4	0:55	Isocratic flow	A: Eluent A	100 %	Flow rate : 1 ml min^{-1}
5	0:60	End of protocol			

Here, Eluent A: water + 0.1 % TFA

Eluent B: acetonitrile + 0.1 % TFA

6.6 Abbreviations

ANN	artificial neural network	FIA	flow injection analysis
αMEM	minimum essential medium, alpha modified	FPLC	fast protein liquid chromatography
AP	alkaline phosphatase	FTIR	Fourier transform infrared
APS	ammonium persulfate	GC	gas chromatography
BCIP	5-bromo-4-chloro-3-indolyl phosphate	GOD	glucose oxidase
BSA	bovine serum albumin	HCl	hydrochloric acid
CAFCA	computer assisted flow control and analysis	HPLC	high performance liquid chromatography
CPR	carbon production rate	IOD	integration optical density
DMEM	Dulbecco's modified eagle medium	iPSC	induced pluripotent stem cell
DCU	digital control unit	IPTG	isopropyl *β-D*-1-thiogalactopyranoside
DO	dissolved oxygen	K_m	Monod substrate saturation constant
DCW	dry cell weight	LAL	*Limulus* amebocyte lysate
DTT	dithiothreitol	M	molar
EC_{50}	half maximal effective concentration	MALDI-TOF	matrix assisted laser desorption ionization-time of flight
E. coli	*Escherichia coli*	M_{CO_2}	molecular weight of carbon dioxide
EDTA	ethylenediaminetetraacetic acid	M_{O_2}	molecular weight of oxygen
EKF	extended Kalman filter	mM	millimolar
Em	emission	μ	specific growth rate
ESC	embryonic stem cell	μ_{calc}	calculated specific growth rate
EU	endotoxin unit	μ_{esti}	estimated specific growth rate
Ex	extinction	μ_{max}	maximum specific growth rate
F^{in}	the volumetric inlet air flow at standard conditions	μ_{set}	specific growth rate set point
FCS	fetal calf serum	MWCO	molecular weight cut-off
FGF	fibroblast growth factor	NBT	nitro blue tetrazolium
FGF-2	basic fibroblast growth factor	NIR	near infrared

Neu5Ac	*N*-Acetylneuraminic acid	TEMED	*N,N,N′,N′*-Tetramethylethylenediamine
OD	optical density	TFA	trifluoroacetic acid
OTR	oxygen transfer rate	TGA	thermal gravimetric analysis
pI	isoelectric point	Tris	tris(hydroxymethyl)aminomethane
PI	proportional integral	UV	ultraviolet
POD	peroxidase	$\dot{V}_F$	feed rate
PSA	polysialic acid	$\dot{V}_{FB}$	feed rate of feedback part
PSC	pluripotent stem cells	$\dot{V}_{FF}$	feed rate of feedforward part
PVDF	polyvinylidenefluoride	V_M	the molar volume of ideal gas at standard conditions
RISP	real-time integrating software platform	V_R	culture volume
rpm	round per minute	$\dot{V}_S$	sample flow rate of the FIA system
RQ	respiratory quotient	X	biomass
S	substrate concentration	$x_{CO_2}^{in}$	the molar fractions of carbon dioxide in the inlet air
S_0	substrate concentration of feed solution	$x_{O_2}^{in}$	the molar fractions of oxygen in the inlet air
S_{set}	substrate set point	$x_{CO_2}^{out}$	the molar fractions of carbon dioxide in the outlet air
SDS-PAGE	sodium dodecyl sulfate polyacrylamide gel electrophoresis	$x_{O_2}^{out}$	the molar fractions of oxygen in the outlet air
SSEA4	stage-specific embryonic antigen 4	$Y_{A/S}$	yield factor of acetate on glucose
TBA	thiobarbituric acid	$Y_{P/S}$	yield factor of PSA on glucose
TCA	tricarboxylic acid	$Y_{X/S}$	yield factor of biomass on glucose

Curriculum Vitae

Personal Data

Name:	Chen, Ran
Gender:	Male
Marital status:	Married
Nationality:	P. R. China
Place of birth:	Hubei, China
Date of birth:	05.09.1981

Education

Sept. 1987 - Jul. 1992	Douhudi primary school, Gongan, China
Sept. 1992 - Jun. 1995	Chanling junior middle school, Gongan, China
Sept. 1995 - Jul. 1999	No. 1 middle school of Gongan, Gongan, China
Sept. 1999 - Jun. 2003	Department of chemistry, Huazhong University of Science and Technology, Wuhan, China Major: Chemistry Engineering and Technology Degree: Bachelor of Engineering
Sept. 2003 - Jun. 2006	School of life science, Nanjing University, Nanjing, China Major: Microbe and Biochemical Pharmacy Degree: Master of Science
Oct. 2006 - Dec. 2010	Ph.D. study at Institute for Technical Chemistry, Leibniz University of Hannover, under the guidance of Prof. Dr. Thomas Scheper

Publications

Papers

Rode, B., Endres, C., Ran, C., Stahl, F., Beutel, S., Kasper, C., Galuska, S., Geyer, R., Muhlenhoff, M., Gerardy-Schahn, R., Scheper, T., 2008. Large-scale production and homogenous purification of long chain polysialic acids from *E. coli* K1. J. Biotechnol. 135, 202-209.

Olmer, R., Haase, A., Merkert, S., Cui, W., Palecek, J., Ran, C., Kirschning, A., Scheper, T., Glage, S., Miller, K., Curnow, E.C., Hayes, E.S., Martin, U., 2010. Long term expansion of undifferentiated human iPS and ES cells in suspension culture using a defined medium. Stem Cell Res. 5, 51-64.

Chen, R., John, J., Rode, B., Hitzmann, B., Gerardy-Schahn, R., Kasper, C., Scheper, T., Comparison of polysialic acid production in *Escherichia coli* K1 during batch cultivation and fed-batch cultivation applying two different strategies. J. Biotechnol. (in press)

Chen, R., John, J., Lavrentieva, A., Müller, S., Tomala, M., Zhao,Y., Zweigerdt, R., Beutel, S., Hitzmann, B., Kasper, C., Martin, U., Rinas, U., Stahl, F., Scheper, T., Effective production of cytokines using membrane adsorbers, illustrated with human basic fibroblast growth factor production from *Escherichia coli*. (in preparation)

Posters

Chen, R., John, J., Hitzmann, B., Scheper, T., 2008. Comparison of polysialic acid production during batch and fed-batch cultivations of *Escherichia coli* K1. Bioperspectives 2008, Hannover, Germany.

Chen, R., Tomala, M., Jain, G., Zhao, Y., Olmer, R., Kasper, C., Stahl, F., Beutel, S., Rinas, U., Hitzmann, B., Martin, U., Scheper, T., 2008. Expression and purification of recombinant human basic fibroblast growth factor from fed-batch cultivation of *E. coli*. The 13th International Biotechnology Symposium, IBS 2008, Dalian, China.

Chen. R., John, J., Tomala, M., Lavrentieva, A., Majore, I., Kasper, C., Stahl, F., Beutel, S., Rinas, U., Hitzmann, B., Scheper, T., 2009. Effect of growth rate on the expression of recombinant human basic fibroblast growth factor during fed-batch cultivation of *E. coli.* DECHEMA Jahrestagung 2009, Mannheim, Germany.

Chen, R., Lavrentieva, A., Majore, I., Kasper, C., Scheper, T., 2010. Biologic activity, lyophilization and long-term stability of a basic fibroblast growth factor produced in *E. coli.* DECHEMA Jahrestagung 2010, Aachen, Germany.